

University of Wollongong

Research Online

Faculty of Science, Medicine & Health - Honours
Theses

University of Wollongong Thesis Collections

2020

Geomorphic evolution and the role of organic matter in a temperate supratidal Melaleuca wetland: Corner Inlet, VIC

Zachary Nagel-Tynan

Follow this and additional works at: <https://ro.uow.edu.au/thsci>

University of Wollongong

Copyright Warning

You may print or download ONE copy of this document for the purpose of your own research or study. The University does not authorise you to copy, communicate or otherwise make available electronically to any other person any copyright material contained on this site.

You are reminded of the following: This work is copyright. Apart from any use permitted under the Copyright Act 1968, no part of this work may be reproduced by any process, nor may any other exclusive right be exercised, without the permission of the author. Copyright owners are entitled to take legal action against persons who infringe their copyright. A reproduction of material that is protected by copyright may be a copyright infringement. A court may impose penalties and award damages in relation to offences and infringements relating to copyright material.

Higher penalties may apply, and higher damages may be awarded, for offences and infringements involving the conversion of material into digital or electronic form.

Unless otherwise indicated, the views expressed in this thesis are those of the author and do not necessarily represent the views of the University of Wollongong.

Recommended Citation

Nagel-Tynan, Zachary, Geomorphic evolution and the role of organic matter in a temperate supratidal Melaleuca wetland: Corner Inlet, VIC, Honours degree of Bachelor of Science, School of Earth, Atmospheric and Life Sciences, University of Wollongong, 2020.
<https://ro.uow.edu.au/thsci/200>

Research Online is the open access institutional repository for the University of Wollongong. For further information contact the UOW Library: research-pubs@uow.edu.au

Geomorphic evolution and the role of organic matter in a temperate supratidal Melaleuca wetland: Corner Inlet, VIC

Abstract

Coastal wetlands are highly productive ecosystems with an exceptional capacity for sequestering organic matter in the accumulating substrate. Recent studies have focused on intertidal saltmarsh and mangrove communities with limited research extending to the supratidal wetland forests, especially in temperate regions. The overall aim to fill the knowledge gap present in current literature by addressing two aims. The aims of this study is to (1) determine the processes driving the development and persistence of supratidal wetland forests in Corner Inlet, Victoria, Australia; and (2) reconstruct the historic vegetation shifts that have occurred in the embayment over the Holocene. A combination of stratigraphic analyses and photogrammetry were used to achieve these aim. Cores were collected to quantify the accumulation and preservation of organic matter across the intertidal-supratidal wetland gradient. Results from stratigraphic logs, bulk density and loss-on-ignition analyses, grain size, and high-resolution core logging (ITRAX) were compiled to determine the contribution and preservation capacity of organic matter in Melaleuca paperbark swamps (MPS) and to produce a paleo-reconstruction of the site. Along the study gradient, an increase in organic matter contribution was observed within the surface organic horizon shifting from the mangrove (5-10% organic matter) through to the MPS communities (up to 66% organic matter). The organic-rich soils of MPS noticeably declined at a greater rate in the more terrestrial substrate further from the seaward edge. This revealed a limitation in the preservation capacity of MPS with depth, with MPS having a greater effectiveness in organic preservation in more marine influenced settings. A time series analysis of historic aerial imagery, and paleo-reconstruction of sedimentary cores were used to reconstruct the historic vegetation shifts across the intertidal-supratidal wetland complex. Seaward migration of the wetland communities was identified during the paleo-reconstruction. Overtime, the infilling estuary revealed marine sands and seagrass meadows shift progressively to mangrove, saltmarsh, herbaceous wetlands and finally MPS. However, recent decadal shifts in the wetland community have inverted to a landward retreat. These results suggest that anthropogenic impacts on the Earth's climate have increased the rate of sea-level rise to a point which exceeds the rate of vertical accretion. The landward retreat of MPS and related rise in sea-level may result in the belowground disruption of preserved organic matter. This may lead to alterations in the global carbon cycle with large proportion of organic matter sequestered in these forests to be remineralised into CO₂, having further implications on anthropogenic climate change.

Degree Type

Thesis

Degree Name

Honours degree of Bachelor of Science

Department

School of Earth, Atmospheric and Life Sciences

Advisor(s)

Jeffrey Kelleway

Keywords

Coastal wetlands, Melaleuc paperbark swamps, organic sequestration, supratidal wetland forests

Geomorphic evolution and the role of organic matter in a temperate supratidal *Melaleuca* wetland: Corner Inlet, VIC

Honours Thesis 2020

Zachary Nagel-Tynan (5732104)

████████████████████

A thesis submitted in part fulfilment of the requirements of the Honours degree of Bachelor
of Science (Environment)

Supervisor: Jeffrey Kelleway

School of Earth, Atmospheric and Life Sciences, University of Wollongong

October 2020



UNIVERSITY
OF WOLLONGONG
AUSTRALIA

Certification

The information in this thesis is entirely the result of investigations conducted by the author, unless otherwise acknowledged, and has not been submitted in part, or otherwise, for any other degree or qualification.



Zachary Nagel-Tynan

October 2020

Contents

| | |
|---|------------|
| List of Figures | vii |
| List of Tables | ix |
| Abstract | x |
| Acknowledgements | xi |
| Abbreviations | xii |
| 1 Introduction | 1 |
| 1.1 Organic Matter in Coastal Wetlands | 1 |
| 1.2 Coastal Wetlands Response to Environmental Change | 2 |
| 1.3 Aims and Objectives | 3 |
| 1.4 Thesis Outline | 4 |
| 2 Literature Review | 5 |
| 2.1 Estuaries | 5 |
| 2.1.1 Estuary Evolution | 7 |
| 2.2 Coastal Wetlands | 10 |
| 2.2.1 Wetland Characteristics and Distribution | 10 |
| 2.2.2 Supratidal Wetland Forests | 11 |
| 2.2.3 Changes in Wetland Distribution and Extent | 12 |
| 2.3 Wetland Substrate Processes | 14 |
| 2.3.1 Importance of Surface Elevation in Coastal Wetlands | 14 |
| 2.3.2 Sediment Accretion in Coastal Wetlands | 14 |
| 2.3.3 Organic Matter Sequestration in Coastal Wetlands | 18 |
| 3 Methods | 19 |
| 3.1 Study Setting | 19 |
| 3.1.1 Geomorphology and Environment | 20 |
| 3.1.2 Water Quality | 23 |
| 3.1.3 Land-use in the Catchment Area | 23 |
| 3.2 Experimental Design | 24 |
| 3.3 Stratigraphic Analyses | 25 |
| 3.3.1 Coring and Water Chemistry | 25 |
| 3.3.2 Stratigraphic Logging and Macrofossil | 27 |
| 3.3.3 Bulk Density and Loss-On-Ignition Analysis | 27 |
| 3.3.4 Micro-XRF | 28 |
| 3.3.5 Grain Size | 28 |

| | | |
|----------|---|------------|
| 3.4 | Photogrammetry | 29 |
| 3.4.1 | Spatial Referencing | 30 |
| 3.4.2 | Time Series Analysis | 30 |
| 4 | Results | 32 |
| 4.1 | Stratigraphic Analysis | 32 |
| 4.1.1 | Field Measurements | 32 |
| 4.1.2 | Mangroves | 33 |
| 4.1.3 | Saltmarsh | 34 |
| 4.1.4 | <i>Melaleuca</i> 1 | 36 |
| 4.1.5 | <i>Melaleuca</i> 2 | 37 |
| 4.1.6 | Intertidal-Supratidal Complex | 39 |
| 4.2 | Photogrammetry | 47 |
| 5 | Discussion | 60 |
| 5.1 | Organic Contribution in Coastal Wetlands | 60 |
| 5.1.1 | Organic Contribution in the Supratidal Zone | 60 |
| 5.1.2 | Organic Contribution in the Intertidal Zone | 61 |
| 5.2 | Long-Term Shifts in Ecosystem Structure | 62 |
| 5.3 | Short-Term Shifts in Ecosystem Structure | 65 |
| 5.4 | Limitations and Further Research | 69 |
| 6 | Conclusion | 71 |
| | References | 72 |
| A | Summary of Stratigraphic Units | 88 |
| B | Table of Macrofossil | 96 |
| C | ITRAX Reference Profiles | 110 |
| D | Data Tables | 111 |
| E | Grain Size Histograms | 125 |
| F | Supplementary Maps | 134 |

List of Figures

| | | |
|-----|--|----|
| 2.1 | Conceptual morphological structure of estuaries, depicting the extremities of river-dominated, tide-dominated, and wave-dominated. Source: Cooper (1993) | 6 |
| 2.2 | Conceptualised wetland accommodation space and zonation. Below mean sea-level represents the subtidal zone, mangrove and saltmarsh represent the intertidal zone, and supratidal wetlands represent the supratidal zone. Source: Rogers <i>et al.</i> (2019a) edited to include supratidal wetlands. | 8 |
| 2.3 | Distribution of wave-dominated estuaries and tide-dominated estuaries across Australia. Source: Harris <i>et al.</i> (2002) | 9 |
| 2.4 | Evolution of a barrier estuary. (a) stages of infilling of an idealised barrier estuary: A= youthful, B=intermediate, C=semi-mature, D=mature. (b) depositional environments/zones as an estuary evolves. Source: Roy <i>et al.</i> (2001) | 9 |
| 2.5 | Conceptual links between the accumulation of mineral and organic matter, and realised accommodation space. Two dimensional model of sediment characteristics representing the accommodation space of a three dimensional wetland. Mineral sedimentation was conceptualised to have a positive linear relationship with accommodation space, though may diminish exponentially or in a polynomial manner with decreasing accommodation space. Accommodation space changes as a result of changes in relative sea-level, mineral and organic sediment accumulation and autocompaction. Sedimentation is variable across sites according to the availability of mineral and organic sediments, and below ground root productivity of surrounding vegetation. Source: Rogers <i>et al.</i> (2019a) | 16 |
| 3.1 | Location map of Corner Inlet. | 19 |
| 3.2 | Catchment area of Corner Inlet. Source: West Gippsland Catchment Management Authority (2014) | 20 |
| 3.3 | Map of the geology of the Corner Inlet catchment area. Source: West Gippsland Catchment Management Authority (2014) | 21 |
| 3.4 | Vegetation community mapping of Corner Inlet. Key codes: 0140 (Mangrove shrubland); 0009 (Coastal saltmarsh aggregate); 0010 (Estuarine wetlands); 0053 (Swamp scrub); 0875 (Blocked coastal stream swamp); 0008 (Wet heathland); 0048 (Unspecified). Source: Victoria. Department of Sustainability and Environment. (2012) | 22 |
| 3.5 | Proportion of each land-use category in the Corner Inlet catchment. Source: Dickson <i>et al.</i> (2013) | 24 |

| | | |
|-----|---|----|
| 3.6 | Core locations along the transect. Red - mangrove, orange -saltmarsh, green - <i>Melaleuca</i> 1, blue - <i>Melaleuca</i> 2. | 25 |
| 3.7 | Conceptual model of the shifting vegetation community within the intertidal-supratidal wetland complex. The transect was broken up into four sites: mangrove; saltmarsh; <i>Melaleuca</i> 1; and <i>Melaleuca</i> 2. Each zone is demonstrated to be positioned higher in elevation to the next (from mangrove to <i>Melaleuca</i> 2), resulting in a declining marine influence. | 25 |
| 3.8 | Map of Corner Inlet spatial analysis extent. The analysis of the intertidal-supratidal wetland complex was separated into two sections. Yellow: Area extent of the whole embayment analysis. Red: Area extent of the transect analysis. | 31 |
| 4.1 | Core photo, stratigraphic units, percentage organic matter and bulk density (left to right) of the Mangrove core (MAN). 0 m AHD is approximately equivalent to mean sea level. | 34 |
| 4.2 | Core photo, stratigraphic units, percentage organic matter and bulk density (left to right) of the Saltmarsh core (SM). 0 m AHD is approximately equivalent to mean sea level. | 35 |
| 4.3 | Core photo, radiograph, stratigraphic units, percentage organic matter, bulk density and elemental analysis (left to right) of the <i>Melaleuca</i> 1 core (MEL1). | 37 |
| 4.4 | Percentage organic matter, bulk density and moisture content (left to right). Organic matter and bulk density data from the primary <i>Melaleuca</i> 1 core, while moisture content was collected separately using the Russian peat corer. 0 m AHD is approximately equivalent to mean sea level. | 37 |
| 4.5 | Core photo, stratigraphic units, percentage organic matter and bulk density (left to right) of the <i>Melaleuca</i> 2 core (MEL2). 0 m AHD is approximately equivalent to mean sea level. | 38 |
| 4.6 | Percentage organic matter, bulk density and moisture content (left to right). Organic matter and bulk density data from the primary <i>Melaleuca</i> 2 core, while moisture content was collected separately using the Russian peat corer. 0 m AHD is approximately equivalent to mean sea level. | 39 |
| 4.7 | Percentage of organic matter downcore with respects to the Australian Height Datum (m AHD) across the four cores: A. Mangrove; B. Saltmarsh; C. <i>Melaleuca</i> 1; D. <i>Melaleuca</i> 2. 0 m AHD is approximately equivalent to mean sea level. | 40 |

| | | |
|------|--|----|
| 4.8 | Time series analysis of the whole embayment area spanning from 1957 to 2020. (A) Reference map of Corner Inlet in 1957, (B) reference map of Corner Inlet in 2020 (C) digitised lines of mangrove seaward edge, (D) digitised lines of mangrove landward, (E) digitised lines of saltmarsh seaward edge, (F) digitised lines of intertidal vegetation landward edge, (G) digitised lines of <i>Melaleuca</i> seaward edge, and (H) digitised lines of <i>Melaleuca</i> landward edge. | 51 |
| 4.9 | Time series analysis of the transect area spanning from 1957 to 2020. (A) Reference map of Corner Inlet in 1957, (B) reference map of Corner Inlet in 2020 (C) digitised lines of mangrove seaward edge, (D) digitised lines of mangrove landward, (E) digitised lines of saltmarsh seaward edge, (F) digitised lines of intertidal vegetation landward edge, (G) digitised lines of <i>Melaleuca</i> seaward edge, and (H) digitised lines of <i>Melaleuca</i> landward edge. The coordinates of the top right corner is -38.904940°S 146.299313°E. | 52 |
| 4.10 | Changes in wetland vegetation distribution across the whole embayment from 1957 to 2020. (A) Reference map of Corner Inlet in 1957, (B) reference map of Corner Inlet in 2020, (C) changes in mangrove distribution, (D) changes in bare ground distribution, (E) changes in saltmarsh distribution, and (F) changes in <i>Melaleuca</i> . Green represents the area of growth; red represents the area of retreat; yellow represents the area that has remained stable. | 55 |
| 4.11 | Changes in wetland vegetation distribution across the transect from 1957 to 2020. (A) Reference map of Corner Inlet in 1957, (B) reference map of Corner Inlet in 2020, (C) changes in mangrove distribution, (D) changes in bare ground distribution, (E) changes in saltmarsh distribution, and (F) changes in <i>Melaleuca</i> . Green represents the area of growth; red represents the area of retreat; yellow represents the area that has remained stable. The coordinates of the top right corner is -38.904940°S 146.299313°E. | 56 |
| 4.12 | Wetland vegetation distribution changes across the (A) whole embayment and (B) transect from 1957 to 2020. | 57 |
| 5.1 | Comparison of <i>Posidonia australis</i> (A) root and (B) rhizome macrofossils. (1) Seagrass macrofossils collected from <i>Melaleuca</i> 1 (MEL1). (2) reference photos of <i>Posidonia australis</i> macrofossil supplied by Oscar Serrano. Collected samples are (1A) MF-27, and (1B) MF-28. Background grid size for in (1) is 5 x 5 mm (Refer to Appendix B). | 63 |

| | | |
|-----|---|-----|
| 5.2 | Comparison of <i>Phragmites australis</i> roots, rhizome and nodes. (1) Root and rhizome macrofossils collected from <i>Melaleuca</i> 1 (MEL1). (2) Living root and rhizome of <i>Phragmites australis</i> . (A) Roots and rhizome casing, (B) rhizome casing, and (C) node. Collected samples are (1A) MF-7, (1B) MF-6, and (1C) MF-1. Background grid size for in (1) is 5 x 5 mm (Refer to Appendix B). | 65 |
| 5.3 | Natural cliffing along the <i>Melaleuca</i> seaward edge. Image taken from within the outline boundary of Figure 5.4 | 67 |
| 5.4 | Lateral expansion of the mangrove community that occurred between (A) 1987 and (B) 2010. | 68 |
| C.1 | Micro-XRF data collected from <i>Melaleuca</i> 1. Ca is environmental proxy for marine influence. Zr is a proxy for coarser sediment grain size. Rb is used as a proxy for terrestrial influence and finer sediment grain sizes. High values Ca/Rb concentrations indicate greater marine influence. High Zr/Rb concentrations are a proxy for coarser grain size. 0 m AHD is approximately equivalent to mean sea level. | 110 |
| F.1 | Aerial photograph of Corner Inlet in 1957 | 134 |
| F.2 | Aerial photograph of Corner Inlet in 1969 | 135 |
| F.3 | Aerial photograph of Corner Inlet in 1978 | 136 |
| F.4 | Aerial photograph of Corner Inlet in 1983 | 137 |
| F.5 | Aerial photograph of Corner Inlet in 1987 | 138 |
| F.6 | Aerial photograph of Corner Inlet in 2010. | 139 |
| F.7 | Aerial photograph of Corner Inlet in 2020. | 140 |

List of Tables

| | | |
|-----|--|-----|
| 2.1 | Types of coastal bodies in eastern Australia based on marine influence. Source: Roy <i>et al.</i> (2001) | 7 |
| 3.1 | Summary of aerial photography used for the time series analysis. Refer to Appendix F for images used. | 30 |
| 4.1 | Core ID, location, vegetation, core measurements, organic matter data, groundwater salinity and water table depth (collection date) | 32 |
| 4.3 | Row by row comparison of similar grainsizes between the stratigraphic units through the profile of the <i>Melaleuca</i> 1 (MEL1) core and the surface 15 cm of the mangrove core (MAN). 0 m AHD is approximately equivalent to mean sea level. | 41 |
| 4.5 | Row by row comparison of similar grain sizes between the stratigraphic units through the profile of the <i>Melaleuca</i> 1 (MEL1) core and the surface 15 cm of the saltmarsh core (SM). 0 m AHD is approximately equivalent to mean sea level. | 44 |
| 4.7 | Area coverage (m ²) and percentage change of the wetland vegetation from 1957 to 2020. (A) Mangrove, (B) bare ground, (C) saltmarsh, and (D) <i>Melaleuca</i> | 58 |
| A.1 | Stratigraphic units of mangrove core (MAN) consisting of depth range in m ADH, colouration, organic content, and grain size. 0 m AHD is approximately equivalent to mean sea level. | 88 |
| A.3 | Stratigraphic units of saltmarsh core (SM) consisting of depth range in m ADH, colouration, organic content, grain size, and additional information. 0 m AHD is approximately equivalent to mean sea level. | 90 |
| A.5 | Stratigraphic units of <i>Melaleuca</i> 1 core (MEL1) consisting of depth range in m ADH, colouration, organic content, grain size, and additional information. 0 m AHD is approximately equivalent to mean sea level. | 92 |
| A.7 | Stratigraphic units of <i>Melaleuca</i> 2 core (MEL2) consisting of depth range in m ADH, colouration, organic content, grain size, and additional information. 0 m AHD is approximately equivalent to mean sea level. | 94 |
| B.1 | Macrofossils collected throughout the profile of <i>Melaleuca</i> 1. Macrofossils are given a sample ID, photo, depth range (0 m AHD is approximately equivalent to mean sea level) description and identification where possible. Background grid size for scaling is 5 x 5 mm. | 96 |
| D.1 | Results of the bulk density and loss-on-ignition analysis of mangrove core (MAN). Samples are presented with an ID, depth range (0 m AHD is approximately equivalent to mean sea level), bulk density (given in g cm ⁻²) and percentage organic matter. | 111 |

| | | |
|------|--|-----|
| D.3 | Results of the bulk density and loss-on-ignition analysis of saltmarsh core (SM). Samples are presented with an ID, depth range (0 m AHD is approximately equivalent to mean sea level), bulk density (given in g cm ⁻²) and percentage organic matter. | 114 |
| D.5 | Results of the bulk density and loss-on-ignition analysis of <i>Melaleuca</i> 1 core (MEL1). Samples are presented with an ID, depth range (0 m AHD is approximately equivalent to mean sea level), bulk density (given in g cm ⁻²) and percentage organic matter. | 117 |
| D.7 | Results of the soil moisture analysis of <i>Melaleuca</i> 1. Samples are presented with an ID, depth range (0 m AHD is approximately equivalent to mean sea level), and percentage moisture content. | 120 |
| D.9 | Results of the bulk density and loss-on-ignition analysis of <i>Melaleuca</i> 2 core (MEL2). Samples are presented with an ID, depth range (0 m AHD is approximately equivalent to mean sea level), bulk density (given in g cm ⁻²) and percentage organic matter. | 121 |
| D.11 | Results of the soil moisture analysis of <i>Melaleuca</i> 2. Samples are presented with an ID, depth range (0 m AHD is approximately equivalent to mean sea level), and percentage moisture content. | 124 |
| E.1 | Results of the grain size analysis of <i>Melaleuca</i> 1 core (MEL1). Sample are presented with a grain size histogram and depth range (0 m AHD is approximately equivalent to mean sea level). | 125 |
| E.3 | Results of the grain size analysis of mangrove core (MAN). Sample are presented with a grain size histogram and depth range (0 m AHD is approximately equivalent to mean sea level). | 132 |
| E.4 | Results of the grain size analysis of saltmarsh core (SM). Sample are presented with a grain size histogram and depth range (0 m AHD is approximately equivalent to mean sea level). | 133 |

Abstract

Coastal wetlands are highly productive ecosystems with an exceptional capacity for sequestering organic matter in the accumulating substrate. Recent studies have focused on intertidal saltmarsh and mangrove communities with limited research extending to the supratidal wetland forests, especially in temperate regions. The overall aim to fill the knowledge gap present in current literature by addressing two aims. The aims of this study is to (1) determine the processes driving the development and persistence of supratidal wetland forests in Corner Inlet, Victoria, Australia; and (2) reconstruct the historic vegetation shifts that have occurred in the embayment over the Holocene. A combination of stratigraphic analyses and photogrammetry were used to achieve these aim. Cores were collected to quantify the accumulation and preservation of organic matter across the intertidal-supratidal wetland gradient. Results from stratigraphic logs, bulk density and loss-on-ignition analyses, grain size, and high-resolution core logging (ITRAX) were compiled to determine the contribution and preservation capacity of organic matter in *Melaleuca* paperbark swamps (MPS) and to produce a paleo-reconstruction of the site. Along the study gradient, an increase in organic matter contribution was observed within the surface organic horizon shifting from the mangrove (5-10% organic matter) through to the MPS communities (up to 66% organic matter). The organic-rich soils of MPS noticeably declined at a greater rate in the more terrestrial substrate further from the seaward edge. This revealed a limitation in the preservation capacity of MPS with depth, with MPS having a greater effectiveness in organic preservation in more marine influenced settings. A time series analysis of historic aerial imagery, and paleo-reconstruction of sedimentary cores were used to reconstruct the historic vegetation shifts across the intertidal-supratidal wetland complex. Seaward migration of the wetland communities was identified during the paleo-reconstruction. Overtime, the infilling estuary revealed marine sands and seagrass meadows shift progressively to mangrove, saltmarsh, herbaceous wetlands and finally MPS. However, recent decadal shifts in the wetland community have inverted to a landward retreat. These results suggest that anthropogenic impacts on the Earth's climate have increased the rate of sea-level rise to a point which exceeds the rate of vertical accretion. The landward retreat of MPS and related rise in sea-level may result in the belowground disruption of preserved organic matter. This may lead to alterations in the global carbon cycle with large proportion of organic matter sequestered in these forests to be remineralised into CO², having further implications on anthropogenic climate change.

Acknowledgements

I wish to acknowledge the traditional custodians of the land in which my study took place, the Gunaikurnai, Bunurong and Boon Wurrung people and their Elders past and present. I acknowledge and respect their continuing culture and the contribution they make to the life of this country.

I would like to thank my supervisor Dr Jeffrey Kelleway for his never-ending patience over the past year. None of this would have been possible without his constant guidance, advice and feedback.

Many thanks to Jeff Kelleway, Kerrylee Rogers and Matthew Holden for their work in the field. Further acknowledgements go out to Kerrylee who provided me with historical imagery of the region, as well as the advice and guidance she provided.

Thanks to those who helped and kept me company in the laboratory: Samantha Houston; Robert Bruckner; Vanessa Mailhammer; Callum Greenshields; and Fabian Boesl.

I would like to express my gratitude to those who proofread my thesis: Samantha Houston; Mark McGivern; Patrick McGivern; Ann Hollifield; Vanessa Mailhammer; Robert Bruckner; Sebastian Garcia; Brooke Conroy; Claudia Stephans; and Nathan Hawkes.

My thanks also go out to Oscar Serrano for his input in macrofossil identification, Robert Bruckner for volunteering his camera for the macrofossil photography, and Courtney Hildebrandt for her assistance in with Lyx.

Last but not least, to my friends and family that have helped me not only through this year, but the years that led to this stage. Particularly to my Nan and Pop, Dimity and James Tynan, whom without I would not be where I am today. I give endless gratitude to the support and guidance they have provided throughout my life.

Abbreviations

| Abbreviation | Terms |
|-------------------------------|---|
| AHD | Australian Height Datum |
| BD | Bulk Density |
| CO ₂ | Carbon Dioxide |
| GCPs | Ground Control Points |
| HAT | Highest Astronomical Tide |
| H ₂ O ₂ | Hydrogen Peroxide |
| ICOLLs | Intermittently Closed/Open Lakes and Lagoons |
| LAT | Lowest Astronomical Tide |
| LOI | Loss-On-Ignition |
| MAN | Mangrove Core |
| MEL1 | <i>Melaleuca</i> 1 Core |
| MEL2 | <i>Melaleuca</i> 2 Core |
| MPS | <i>Melaleuca</i> Paperbark Swamp |
| MSL | Mean Sea-Level |
| N | Ammonium, nitrate and nitrite |
| NPP | Net Primary Production |
| P | Phosphate |
| RMS | Root Mean Square |
| RSL | Relative Sea-Level |
| RTK-GPS | Real-Time Kinematic Global Positioning System |
| SEPP | State Environment and Protection Policy |
| SLR | Sea-Level Rise |
| SM | Saltmarsh Core |
| SOI | Southern Oscillation Index |

1 Introduction

1.1 Organic Matter in Coastal Wetlands

The production and preservation of organic matter within terrestrial and marine ecosystems plays a significant role in the global carbon cycle (Janzen, 2004). Forested and wetland communities are of particular importance due to their high productivity of organic matter above- and belowground (Dixon *et al.*, 1994; Trettin and Jurgensen, 2002; Saintilan *et al.*, 2013; Sohn *et al.*, 2013). Forested areas contain approximately 80% and 40% of the global above- and belowground terrestrial carbon, respectively (Dixon *et al.*, 1994). Approximately 18-30% of the total belowground carbon stores can be attributed to wetlands areas, despite covering only 2-3% of the Earth's terrestrial surface (Trettin and Jurgensen, 2002). Preservation of organic matter below the surface is influenced by a complex interaction of biotic and abiotic components of an ecosystem. Factors impacting preservation include climate, soil chemistry and composition, and vegetation (Lal, 2005; Pester *et al.*, 2012). The interaction occurring between these factors in coastal ecosystems allows for the efficient preservation of organic material. This signifies the importance of organic accumulation and preservation in coastal wetlands .

Coastal wetlands' distribution is governed by the combination of biotic and abiotic factors associated with low energy coastal areas (Pennings *et al.*, 2005). Tidal wetlands are a subcategory of coastal wetlands that are positioned around the tidal frame, and are categorised into three zones: subtidal, intertidal, and supratidal.

The surge in research surrounding coastal wetlands has been focused on the role inundation plays in preservation and productivity of intertidal and subtidal wetland communities (saltmarsh, mangrove and seagrass communities) (Kirk, 2004; Dise, 2009; Del Grosso *et al.*, 2010; McLeod *et al.*, 2011; Howard *et al.*, 2014; Morris *et al.*, 2016). Examination of sediment cores have been used to address the contribution of organic material of these wetland communities in the past (Kelleway *et al.*, 2017b; Adame *et al.*, 2019). Limited research has been undertaken to understand these processes in the wetland vegetation positioned above the intertidal zone. Supratidal wetland forests are forested communities positioned above highest astronomical tide (HAT) in the supratidal zone. Due to the positioning of supratidal wetland forests beyond the astronomical tidal frame they receive aperiodic inundation from extreme tides and/or meteorological events (Adame *et al.*, 2019). The supratidal wetland forests of Australia are largely dominated by the genera *Melaleuca* and *Casuarina* (Boon *et al.*, 2016). *Melaleuca* paperbark swamps (MPS) are a supratidal wetland forest commonly found along Australian coastlines that are dominated by *Melaleuca*, a genus of trees and shrubs from the family Myrtaceae (Barlow, 1988). The implications of anthropogenic draining and clearing of many wetland ecosystems has led to significant declines in MPS distribution and abundance (Bowkett and Kirkpatrick, 2003; Robinson *et al.*, 2006). Studies concerned with the organic contribution of MPS have only

included those in tropical climates (Adame *et al.*, 2019; Tran *et al.*, 2013a), with currently no published research focusing on the role of organic matter in temperate supratidal wetland forests. Further research of MPS, specifically within temperate climates is required to broaden the understanding of organic matter accumulation within supratidal wetland forests.

1.2 Coastal Wetlands Response to Environmental Change

A coastal wetland's ability to increase surface elevation in response to changing sea-level is a key component in maintaining the stability of ecosystem structure and function (Alongi, 2014; Baker *et al.*, 2009; Woodroffe *et al.*, 2016). To remain stable, surface elevation must increase at a similar rate to that of rising sea-level (Kirwan and Megonigal, 2013; Morris *et al.*, 2016; Reed, 1995). Changes to surface elevation are a function of surface and belowground processes. The vertical accretion of sediment fills the available accommodation space of the wetland, raising surface elevation (Rogers *et al.*, 2019a). Autocompaction of sediments, decomposition of stored organic material, and erosion can reduce surface elevation by decreasing sediment volume, thereby raising relative sea-level (RSL) (Morris *et al.*, 2016). Present day estuaries of south-east Australia formed during the post-glacial marine transgression and subsequent sea-level rise (SLR) of the Holocene (Roy *et al.*, 2001). Estuaries are a common location for coastal wetlands, as they are typically protected, low energy environments. Present day mean sea-level for Australia was reached approximately 2 kya (Rogers *et al.*, 2019b). Before modern standards, there was a steady rise in sea-level until 5 kya, preceded by sea-level sharply falling to approximately 4m below present day sea-level around 6 kya. The stable sea level over the last 2 ky has led to sediment accumulation and seaward migration within wetland communities.

A period of stable sea-level has resulted in progressive infilling of estuaries (Dalrymple *et al.*, 1990; Zaitlin *et al.*, 1994). The slow rate of infilling that ensue the post-glacial marine transgression formed the ideal conditions within the intertidal zones of Australia for ecotonal saltmarsh-mangrove communities to exist (Adam, 1993; Roy *et al.*, 2001). Changes in south-east Australia coastal wetlands distribution during the Holocene has been observed using sedimentary cores. Cores sampled from contemporary saltmarsh across multiple sites contain remnants of ancient mangrove communities in the form of preserved macrofossils (Saintilan and Williams, 1999a; Saintilan and Wilton, 2001).

During rising sea-level, vertical accommodation space increases, paving the way for further sedimentation and geomorphic evolution of the coastal zones of Australia. If changes in RSL exceed the rate of vertical accretion, vegetation communities will begin to encroach landwards from the stress of changing environmental conditions. Despite SLR increasing accommodation space which allows for further accretion of organic matter, continuous rise may lead to reduced organic preservation. As sea-level rises, the rate of erosion may increase, exposing previous sequestered organic matter (DeLaune and White, 2012; Kirwan

and Mudd, 2012). Similarly, stable or diminishing sea-level have been proposed to deplete organic matter as a result of substrate development reaching upper limit of accommodation space, that being HAT, and becoming increasing terrestrial (Rogers *et al.*, 2019a). Under future projections for anthropogenically driven SLR, the threshold for exposing sequestered organic matter may potentially be reached (Oppenheimer *et al.*, 2019; Rogers *et al.*, 2019a). Anthropogenic clearance of wetlands also poses a threat to the effectiveness of sequestering organic material.

Aerial photography has been used to assess decadal changes within coastal wetlands (Buckney, 1987; Chafer, 1998; Rogers *et al.*, 2005). In south-east Australia a landward migration has been observed surrounding the mangrove and saltmarsh communities (Rogers *et al.*, 2005; Kelleway *et al.*, 2016b; Whitt *et al.*, 2020), however there has been minimal research extending beyond the impacts on intertidal wetlands into the supratidal wetland forests. Sensitivity to relative SLR has been suggested to play a role in the diminishing coverage of supratidal wetland forests in Australia (Bowman *et al.*, 2010; Kelleway *et al.*, 2018) and globally (Kirwan *et al.*, 2007; Schieder *et al.*, 2018). These changes have been suggested to have number potential drivers, these include changes to temperature (Whitt *et al.*, 2020), sedimentation regimes (Saintilan and Williams, 1999b), autocompaction of substrate (Rogers *et al.*, 2006), and alterations to the regions hydrology (Saintilan and Williams, 1999b). Research into coastal wetlands' response to a changing environment has been predominately dedicated to the intertidal saltmarsh and mangrove. This has left critical knowledge gaps within present literature surrounding the supratidal wetland forests, including MPS.

1.3 Aims and Objectives

This study will address the current knowledge gap surrounding supratidal wetland forests, focusing on MPS. Sediment cores will be taken to determine the changes in vegetation distribution that have occurred during the Holocene (hereafter referred to as long-term changes). They will also help quantify the role that organic matter plays in the surface organic horizon and preservation of organic matter through the substrate. Historic aerial photography will be used to assess the changes in wetland distribution over the last 70 years (hereafter referred to as short-term changes).

Aim 1: Determine the processes driving the development and persistence of supratidal wetland forests

Objectives:

- Characterise contributions of organic and mineral components in the substrate across the intertidal-supratidal gradient.

- Assess relationships between organic matter preservation, stratigraphic composition and hydrology.

Aim 2: Reconstruct historic vegetation shifts across an intertidal-supratidal wetland complex (Corner Inlet, Victoria)

Objectives:

- Map distribution changes of intertidal and supratidal vegetation communities over a 70-year period
- Characterise and correlate sedimentary strata across the intertidal-supratidal gradient.
- Identify and assess macrofossil distribution in sediment profiles to determine vegetation communities present.

Organic contributions in previous studies of supratidal wetland forests have shown a high proportion of organic to mineral matter within the near surface sediment. It is hypothesised that MPS will have an organic-rich surface and potentially demonstrate an efficient capacity for organic matter preservation with depth. The paleo-reconstruction of these wetlands throughout the Holocene is hypothesised to follow the process of estuary evolution. As the estuary begins to infill the vegetation will shift to accommodate the new seaward moving foreshore. Recent mapping of the temperate wetlands of south-east Australia have revealed an expansion of mangrove forest into the upper intertidal saltmarsh. The mapping of Corner Inlet wetlands in this project is hypothesised similar landwards shift will occur in vegetation communities, with mangroves encroaching into saltmarsh communities.

1.4 Thesis Outline

This thesis is comprised of the following elements. The first is a review of the current literature surrounding estuarine evolution and the structure and changes that occur within coastal wetland communities. The literature review also addresses the role of sediment accumulation, both organic and mineral, and the influence of these on wetland surface dynamics, and therefore wetland structure and function. The methodology used to complete this study is presented and followed by the collective results for each analysis. The results have been interpreted in the context of existing literature to address the aims of this study. Finally, the conclusion of the findings of the study are presented.

2 Literature Review

This literature review consists of three primary topics: (1) estuaries, to understand the environmental setting of the coastal wetlands of this project; (2) coastal wetlands, to outline the structure and function of these vegetative communities; (3) and the role of sedimentation within coastal wetlands to identify the processes that control the stability or dynamism of the wetlands. A review of the geomorphic processes shaping modern estuaries is focused on research of south-east Australian estuaries. This section explain the processes driving estuarine evolution from young to mature estuaries. Narrowing in from the estuary scale, an assessment of coastal wetlands of was undertaken. This is focused on the characteristics and distribution of intertidal and supratidal wetlands within an estuary, along with the changes that occur in wetlands. This is followed by an explanation of the role of organic and mineral sedimentation in coastal wetlands, controlling whether wetlands are dynamic or stable.

2.1 Estuaries

The term *estuary* refers to a body of water where the mixing of freshwater and marine saltwater occurs. Sedimentary inputs within estuaries are sourced from fluvial and marine settings, with morphological influences from fluvial, tidal, and wave processes (Boyd, 1992). An estuary's extent ranges from the upper limits of the fluvial system impacted by saline intrusion, through to its coastal opening (Woodroffe, 2002). The morphology and evolution of an estuary is determined by two aspects: the dominant physical processes (fluvial, tidal, or wave) of the estuary; and the evolution of the coastal surroundings, involving factors such as variations in relative sea-level (RSL), sediment input and output, sediment type, and shoreline shape (Boyd, 1992; Roy *et al.*, 2001). Three main estuary types are informed by the physical processes operating within the estuary: river dominated, tide-dominated and wave-dominated (Figure 2.1) (Roy *et al.*, 2001).

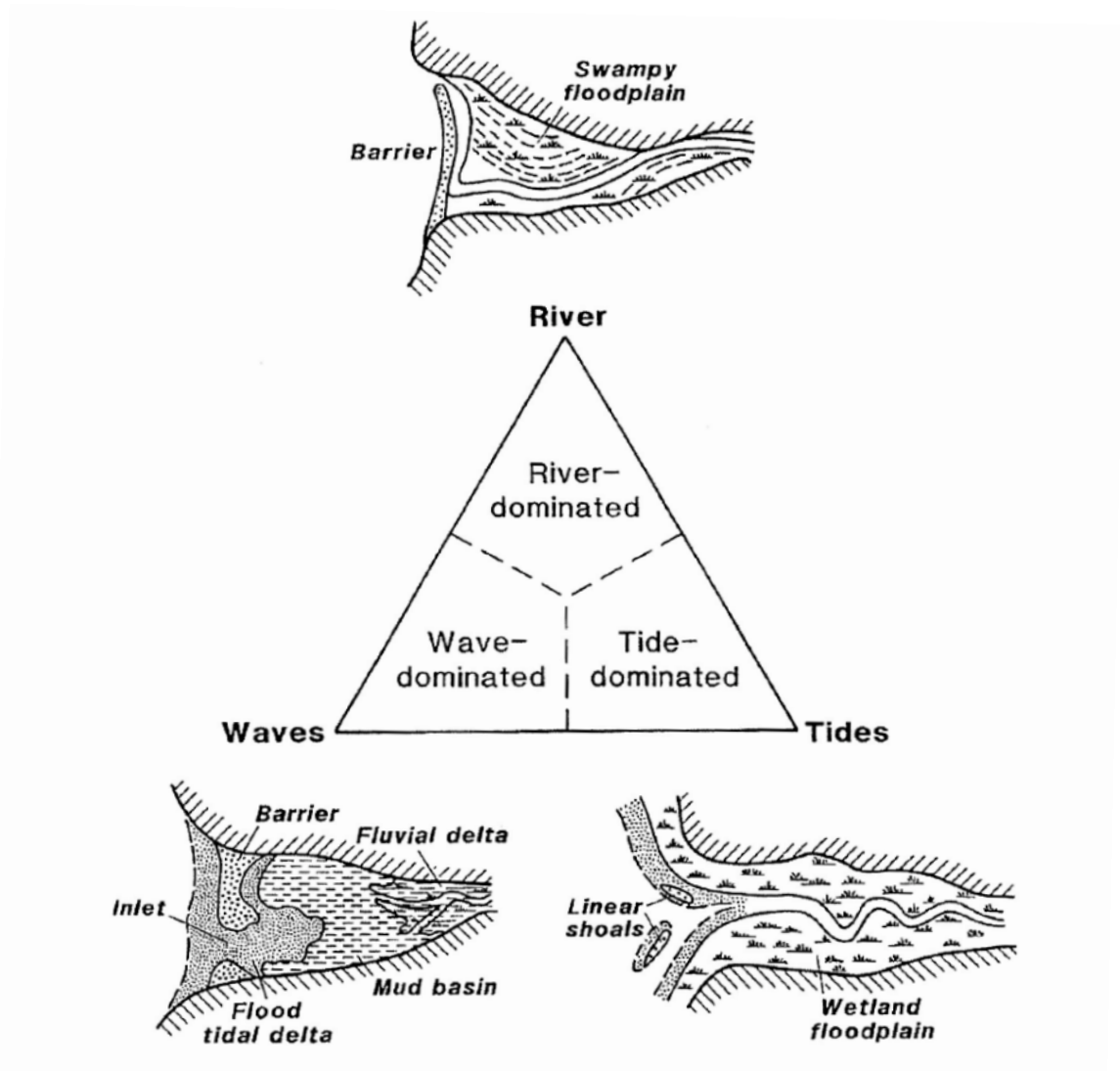


Figure 2.1: Conceptual morphological structure of estuaries, depicting the extremities of river-dominated, tide-dominated, and wave-dominated. Source: Cooper (1993)

Present day estuaries of south-east Australia formed during the post-glacial marine transgression and subsequent SLR of the Holocene (Roy *et al.*, 2001). These estuaries are a common location for coastal wetlands, as they are typically protected, low energy environments. Many of south-east Australia's modern estuaries were formed over the course of the Holocene as a result of the post-glacial marine transgression and subsequent SLR (Roy *et al.*, 2001). In response to this, fluvial systems began to drown and experienced a landwards shift as the rate of SLR surpassed the rate of sedimentation (Roy, 1994; Zaitlin *et al.*, 1994). As sea-level stabilised, the landward regression of estuaries halted and the rate of sedimentation at this stage exceeded SLR, resulting in the progressive infilling of estuaries (Dalrymple *et al.*, 1990; Zaitlin *et al.*, 1994).

2.1.1 Estuary Evolution

Estuaries along eastern Australia can be divided into five groups relating to the prevalence of marine influence (Table 2.1) (Roy *et al.*, 2001) . Open marine embayments have a strong marine influence with limited influx of fresh water from fluvial processes (Roy *et al.*, 2001). This is a common early transitional phase in estuary evolution, after which young systems may experience sediment infill, thereby constricting estuarine area over time and decreasing available accommodation space (Cooper, 2001; Roy, 1994). This process changes the biological communities and hydrological characteristics of the estuary (Hodgkin and Kendrick, 1984; Roy, 1984; Roy *et al.*, 2001). The effective accommodation space of tidal coastal wetlands is bounded between the underlying bedrock and HAT (Figure 2.2; Rogers *et al.*, 2019a). The realised accommodation space is the zone that has been infilled by sediment, changes within this zone result in vertical change of the wetlands. Available accommodation space is the potential space that sediment can infill. As mineral and organic sediments accumulate the available accommodation space of the wetland decreases in one of two ways: vertically or horizontally.

Table 2.1: Types of coastal bodies in eastern Australia based on marine influence. Source: Roy *et al.* (2001)

| Groups | Types (and examples) | Mature forms* |
|-------------------------------|---|--------------------|
| I. Bays | 1. Ocean embayments (Botany Bay) | |
| II. Tide-dominated estuaries | 2. Funnel-shaped macrotidal estuary (South Alligator River, Northern Territory) | Tidal estuaries |
| | 3. Drowned valley estuary (Hawkesbury River) | |
| | 4. Tidal basin (Moreton Bay) | |
| III. Wave-dominated estuaries | 5. Barrier estuary (Lake Macquarie) | Riverine estuaries |
| | 6. Barrier lagoon (The Broadwater/South Stradbroke Island) | |
| | 7. Interbarrier estuary (Tilligerry Creek, Port Stephens) | |
| IV. Intermittent estuaries | 8. Saline coastal lagoon (Smiths Lake) | Saline creeks |
| | 9. Small coastal creeks (Harbord Lagoon, Sydney) | |
| | 10. Evaporative lagoons (The Coorong, South Australia) | |
| V. Freshwater bodies | 11. Brackish barrier lake (Myall Lakes) | Terrestrial swamps |
| | 12. Perched dune lake (Lake Hiawatha) | |
| | 13. Backswamp (Everlasting Swamp, Clarence River) | |

*Mature forms refer to infilled estuaries.

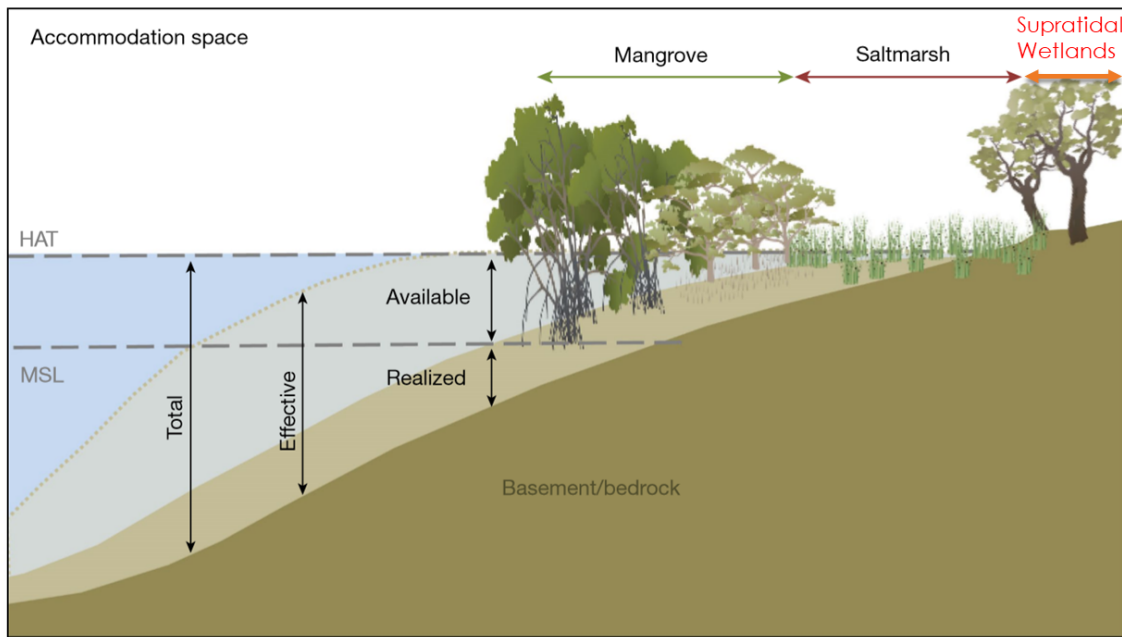


Figure 2.2: Conceptualised wetland accommodation space and zonation. Below mean sea-level represents the subtidal zone, mangrove and saltmarsh represent the intertidal zone, and supratidal wetlands represent the supratidal zone. Source: Rogers *et al.* (2019a) edited to include supratidal wetlands.

During the infilling stage, dominant processes morph the estuary into one of four groups (Groups II-V of Table 2.1). Australian estuaries are predominantly tidal-dominated or wave-dominated. There is a clear geographical separation between the tidal-dominated estuaries characteristic of northern Australia and the wave-dominated systems across much of southern Australia (Figure 2.3; Harris *et al.*, 2002; Hodgkin and Hesp, 1998; Woodroffe, 1993). Dominant wave action along the south-east coast of Australia provides a large supply of marine sediment to estuaries, compared to their tidal and river counterparts (Dalrymple *et al.*, 1992). Wave-dominated estuaries are categorised by their tidal driven inlets, with an enclosing or semi-enclosing supratidal barrier formed by wave-deposited sediments (Figure 2.1; Roy *et al.*, 2001). Barriers form as sediment is transported from the continental shelf and deposited along the coastline by wave energy (Woodroffe, 2002). The barrier feature of wave-dominated estuaries acts as an effective sediment trap, limiting coastal regression as the estuaries tend to experience an initial period of rapid infilling (Heap *et al.*, 2004). This causes the shape of the estuary to become increasingly channelised (Cooper, 1993). As the infilling progresses, an estuary reaches the latter stages of maturity and takes on more river-dominated characteristics (Figure 2.4; Roy *et al.*, 2001). After the infill process is complete, the morphology of the estuaries resembles that of a river channel with a wave-dominated delta (Dalrymple *et al.*, 1990; Harris *et al.*, 2002).

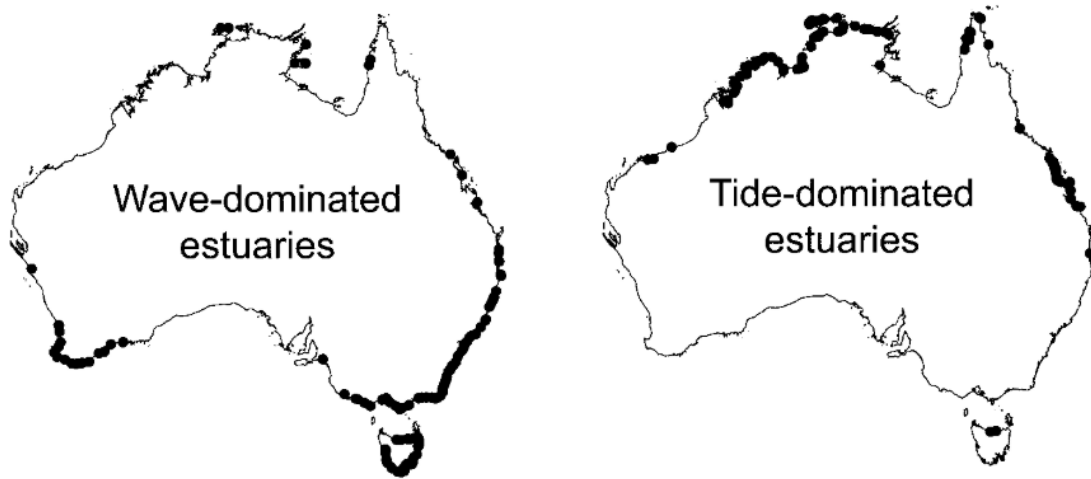


Figure 2.3: Distribution of wave-dominated estuaries and tide-dominated estuaries across Australia. Source: Harris *et al.* (2002)

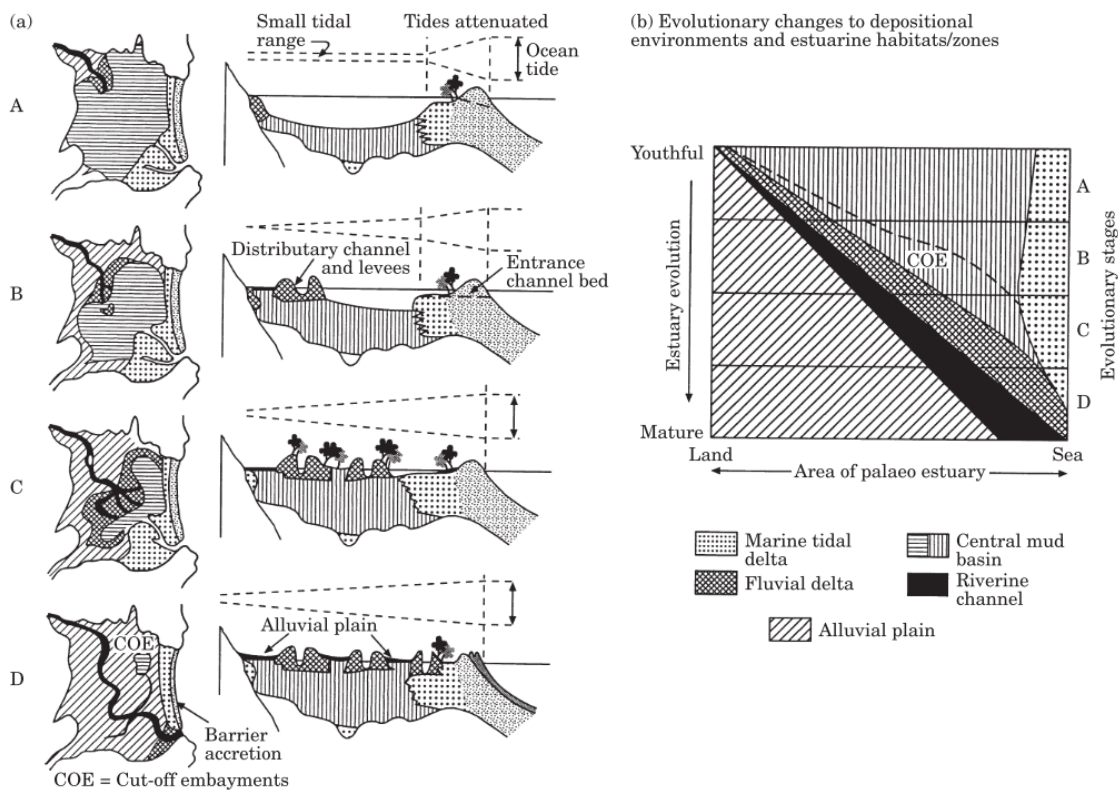


Figure 2.4: Evolution of a barrier estuary. (a) stages of infilling of an idealised barrier estuary: A= youthful, B=intermediate, C=semi-mature, D=mature. (b) depositional environments/zones as an estuary evolves. Source: Roy *et al.* (2001)

The small catchment size of many south-east Australian estuaries minimises fluvial inputs (Roy *et al.*, 2001). This can be attributed to periodic low rainfall events reducing the sediment supply of fluvial systems. In the event of low fluvial sedimentation and heavy input

wave-deposited sediments, the barrier can fully enclose the estuary, creating an isolated lagoonal system. This closure can span a few days or up to years (McSweeney *et al.*, 2018). Systems of this nature are referred to as Intermittently Closed/Open Lakes and Lagoons (ICOLLs). This closure starves the estuary of marine sediment, with terrestrial sediments delivered from fluvial processes supplying the estuary (Roy *et al.*, 2001). The channel infilling the estuary begins to deposit coarse sediments forming a fluvial delta at the head of the channel, while the finer sediments infill the remaining accommodation space of the central basin (Figure 2.4; Woodroffe, 2002; Sloss *et al.*, 2005; Sloss *et al.*, 2006; Woodroffe, 2002). The finer grained silt and muds are dark in colouration due to the carbon rich content (Roy *et al.*, 2001). Infilling along the boundaries of the estuary sustains suitable conditions for wetland vegetation to inhabit.

2.2 Coastal Wetlands

2.2.1 Wetland Characteristics and Distribution

Coastal wetlands are positioned around low energy coasts, with their distribution determined by biotic and abiotic factors (Pennings *et al.*, 2005). They can be categorised according to a range of criteria. Tidal wetlands are a category of wetlands positioned and influenced by the tides. Tidal wetland communities are categorised into three zones within the tidal frame: subtidal, intertidal, and supratidal (Figure 2.2). Coastal wetland zonation is informed by the vegetation community's tolerance to the biotic and abiotic stressors present, with salinity and inundation being the primary factors (Crowley and Gagan, 1995; Pennings *et al.*, 2005).

The subtidal zone is located below the lowest astronomical tide (LAT) and experiences constant inundation. Seagrass meadows are a common wetland community located in the subtidal and lower intertidal zone. Above this is the intertidal zone, positioned between the LAT and HAT. These zones experience periodic inundation with respects to their position in the tidal frame and tidal regime of the area. Mangroves and saltmarshes are common upper intertidal vegetation communities. These communities commonly coexist in south-east Australia, forming ecotonal communities within the intertidal zone; in temperate Australia, mangroves are typically located above MSL in the tidal frame regions and saltmarshes typically positioned further landwards in the upper intertidal zone above mean highwater neap tidal (Allen, 2000; Kelleway *et al.*, 2017b; Perillo *et al.*, 2018). Lower intertidal communities consist of mudflats and/or seagrass. Located above the HAT, the supratidal zone is unaffected by surface inundation from astronomic tidal activity but may be infrequently inundated during extreme tides and/or meteorological events such as storms.

Global estimates of mangrove coverage range between 137,760 – 152,308 km² with increasing distribution and species diversity moving towards tropical regions of middle latitudes (Spalding, 2010; Giri *et al.*, 2011; Friess *et al.*, 2012). The distribution patterns of mangrove species can be attributed to their lower tolerance of as a majority of the

11,000 km² of mangrove forests are positioned in the tropical wetlands in northern Australia (Galloway, 1982). In contrast, the distribution and diversity of saltmarsh species shows an inverse trend to mangroves, favouring more temperate climates and have a widely varied global coverage estimated to be between 22,000-400,000km² (Duarte *et al.*, 2013; McLeod *et al.*, 2011). Saltmarshes tend to prefer temperate climates, observed in assessments of species biodiversity undertaken across Australian saltmarshes (Adam, 1993). The temperate wetlands of southern Australia contain more than 30 species of saltmarsh, which is over three times that of the northern tropics of Australia, containing less than 10 species (Adam, 1993; Saintilan, 2009). The temperate conditions of south-east Australia support the coexistence of saltmarsh and mangrove communities within the upper intertidal zone (Adam, 1993). This is complimented by the slow infill following the post-glacial marine transgression, which formed an ideal intertidal zone that allows both communities to coexist (Roy *et al.*, 2001).

In recent decades there has been an increasing focus on the ecosystem services provided by coastal wetlands. Ecosystem services are 'the benefits people obtain from ecosystems' (MEA, 2005) and serve as justification for the conservation and restoration of many ecosystems (Mitsch and Gossilink, 2000; Boyd and Banzhaf, 2007; Kelleway *et al.*, 2017a). Coastal wetlands provide habitat for fisheries, act as filtration systems for nutrients and pollutants, sequester and store carbon, and provide many other ecological benefits (Kelleway *et al.*, 2017a). The global annual ecosystem service provided by intertidal wetland communities alone is estimated at US\$24.8 trillion (de Groot *et al.*, 2012). Despite the predominant tropical distribution of mangroves, global climate change is causing a poleward migration of many temperate and tropical ecosystems (Walther *et al.*, 2002). This disruption is changing the structure and function of many wetland communities through the displacement of native species and alteration of biodiversity patterns (Kelleway *et al.*, 2017a).

2.2.2 Supratidal Wetland Forests

Supratidal wetlands support forested communities located in the supratidal zone above the HAT. Compared to their lower elevation counterparts (saltmarshes and mangroves), supratidal wetland forests only experience inundation in the event of extreme tides and/or meteorological events. *Melaleuca* Paperbark Swamps (MPS) are a wetland forest dominated by *Melaleuca*, a genus of trees and shrubs from the Family Myrtaceae. MPS that grow along freshwater and estuarine waters of the coast have an extensive range covering ~6.4 million ha across Australia (ABARES, 2016; Jeanes, 1996; Robinson *et al.*, 2006; Raulings *et al.*, 2007; Tran *et al.*, 2013a), though much of this distribution is not within coastal catchments. The salt tolerance of many *Melaleuca* species allows for their distribution within the supratidal zone of coastal Australia (Salter *et al.*, 2007; Tran *et al.*, 2013b). Water salinity is a limiting factor to the range of water regimes tolerable by *Melaleuca*

(Salter *et al.*, 2007, 2010) Anthropogenic draining and clearing of many wetland ecosystems has influenced a significant decline in abundance and distribution of MPS (Bowkett and Kirkpatrick, 2003; Robinson *et al.*, 2006).

The supratidal MPS of tropical and sub-tropical Australia have been the subject of research interest in recent years. Adame *et al.* (2019) studied five palustrine *Melaleuca* wetlands in tropical Queensland determining their carbon storage capability. However, the temperate supratidal MPS, which span southern New South Wales to southern Western Australia are largely unstudied. *Melaleuca ericifolia*, *Melaleuca quinquenervia* and *Melaleuca lanceolata* are the major coastal species of *Melaleuca* along the coastlines of temperate Australia (Boon *et al.*, 2016). *M. ericifolia* dispersal mechanisms are unique in that - unlike most *Melaleuca* species, which use seeds in dispersion and reproduction to form a new individual plant - they are an extensively clonal species and produce physically independent ramets (Ladiges *et al.*, 1981). This process is potentially key in their success as coastal wetland species as it is a method that reduces the reproductive capability but increases the survivability and persistence of the species in otherwise unfavourable environmental conditions (Eskert, 2002; Ladiges *et al.*, 1981).

2.2.3 Changes in Wetland Distribution and Extent

Elevation and related conditions control the distribution and structure of vegetation in the coastal zone. This meaning that changes in vegetation composition and/or structure can be used to reflect other environmental changes. An example of vegetation structure can be observed in the poleward advancement of *Avicennia marina* into the saltmarsh communities of the south-east Australian wetlands (Saintilan *et al.*, 2014). Changes in temperature threshold has been theorised to be responsible for recent mangrove expansion due to extreme freeze events controlling the distribution of the cold-sensitive mangroves in the United States (Osland *et al.*, 2013; Osland *et al.*, 2017). In south-east Australia, studies have suggested SLR provokes change in surface elevation and distribution within a wetland ecosystem. As wetlands increase surface elevation through the accumulation of sediment, biomass, and soil water volume they may adjust to rising sea-level (Saintilan *et al.*, 2018). If the rate of vertical accretion is equal to SLR, the vegetation remains stable, otherwise a landwards regression of wetland vegetation occurs. In south-east Australia, saltmarshes typically have a lower capacity to build surface elevation compared to mangrove communities, leading to the encroachment of mangroves into saltmarsh as elevations between the two communities begin to level (Rogers *et al.*, 2005). Higher precipitation rates have also been linked to the mangrove encroaching into saltmarsh regions (Eslami-Andargoli *et al.*, 2010). Given these factors, a competitive advantage is given to mangrove communities over saltmarsh, which restricts their extent within the wetland complex in response to SLR, although this is dependent on whether the saltmarsh are able to migrate upslope (Saintilan *et al.*, 2018). In the event that sedimentation exceeds SLR and the estuary infills, wetland vegetation may

undergo a seaward shift, as the estuary morphology experiences increased vertical accretion and lateral progradation (Roy *et al.*, 2001).

Sedimentary records have been used to identify historic lateral shifts of coastal wetland vegetation, including both sea- and landward directions. Saintilan and Hashimoto (1999) observed mangroves encroaching into tidal saltmarsh along the Hawkesbury River, NSW, Australia. Within the underlying sediment, preserved mangrove roots were found indicating previous occupation of mangroves beneath the contemporary saltmarsh plains, with similar findings from (Kelleway *et al.*, 2017b). This demonstrates the shifts that occur between communities within the wetland over time as a result of changes in relative sea-level. Despite the dynamic nature of coastal wetlands, they have been shown to have the potential to persist in changing environments over hundreds to thousands of years. The *Posidonia oceanica* meadows of Portlligat Bay, Spain have remained stable for 5616 ± 46 Cal yr BP (Lo Iocano *et al.*, 2008). This corresponds to the beginnings of the highstand following the last glacial maximum (Lambeck and Chappell, 2001). For this to occur, the rate of sedimentation would have matched the rate of SLR with both rising at a rate of 1.1 m/kyr as sea-level sat 3-7 m below present-day level (Lambeck and Bard, 2000; Lo Iocano *et al.*, 2008). Rozaimi *et al.* (2016) study of *Posidonia australis* meadows in Oyster Harbour, Western Australia quantified the percentage organic matter within the subtidal wetland ($9.07 \pm 0.36\%$). The eutrophication-driven loss in seagrass distribution has resulted in the remineralisation of otherwise sequestered organic material. Under the assumption that all organic matter stored in the shallow sediments was remineralised, 37-41 Gg CO₂ was produced as a result. These findings further emphasise the importance of wetland ecosystems in the global carbon cycle.

Aerial photograph records have been used in south-east Australia to characterise and quantify vegetation shifts as far back 1930s. Saltmarsh decline and mangrove expansion has been heavily documented across Australia and has been observed across numerous estuaries (Saintilan and Williams, 1999b; Rogers *et al.*, 2005; Jupiter *et al.*, 2007). South-east Australian saltmarsh coverage has declined: 25% in Lake Macquarie (Winning, 1990); 67% in the Hunter Valley (Buckney, 1987; Williams *et al.*, 1999); 49% lost within the Minnamurra estuary (Chafer, 1998) ;and over 80% lost across Homebush Bay within the Paramatta River (Clarke and Benson, 2010). Historical aerial photography has also been used to observe changes to MPS (Williams, 1984; Bowman *et al.*, 2010). Bowman *et al.* (2010) found that coverage MPS in Kakadu Nation Park declined by 5% from 1964 to 2004 as a result of damage from feral ungulates and saltwater intrusions. In contrast to this, the mangrove communities of the Kakadu region have increased their distribution by 17% (Williamson *et al.*, 2011).

Focus has been placed on the intertidal and subtidal communities and how they respond to the pressures of SLR and other environmental factors, though there is limited research available on the response of the supratidal wetland forest. Invasive fauna capable of impacting the surrounding vegetation and soil present a potential threat to the distribution of

MPS. This is recognised by the dieback of MPS in Kakadu National Park. The alterations to the hydrology of the area have allowed tides to penetrate further inland increasing soil salinity, and thus affecting the health of MPS (Bowman *et al.*, 2010; Finlayson *et al.*, 1993). Currently, there is limited insight into the lateral changes that occur amongst the supratidal wetland forest, though there is a critical knowledge gap surrounding the vertical processes and the processes involved in building surface elevation.

2.3 Wetland Substrate Processes

2.3.1 Importance of Surface Elevation in Coastal Wetlands

A coastal wetland's ability to increase surface elevation in response to changing sea level is a key component in maintaining the stability of ecosystem structure and function (Baker *et al.*, 2009; Alongi, 2014; Woodroffe *et al.*, 2016). To remain stable, surface elevation must increase at a similar rate to the rate of rising sea-level (Kirwan and Megonigal, 2013; Morris *et al.*, 2016; Reed, 1995). Changes to surface elevation are a function of surface and belowground processes. The vertical accretion of sediment fills the available accommodation space of the wetland, raising surface elevation (Rogers *et al.*, 2019b). Autocompaction of sediments, decomposition of stored organic material, and erosion can reduce surface elevation by decreasing sediment volume, thereby raising relative sea-level (RSL) (Morris *et al.*, 2016). Isostatic and tectonic processes can also cause the subsidence of wetlands over an extended period of time, lowering their absolute elevation, resulting in a rise in RSL. Groundwater is considered to have minor impact on the surface elevation of mangroves and saltmarsh at a diurnal scale attributed to evapotranspiration (3 mm variation between spring neap high tide and low tide) (Rogers and Saintilan, 2008). The main variation caused by changes in groundwater comes as a result of the Southern Oscillation Index (SOI). This accounts for 80% of the variability as observed by Rogers and Saintilan (2008) with changes of 4mm up to 25 mm variation between drought and pre-drought conditions. It is not yet known to what extent variations in groundwater may influence surface elevation dynamics in supratidal wetlands. Hydrodynamic energy (including the role of tides) influences vertical and lateral accretion of sediment, however there are components which can reduce the surface elevation of a wetland. Eustatic SLR can also result in a rise in RSL. These processes can reverse the otherwise dominant vertical and lateral evolution of wetlands.

2.3.2 Sediment Accretion in Coastal Wetlands

Within wetlands there are two primary origins of sediment influx: autochthonous material, internally derived from predominantly plant productivity within the wetland ecosystem; and, allochthonous materials externally derived, which are primarily mineral based with limited

organic components (French, 2006; Baker *et al.*, 2009; Saintilan *et al.*, 2013; Krauss *et al.*, 2014). In order to understand the long-term evolution of coastal wetlands the contributions of organogenic and minerogenic processes will be reviewed here.

2.3.2.1 Contribution of Mineral Matter to Wetland Substrates

Mineral sediments are deposited when material introduced by tidal activity settles out of the water column and onto the surface (Marion *et al.*, 2009). Areas that experience increased inundation depth (i.e. locations lower in the tidal frame) typically have a higher depositional rate than those that sit higher in the tidal frame (Kirwan and Megonigal, 2013; Morris *et al.*, 2016) (Figure 2.5). For example, in temperate Australia, mangrove forests typically sit lower in the tidal frame than adjacent saltmarsh and are therefore subject to higher rates of mineral accumulation. Calcareous organisms are able to build the mineral components of wetlands substrates in the form of biogenically derived carbonate sediments (Wang and Li, 2011).

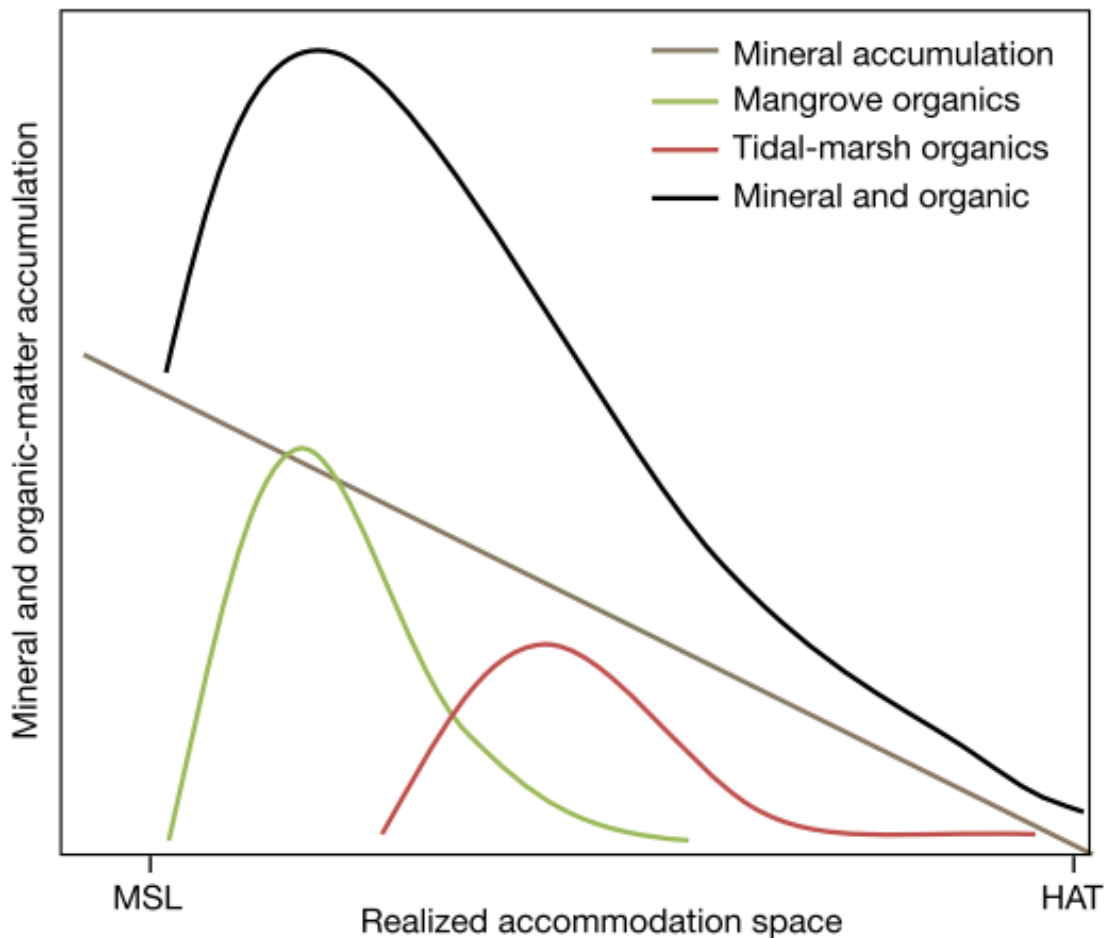


Figure 2.5: Conceptual links between the accumulation of mineral and organic matter, and realised accommodation space. Two dimensional model of sediment characteristics representing the accommodation space of a three dimensional wetland. Mineral sedimentation was conceptualised to have a positive linear relationship with accommodation space, though may diminish exponentially or in a polynomial manner with decreasing accommodation space. Accommodation space changes as a result of changes in relative sea-level, mineral and organic sediment accumulation and autocompaction. Sedimentation is variable across sites according to the availability of mineral and organic sediments, and below ground root productivity of surrounding vegetation. Source: Rogers *et al.* (2019a)

Vegetation structure also plays a role in the sedimentation rates of mineral matter (Wolanski *et al.*, 1992). Sediment is deposited at a higher rate as the energy of the water is lowered by vegetation. Mangrove pneumatophores have been found to be successful and trapping sediment with a preference to accumulate clay minerals (Furukawa *et al.*, 1997). Once mineral matter is deposited, unless eroded, it remains stable and does not break down in the substrate. The sediment volume is still subjective to change. Root development can increase sediment volume, where auto compaction of sediment is responsible for a reduction in volume (Morris *et al.*, 2016).

2.3.2.2 Contribution of Organic Matter to Wetland Substrates

Coastal wetland vegetation's high net primary production (NPP) is a result of photosynthetic processes converting inorganic CO₂ from the atmosphere to provide sustenance for plant growth (Nixon, 1980; Alongi, 2002; Dise, 2009; Del Grosso *et al.*, 2010). The NPP of wetland ecosystems are comparable to the productivity of the most efficient terrestrial ecosystems (Alongi, 2009; Alongi, 2014). This can be attributed to their efficient nutrient derivation and water usage under saline conditions, which increase the production of organic material (Dise, 2009). This organic matter can be added to the belowground system through root and rhizome growth or accumulated on the surface through leaf litter (Finlayson *et al.*, 1993; Morris *et al.*, 2016).

Climatic conditions, salinity levels and nutrient availability control the NPP of coastal wetlands, with hydrological characteristics and temperature dictating the production of organic matter (Kirk, 2004; Del Grosso *et al.*, 2010; McLeod *et al.*, 2011). Tidal inundation duration and frequency have the capability to shift NPP, with frequency shown to play a more substantial role in controlling this variation (Kirk, 2004). NPP was found to be at its maximum when tidal inundation is at an intermediate level, showing diminishing results with extreme inundation. The reasoning for this is explained by limitations placed on aerobic respiration through periodic inundation restricting oxygen availability (Kirk, 2004). An increasing temperature will result in NPP to increase (Del Grosso *et al.*, 2010; McLeod *et al.*, 2011), while also causing an increase in aerobic and anaerobic respiration which lower the preservation of the stored carbon (Chmura *et al.*, 2003; Dise, 2009; Kirwan and Blum, 2011).

Contrary to the stability of mineral matter, organic matter is subject to the physical and biochemical processes involved in the organic decomposition (Zhao *et al.*, 2015). The aerobic decomposition of litter continues the cycling of N and P within soils, assisting the productivity of wetland vegetation (Zhao *et al.*, 2015). The microorganisms involved in the breakdown of organic matter rely on aerobic conditions to decompose organic matter (Kirk, 2004). As tidal inundation controls substrate saturation, it also influences the rate at which microbes are able to remineralise organic matter (Morris *et al.*, 2016; Howard *et al.*, 2014). Accommodation space and position within the tidal frame can impact the longevity of organic matter stored in sediment. As available accommodation space is depleted and the wetland surface sits higher in the tidal frame, the soil will experience increased exposure to oxygen, encouraging decomposition (Rogers *et al.*, 2019b). Due to the numerous environmental factors controlling the production and preservation of organic matter, carbon stocks vary according to geomorphic settings (Kelleway *et al.*, 2016a).

2.3.3 Organic Matter Sequestration in Coastal Wetlands

The carbon cycling of vegetated areas plays a significant role within the global carbon cycle (Janzen, 2004). Forest and wetland communities store a large proportion of the Earth's above- and belowground carbon stores, with forested areas storing ~80% of the terrestrial aboveground carbon and ~40% of all belowground terrestrial carbon (Dixon *et al.*, 1994; Trettin and Jurgensen, 2002). Wetlands contribute between 18-30% of the total global belowground carbon despite covering 2-3% of the Earth's terrestrial surface (Trettin and Jurgensen, 2002). Coastal wetlands have exceedingly high quantities of carbon sequestered with respect to the extent of their global distribution and compared to that of terrestrial ecosystems (Dise, 2009; Howard *et al.*, 2014; McLeod *et al.*, 2011). The high potential of coastal wetlands to store carbon can be attributed to limited oxygen availability due the periodic inundation of coastal wetlands. The aerobic limitations along with the high NPP associated with wetland ecosystems allow for coastal wetlands to store significant amounts of carbon. This combined with their high NPP are the reason coastal wetlands are highly effective carbon stores. Their affinity for carbon sequestration has led to increased recognition surrounding the importance of blue carbon ecosystems within the global carbon cycle.

3 Methods

3.1 Study Setting

Corner Inlet is an ocean embayment estuary located approximately 200 km south-east of Melbourne in the South Gippsland region of Victoria, Australia (Figure 3.1). It is the southern-most marine embayment and intertidal system of mainland Australia. The estuary has an area of 600 km² and relatively small catchment area of 2300 km², which stretches from Woodside to Wilson Promontory (Figure 3.2; Dickson *et al.*, 2013). Corner Inlet is positioned within the temperate warm summer – cool winter climatic zone (BOM, 2020). It has a mean annual precipitation of 1055.7 mm and an average maximum temperature of 16.4°C (BOM, 2020). Corner Inlet’s tides are semi-diurnal with a tidal range of 2.9 m (Gilmour, 2014).

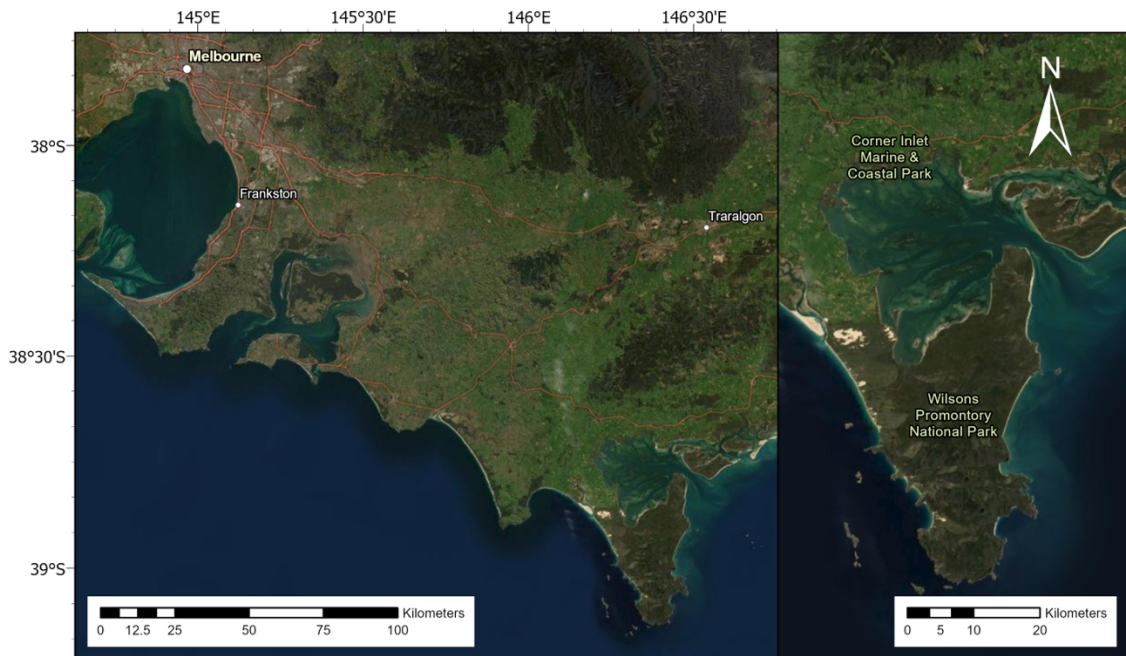


Figure 3.1: Location map of Corner Inlet.

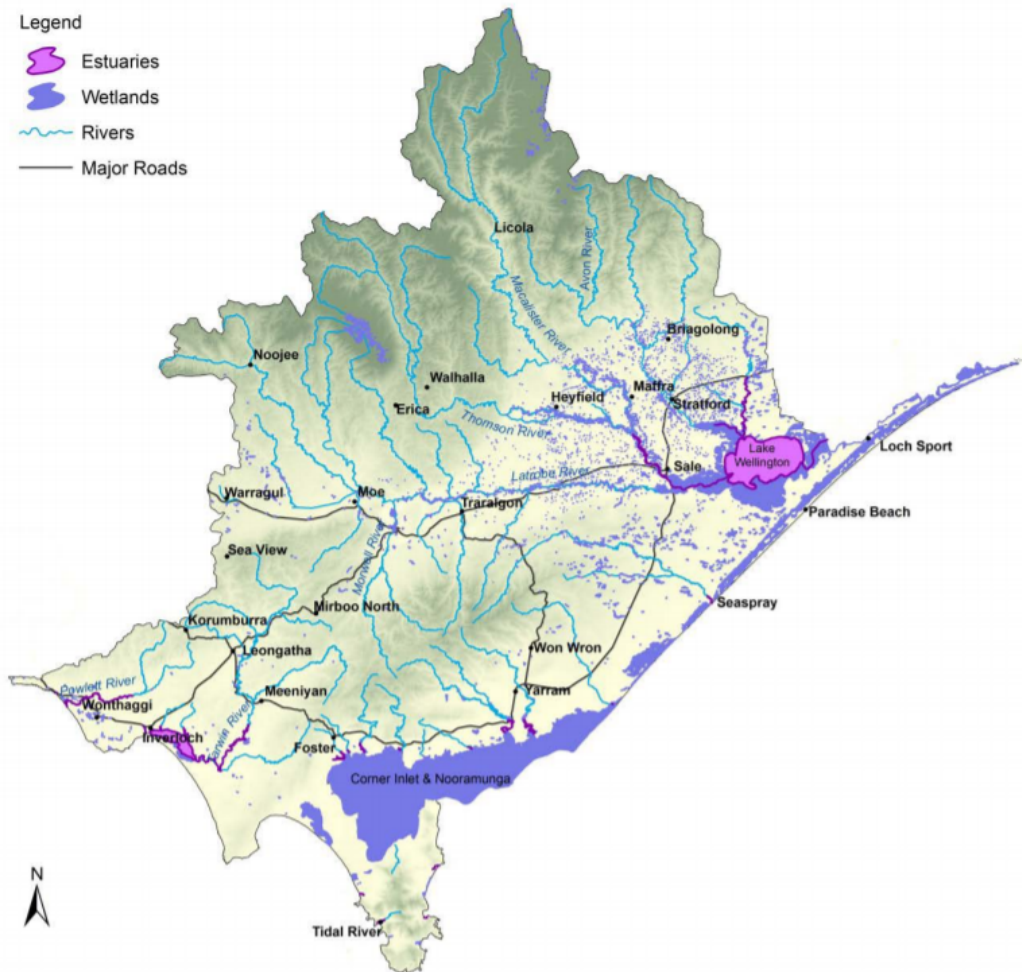


Figure 3.2: Catchment area of Corner Inlet. Source: West Gippsland Catchment Management Authority (2014)

3.1.1 Geomorphology and Environment

Corner Inlet is positioned south of the Strzelecki Ranges, which provide the primary higher catchment for the coastal region (Figure 3.2; Figure 3.3; Dickson *et al.*, 2013). These ranges reach elevations of 600-700 m and drain in a north-west and south-east direction. The south-east drainage basin connects and transports sediment to Corner Inlet via the Agnes, Albert, Franklin and Tarra Rivers. The Lower Cretaceous Strzelecki Group forms the basis of the range. This group consists of thick layers fluvial-derived sandstone, siltstone conglomerates, and minor coal beds. The granite intrusions that form the foundations of Wilsons Promontory connect to the mainland through dune, wetland and sand deposits overlying a basal sandstone and siltstone.

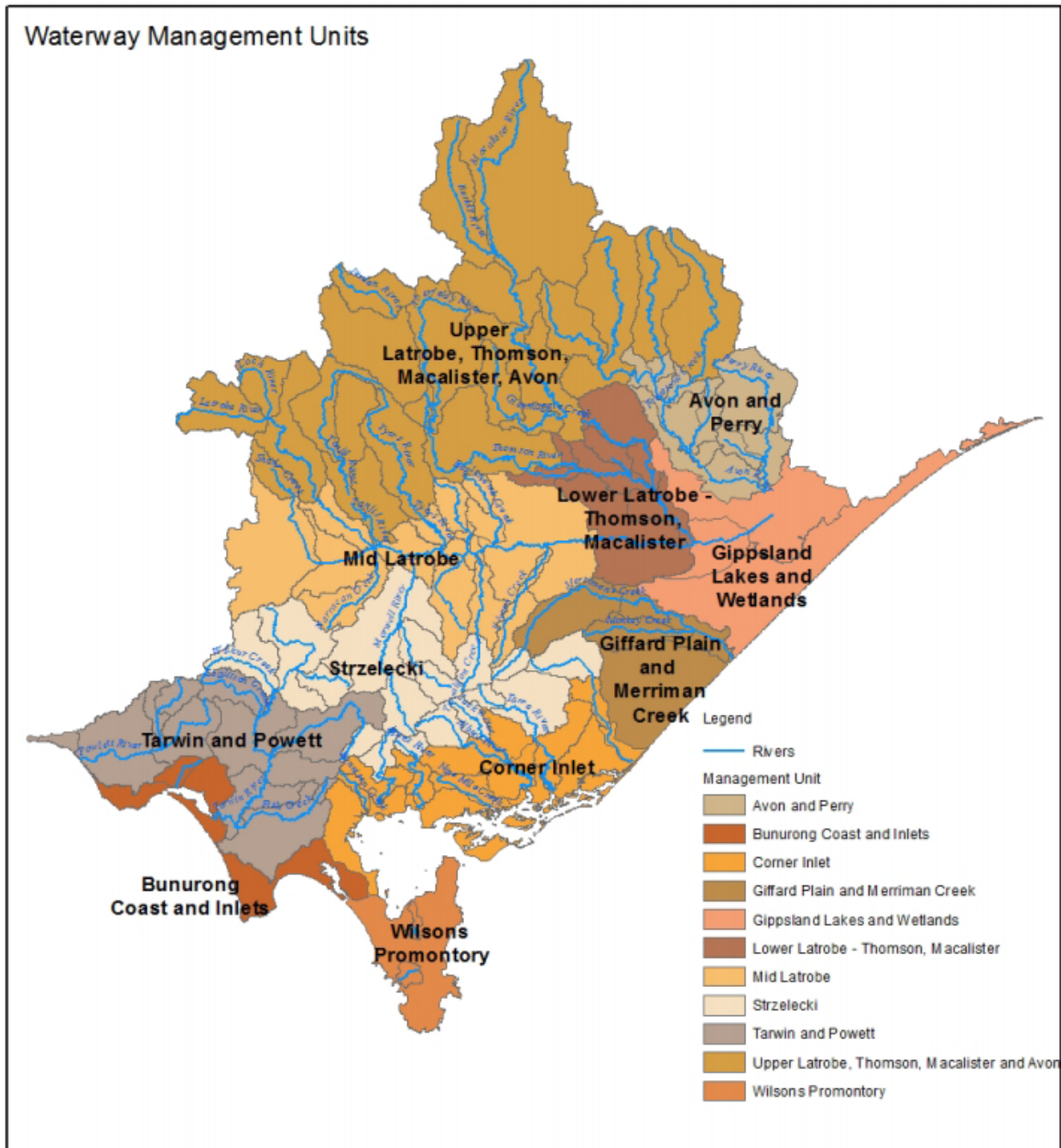


Figure 3.3: Map of the geology of the Corner Inlet catchment area. Source: West Gippsland Catchment Management Authority (2014)

The mainland surrounding Corner Inlet consists predominately of relatively flat depositional terrace (1.0 – 1.7 m AHD). These encompassing terraces formed in the Holocene during a period of higher RSL (Bird, 1993). Behind the depositional terrace are steeply rising bluffs reaching above 3 to 5 m AHD. These bluffs formed as the coastlines of a previously higher sea-level (Bird, 1993).

Corner Inlet’s wetland complex is composed of subtidal aquatic beds and sandy shores, intertidal flats, intertidal mangrove forests and saltmarshes, through to the supratidal MPS and herbaceous wetlands (Figure 3.4). Dieback of the supratidal MPS can be observed along the wetlands of Corner Inlet. This along with the landwards encroachment of the

mangrove forest suggest that the wetlands of the area are currently shifting landwards. The cool wet climate and high tidal variation of Corner Inlet, along with the evidence of shifting vegetation communities through field observations makes these wetlands a point of interest in understanding the processes and driving forces in supratidal MPS evolution and stability/dynamism.

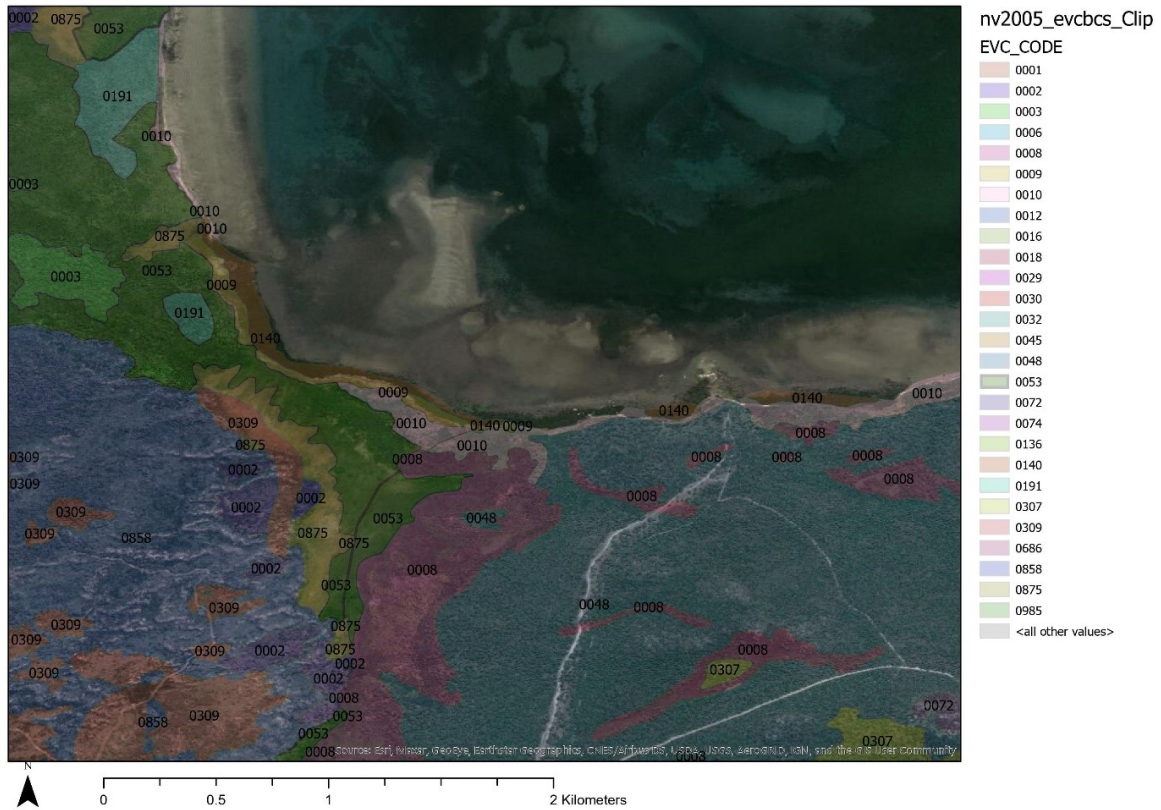


Figure 3.4: Vegetation community mapping of Corner Inlet. Key codes: 0140 (Mangrove shrubland); 0009 (Coastal saltmarsh aggregate); 0010 (Estuarine wetlands); 0053 (Swamp scrub); 0875 (Blocked coastal stream swamp); 0008 (Wet heathland); 0048 (Unspecified). Source: Victoria. Department of Sustainability and Environment. (2012)

Corner Inlet is listed as a Wetland of International Importance under the Ramsar treaty and is one of 65 in Australia. The treaty site encompasses Corner Inlet and Nooramunga. The area in which the treaty covers is locked at its time of listing and changes to the extent of the wetland are not considered. The Ramsar treaty is also limited to the boundaries of the intertidal zone and subtidal, excluding the MPS. The West Gippsland Catchment Manage Authority also developed a Water Quality Improvement Plan for the Corner Inlet catchment. This plan aims to reduce the sediment and nutrient loads to the surrounding waterways, estuary, and marine environments of the Corner Inlet Ramsar Site (Dickson *et al.*, 2013)

3.1.2 Water Quality

The surface water salinity of Corner Inlet is usually equal to that of ocean-water, with heightened periods of salinity during summer due to increased evaporation (Dickson *et al.*, 2013). Heavy metal and pesticides concentrations within the waterways of Corner Inlet have not been shown to be a significant issue. P (Phosphate) levels are low within the estuary, however N (ammonium, nitrate and nitrite) concentrations were significant with some sites 20 times the guidelines for estuary proposed by the State Environment and Protection Policy (SEPP). Silt and clay deposition occurs primarily in the upper reaches of Corner Inlet's tributaries prior to entering the embayment. The fine sediments that do enter the embayment during periods of high flow do not settle in the main channel or sandflats, and are primarily deposited in the backwater areas of the embayment.

3.1.3 Land-use in the Catchment Area

The dominant land-use activity in Corner Inlet's catchment area consists of agricultural practices (50% of total land-use) (Figure 3.5; Dickson *et al.*, 2013). This is predominately dryland grazing (cattle and sheep) and dairying comprising approximately 40% and 10% of total land-use respectively. Much of the surrounding agricultural practice is adjacent to the tributary waterways of Corner Inlet. Forestry land-use covers approximately 21% of the catchment area, with 3% of forests logged each year. Corner Inlet is included within the 28% of protected areas covered by Parks and Reserves. Urbanisation within the catchment area is limited to less than 1% of the total catchment area. Urban expansion is estimated to increase to 2.3% coverage over the next 30 years.

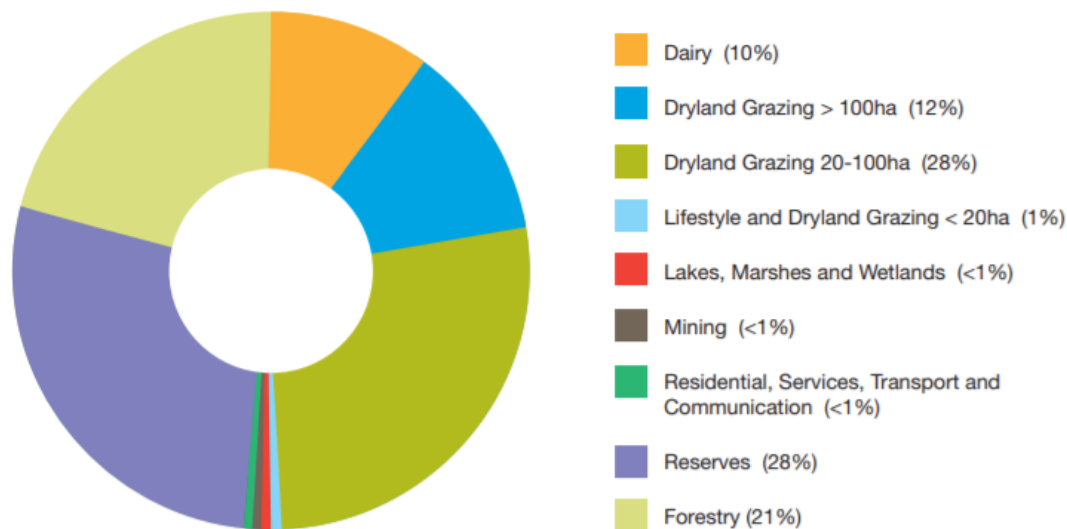


Figure 3.5: Proportion of each land-use category in the Corner Inlet catchment. Source: Dickson *et al.* (2013)

3.2 Experimental Design

This study was divided into first, a stratigraphic analysis and second, a geospatial analysis. The stratigraphic analysis involved collection of sediment cores and deployment of water level and salinity loggers along a transect (Figure 3.6). The transect was divided into four sites: Mangrove; Saltmarsh; a *Melaleuca* site near the saltmarsh (*Melaleuca* 1); and a second *Melaleuca* site (*Melaleuca* 2) closer the inland herbaceous vegetation (Figure 3.7). Two *Melaleuca* sites were selected to assess any variation that occurs between forests closer to the coastal zone to those further inland. The cores collected underwent laboratory analyses to determine the stratigraphy, bulk density, organic matter composition, and grain size. This provided insight into the long-term changes that are occurring across the wetland and the role of organic material in MPS. The geospatial component involved a decadal time series analysis of the wetland vegetation over the last 63 years to develop an understanding of the short-term variation occurring across the wetland. With these combined approaches, long- and short-term changes can be used to reconstruct the historic vegetation shift of the study site.

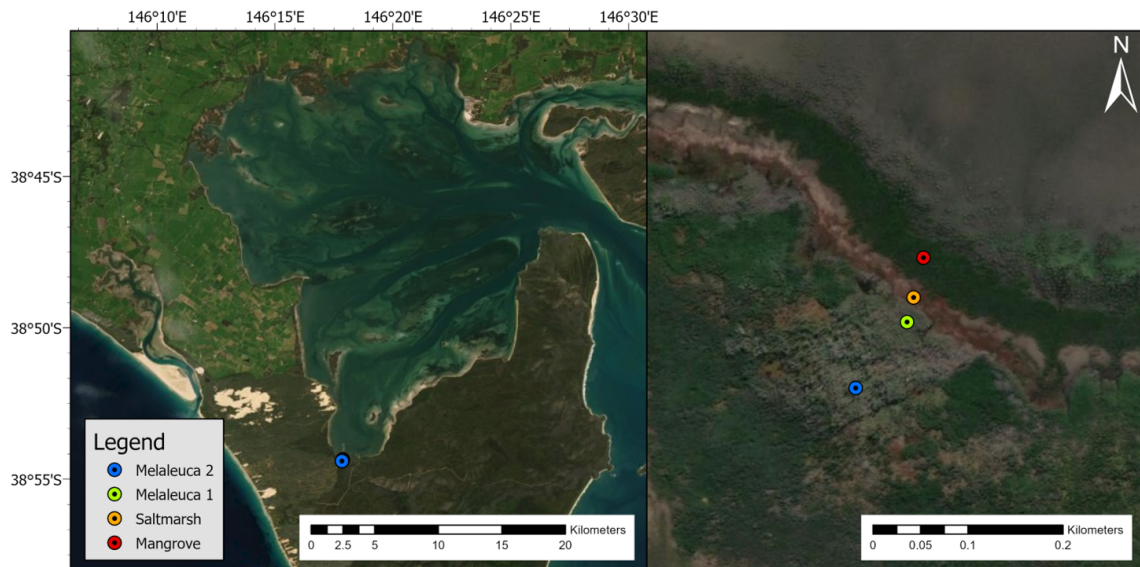


Figure 3.6: Core locations along the transect. Red - mangrove, orange - saltmarsh, green - *Melaleuca 1*, blue - *Melaleuca 2*.

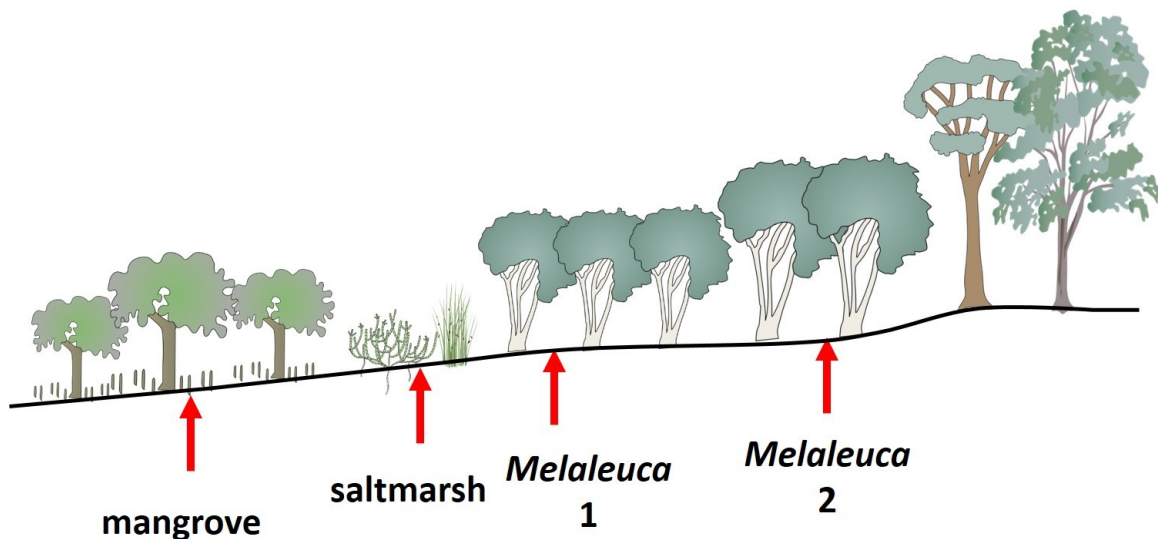


Figure 3.7: Conceptual model of the shifting vegetation community within the intertidal-supratidal wetland complex. The transect was broken up into four sites: mangrove; saltmarsh; *Melaleuca 1*; and *Melaleuca 2*. Each zone is demonstrated to be positioned higher in elevation to the next (from mangrove to *Melaleuca 2*), resulting in a declining marine influence.

3.3 Stratigraphic Analyses

3.3.1 Coring and Water Chemistry

One core was taken at each site: mangrove (MAN), saltmarsh (SM), *Melaleuca 1* (MEL1), and *Melaleuca 2* (MEL2). To take the sediment cores, a 3 m aluminium tube with an internal

diameter of 74 mm was forced into the ground using a sledgehammer. To prevent roots from inhibiting the coring, the edges of each tube were sharpened in order to cut through larger roots. A brace was then placed around the core for extraction, upon which the core was immediately capped to prevent sediment loss. Cores were then kept below 4°C awaiting further analyses. The collection of cores follows the methodology of Kelleway *et al.*, 2016a. Coring of this nature causes compaction of the sediment. To counteract this, a compaction correction factor must be applied down core for any further sampling.

The equation for the to determine the compaction correction factor is:

$$C = \frac{l_1}{l_2}$$

Where:

C = Compaction correction factor

l_1 = Compacted length

l_2 = True length

Cores were split in half along their length in the laboratory to undergo stratigraphic logging, macrofossil collection, bulk density (BD) and loss on ignition (LOI) analysis, and grain size analysis. Compaction correction factors were used to determine the relationships between the ‘compacted length’ and ‘true length’. The length of soil profile within the tube was divided by the length of the core barrel taken to provide a linear compaction correction factor across the core. The correction factor can then be used to find the required depth to be sectioned for each core.

Soil moisture measurements were collected using a 1 m Russian peat core to avoid soil compaction and the addition of water. The surface 20 cm was collected and sectioned into 1 cm samples. Wet samples were weighed and placed in an oven at 60°C to be dried. Dried samples were then weighed, and the water content was determined for the near surface soil.

The equation for the to determine the moisture content is:

$$W\% = \frac{(m_t - m_d)}{m_t} \times 100\%$$

Where:

$W\%$ = Percentage moisture content

m_t = mass of undried sub-sample

m_d = mass of dried sub-sample

Water level and salinity logging was undertaken to understand the role of ground water and surface tidal inundation across the study site. Single ground water standpipes were installed at each core location. Within each of the standpipes a continuous water level logger was installed, and salinity level loggers were installed at each of the MPS sites. As a result of COVID-19 restrictions, collection of this data was prevented and thus data is limited to a single point in time. A Trimble Real-Time Kinematic Global Positioning System (RTK-GPS; horizontal error = 8 mm; vertical error = 15 mm) was used to survey the study transect. Three replicate coordinates were taken at each core and along the transect location. Elevation of each site were taken with respect to the Australian Height Datum (AHD), where 0 m elevation is the approximate MSL of Australia.

3.3.2 Stratigraphic Logging and Macrofossil

Cores were inspected to determine the distribution of sedimentary strata, roots and macrofossils throughout the depth of each core. Strata were separated through distinguishing characteristics including: grain size; colouration; quantity of preserved organic matter; and evidence of inorganic carbon.

Macrofossils are an indicator for the prevailing vegetation at the time. Significant macrofossils (seeds, roots, rhizomes etc) exposed down core were extracted in an initial inspection to be identified using microscopy. After the remaining stratigraphic analyses were completed a secondary thorough inspection was undertaken using the remnants of the core. The true depths of each macrofossil were recorded, identified and photographed using a light microscope. To identify the samples, available material was compiled to assess possible origins for the specimens.

3.3.3 Bulk Density and Loss-On-Ignition Analysis

BD and LOI provide information on the organic and mineral contents of the strata. Johnson et al., (2007) found significant variation within the surface 20-30 cm within wetlands sediments. A higher sensitivity was used for the surface 30 cm to capture this variation, with samples taken every 2 cm. Beyond 30 cm depth, 2 cm samples were taken in 5cm increments. Each sample was weighed in pre-weighed aluminium trays and dried at 60°C. Samples were weighed again after 24 hours to determine water loss and were then returned to the oven. This process was repeated until samples showed no significant change over 24 hours of drying.

The equation for the to determine the bulk density is:

$$\rho = \frac{g}{v}$$

Where:

ρ = bulk density

g = weight of dry sample

v = compaction-corrected volume of sub-sample from aluminium tube

The dried samples were homogenised in a mortar and pestle until a fine powder was achieved and quartz grains were smaller than 0.5 mm. In a LOI analysis, 2-4 g is considered optimal to prevent an under- or overestimated result (Heiri *et al.*, 2001). 2 g of the homogenised samples were then dried at 105°C for 24 hours to remove any remaining moisture before being analytically weighed. Samples were placed into a muffle furnace at 550°C for four hours to remove all organic matter (Heiri *et al.*, 2001). Samples were then weighed post ignition to record a change in weight.

3.3.4 Micro-XRF

The core taken from the *Melaleuca* 1 site (MEL1) underwent a high-resolution logging using micro-XRF (ITRAX Core Scanner) to inform the environmental reconstruction of the site. The core was scanned using a molybdenum tube set at 30 kV and 55 mA, with a dwell time of 10 s and step size of 1 mm. Three environmental proxies were selected on the basis of their suitability in marine or estuarine sediments: Ca/Rb, Zr/Rb, and Br.

Ca/Rb was used as a proxy for sediment origin, with Ca-rich sediment having a marine provenance as opposed to the low Ca sediments of terrigenous source (West *et al.*, 2004; Rothwell *et al.*, 2006; Wolters *et al.*, 2010; Hughes *et al.*, 2010). Ca has a predominantly marine origin and was therefore selected as a marker for the marine influence within the core (West *et al.*, 2004; Wolters *et al.*, 2010). Similar rationale was used in assigning Rb as the terrestrial proxy for this ratio, as it is largely associated with sediments of terrigenous origins (Rothwell *et al.*, 2006; Hughes *et al.*, 2010). Zr/Rb was selected as a proxy for grain-size as Zr is found within zircon crystals which do not break down into smaller sediments such as clays, as opposed to Rb which easily breaks down into clays (Hughes *et al.*, 2010). Br was used as a proxy for the productivity of wetland vegetation with higher values equating to a greater influence from the surrounding vegetation (Ziegler *et al.*, 2009).

3.3.5 Grain Size

Grain size acts as an indicator for the energy of an environment at time of deposition. Organic matter is capable of being any size based of the source material structure and its degree of humification, providing false readings during the analysis. To counteract this, a

30% hydrogen peroxide (H₂O₂) was added to samples until there was no visible reaction taking place, this time ranged from 2 to 14 days based of the organic content (Gray *et al.*, 2010). The samples were dried and weighed, before removing sediments with a grain size >2 mm through wet sieving. The samples were disaggregated using a sonicator for 2 minutes before processing. The samples were processes using the Malvern Mastersizer-X which uses laser diffraction to count and sort sediment based on grain size. The Mastersizer produces three values, along with an average of both., with the average being used to show the grain size of selected strata downcore. The removed sediment was dried and weighed to assess the proportion of sediments not measured by the Mastersizer.

3.4 Photogrammetry

An assessment of aerial photography spanning from the 1950s to present was produced in this study (Table 3.1). This was used compare the lateral changes of wetland communities over a short-term decadal period. Georectification and interpretation were undertaken at a resolution of 1:1000.

Table 3.1: Summary of aerial photography used for the time series analysis. Refer to Appendix F for images used.

| Year | Image Type | Pixel Size (cm ²) | Image Description | Source |
|------|-----------------|-------------------------------|---|----------------------|
| 1957 | Black and White | 2025 | Average quality, boundaries not well defined | Victorian Government |
| 1969 | Colour (RGB) | 2025 | Average quality, boundary between saltmarsh and mangrove not well defined | Victorian Government |
| 1978 | Black and White | 225 | Good quality, boundary between saltmarsh and mangrove not well defined | Victorian Government |
| 1983 | Colour (RGB) | 225 | Good quality, clear boundaries | Victorian Government |
| 1987 | Colour (RGB) | 900 | Good quality, boundary between saltmarsh and mangrove not well defined | Victorian Government |
| 2010 | Colour (RGB) | 2500 | Average quality, colouration made vegetation boundaries difficult to distinguish, juvenile mangroves blended with dark sections | Google Earth |
| 2020 | Colour (RGB) | 3600 | Poor quality, grainy, saltmarsh boundary unclear | Google Earth |

3.4.1 Spatial Referencing

Historic aerial photography was imported into ArcGIS 10.7.1. The images were georectified to the present-day imagery with a minimum of 15 ground control points (GCPs) selected across each site. GCPs included granite outcrops and significant mangrove canopies, and were focused around the area of interest. A second order transformation was used across all imagery and a root mean square (RMS) error from the georectified images was assessed and recorded. Georectification was considered inaccurate if the RMS error value was greater than 0.1.

3.4.2 Time Series Analysis

An area covering the south-west corner of the wetlands through to Millers Landing was selected for the analyses as a result of the extent of available imagery (hereafter referred to as whole embayment). An approximately 100 m wide boundary encompassing transect

was selected alongside this for a localised assessment around the coring locations. Images were analysed in reverse sequential order from present day back to 1957. Boundaries were devised by digitising polylines across visually interpreted vegetation boundaries. These boundaries were classified into six regions: mangrove seaward edge; mangrove landward edge; saltmarsh seaward edge; intertidal landward edge; *Melaleuca* seaward edge; and *Melaleuca* landward edge. These regions were assessed based on the changes in colour, tone, and texture with respect to the modern image coupled with field reconnaissance. Polygons were created around four areas to assess the changes in area of the wetlands. These areas included: mangrove; saltmarsh; bare ground; *Melaleuca*. This was achieved through tracing the polylines developed to polygons with a defined area. Mangrove and *Melaleuca* area were determined by their seaward and landward extents. Bare ground was designated as the barren area between vegetation communities and saltmarsh was determined using the saltmarsh seaward edge and intertidal landward edge. A 2010 assessment of *Melaleuca* in Corner Inlet was excluded due to the lack of clarity between vegetation.

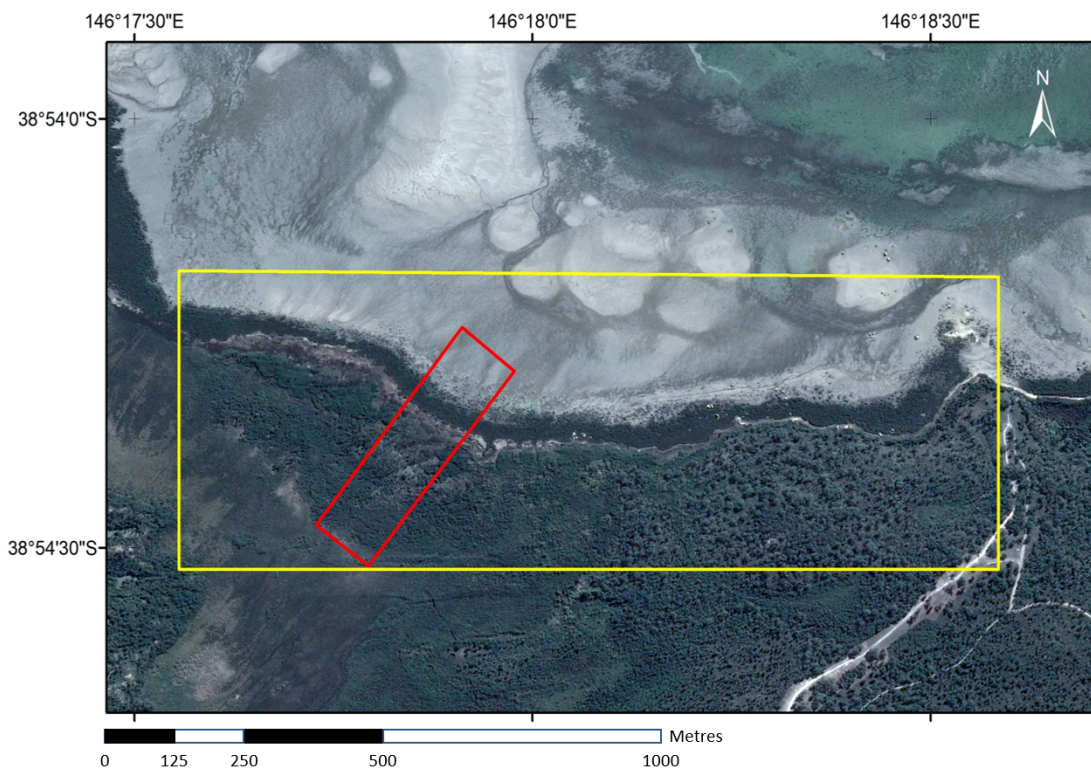


Figure 3.8: Map of Corner Inlet spatial analysis extent. The analysis of the intertidal-supratidal wetland complex was separated into two sections. Yellow: Area extent of the whole embayment analysis. Red: Area extent of the transect analysis.

4 Results

4.1 Stratigraphic Analysis

4.1.1 Field Measurements

The salinity across each cores declines in a landwards directions with MAN having the highest salinity at 32.9 ppt and MEL2 with the lowest at 3.03 ppt (Table 4.1). Water table levels show alternating depths from low (MAN and MEL1) to high (SM and MEL2) moving landwards. Changes in ground cover vegetation were observed across each site, including amongst the two MPS sites, with the ground cover vegetation of MEL2 consisting of more terrestrial species.

Table 4.1: Core ID, location, vegetation, core measurements, organic matter data, groundwater salinity and water table depth (collection date)

| Site | Mangrove | Saltmarsh | <i>Melaleuca</i> 1 | <i>Melaleuca</i> 2 |
|-----------------------------------|------------------------|--|-----------------------------|--|
| Core ID | MAN | SM | MEL1 | MEL2 |
| Latitude | -38.905771 | -38.906074 | -38.906257 | -38.906730 |
| Longitude | 146.297979 | 146.297858 | 146.297803 | 146.297326 |
| Vegetation (Tree) | <i>Avicennia maina</i> | N/A | <i>Melaleuca ericifolia</i> | <i>Melaleuca ericifolia</i> |
| Vegetation (Ground Cover) | N/A | <i>Selliera radicans</i> , <i>Samolus repens</i> , <i>Sarcocornia spp.</i> , <i>Triglochin striatum</i> | <i>Selliera radicans</i> | Fresh to brackish water herbaceous vegetation, grasses |
| Core Length (m) | 2.17 | 2.54 | 2.61 | 2.52 |
| Compaction Correction Factors | 0.77 | 0.78 | 0.77 | 0.65 |
| Surface Organic Horizon Depth (m) | 0.35 | 0.45 | 0.65 | 0.25 |
| Salinity (ppt) | 32.9 | 23.4 | 17.63 | 3.03 |
| Water Table (cm below surface) | 3 | 20 | 9 | 32 |

4.1.2 Mangroves

MAN is characterised by organic matter concentrations <10% throughout the profile, though variation in organic matter does occur at a lower scale (Figure 4.1). There are three primary peaks in the organic matter profile begin with the surface organic horizon. The surface 0.35 m correlates to MAN-A which is characterised by the fine silts and clays of MAN-A with fine roots found throughout, and MAN-B where contribution of sands increase coinciding with a reduction in density of fine roots. Organic matter in these layers range from 2.1-8.9% and gradually decrease with depth. The grain size of MAN surface sediments is a mix of sand and finer sediments (Refer to Appendix E). The coarser profile continues through MAN-C where organic matter increases to 5.6% with fine root material found throughout this unit. The grain size of MAN-C fines downwards for 3 cm before returning to predominately silt and clay. Organic matter gradually decreases to 1.7% until reaching the carbonate heavy MAN-D. The organic matter peak of MAN-E appears more continuous than previous peaks, maintaining a range of 3.1-5.8% across the layer. The gradual diminish of organic matter begins in MAN-F and continues through the remaining core.

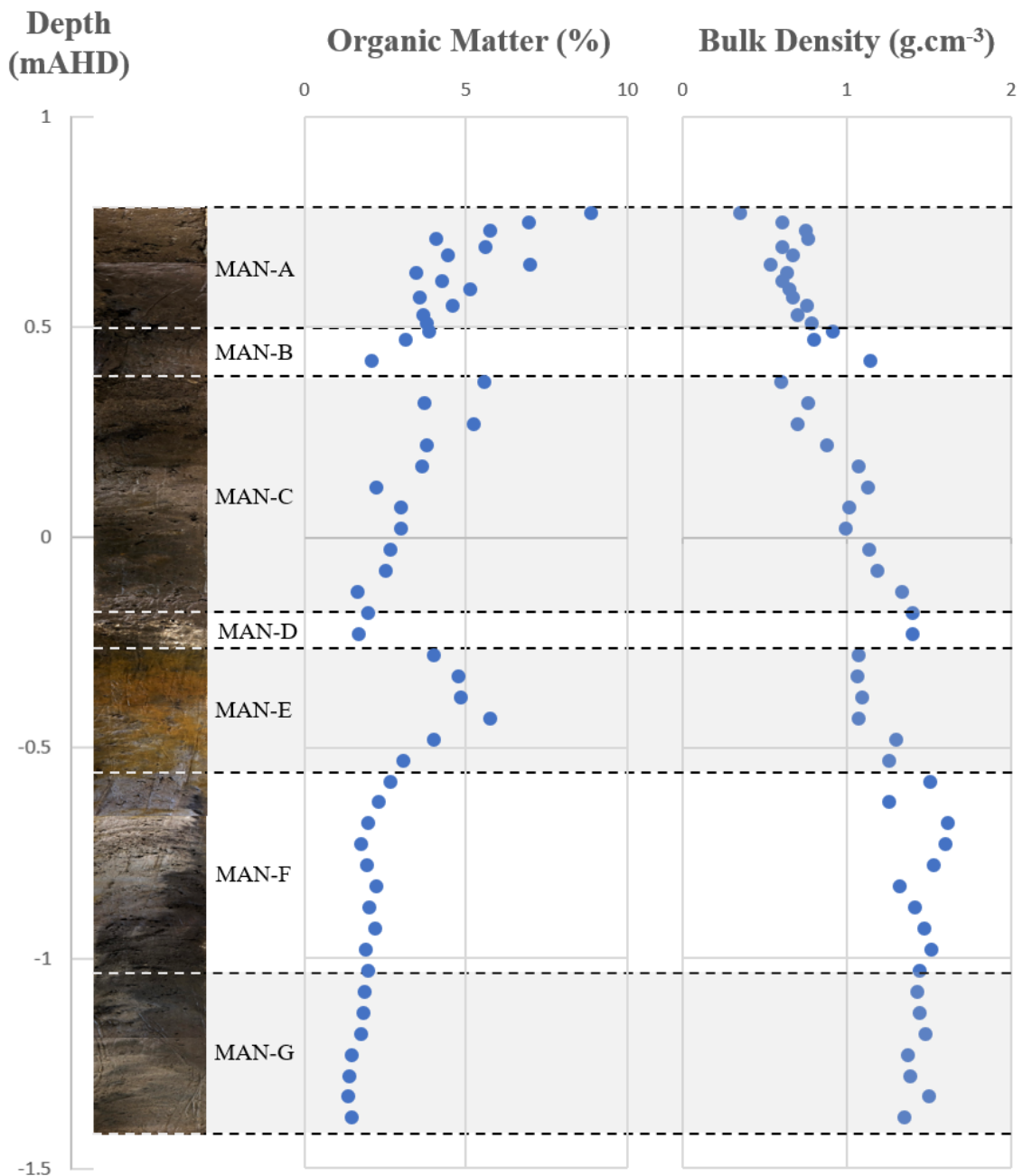


Figure 4.1: Core photo, stratigraphic units, percentage organic matter and bulk density (left to right) of the Mangrove core (MAN). 0 m AHD is approximately equivalent to mean sea level.

4.1.3 Saltmarsh

SM displays an organic-rich surface horizon comprising of ~20-60% organic material in the initial 0.45 m of the core (SM-A to SM-E). The grain size of MAN surface sediments consists predominately finer sediments (Refer to Appendix E). Organic matter sharply changes between SM-A to SM-C below which there is a steady decline from SM-D. Consistent presences of fine to coarse root material and very fine dark brown sediments

correlates to this high in surface organics. SM-F is characterised by its shift to coarse sediments with a dark grey colouration. This unit's low density of root preservation in this layer, coincides with the stable period of low organic matter (~2-3%). Organic matter increases in SM-G ranging from 4-6% following the return of finer sediments, well preserved roots material. This layer is mottled with yellowish brown colouration, which correlates to a similar MAN-E within the MAN core. Organic matter declines moving through the profile into the light coloured, sand dominated SM-H.

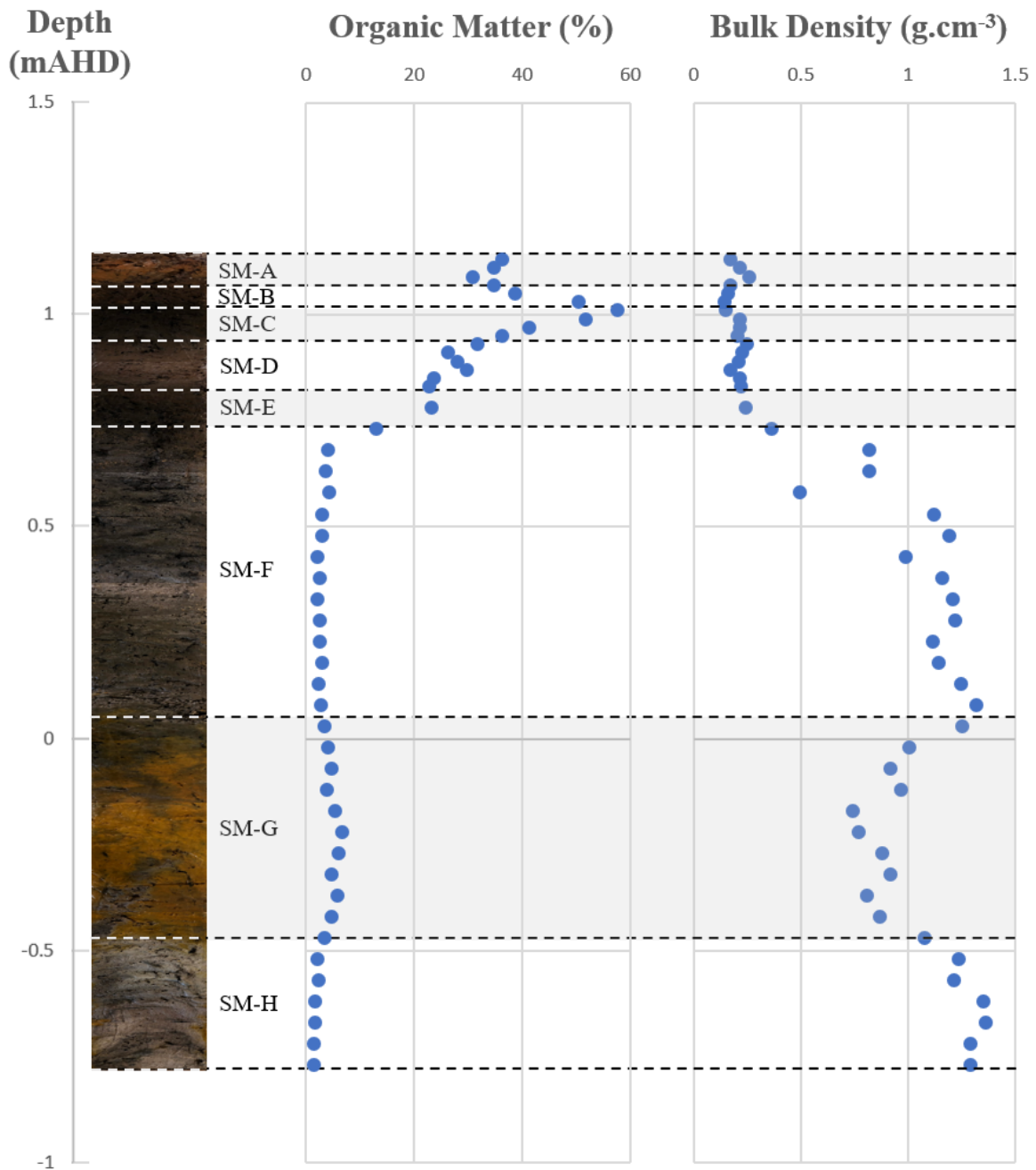


Figure 4.2: Core photo, stratigraphic units, percentage organic matter and bulk density (left to right) of the Saltmarsh core (SM). 0 m AHD is approximately equivalent to mean sea level.

4.1.4 *Melaleuca 1*

The surface organic horizon of MEL1 shows the greatest proportion of organic contribution (up to 66%) amongst the cores studied, while also extending deeper (0.65 m) than its intertidal counterparts (Figure 4.3). MEL1-A has a stable organic concentration sitting around 60% before beginning to decline over MEL1-B to MEL1-C. Br and Ca:Rb concentrations through the surface profile follow the organic composition of the units. MEL1-D sees an increase in grain size, Zr:Rb and low period in percentage organic matter. Below MEL1-D, MEL-E experiences increased grain size, and Zr:Rb, while the inverse occurs for organic composition and Ca:Rb. The grain size and colouration of this unit correlates to both MAN-E and SM-G, along with the corresponding increase in organic content. Similarly to MAN and SM this unit overlays the sand dominated sediments with low organic contribution. MEL1-F is a unique unit amongst the cores being grey in colour, comprised of sands tightly packed with fine sediment and has a tacky texture. The remainder of MEL1 is then followed by similar sands to that found the bottom of MAN and SM. Preserved macrofossils were consistent throughout the profile, comprised of primarily root and rhizome casings. There was a clear shift preserved detritus below approximately 0.43 and 0.2 m AHD (MF-10 and MF-13 respectively; Refer to Appendix B). Soil moisture in MEL1 remains mostly stable at ~80% in the surface 20 cm, which is consistent with the stable surface organic horizon (Figure 4.4). The overall grain size throughout the profile of MEL1 fined upwards (Refer to Appendix E). Shifting from sandy sediments between MEL1-F and MEL1-J, to a mix of sand and finer sediments above this until MEL1-C. MEL1-A through to MEL1-C consists predominantly of finer sediments.

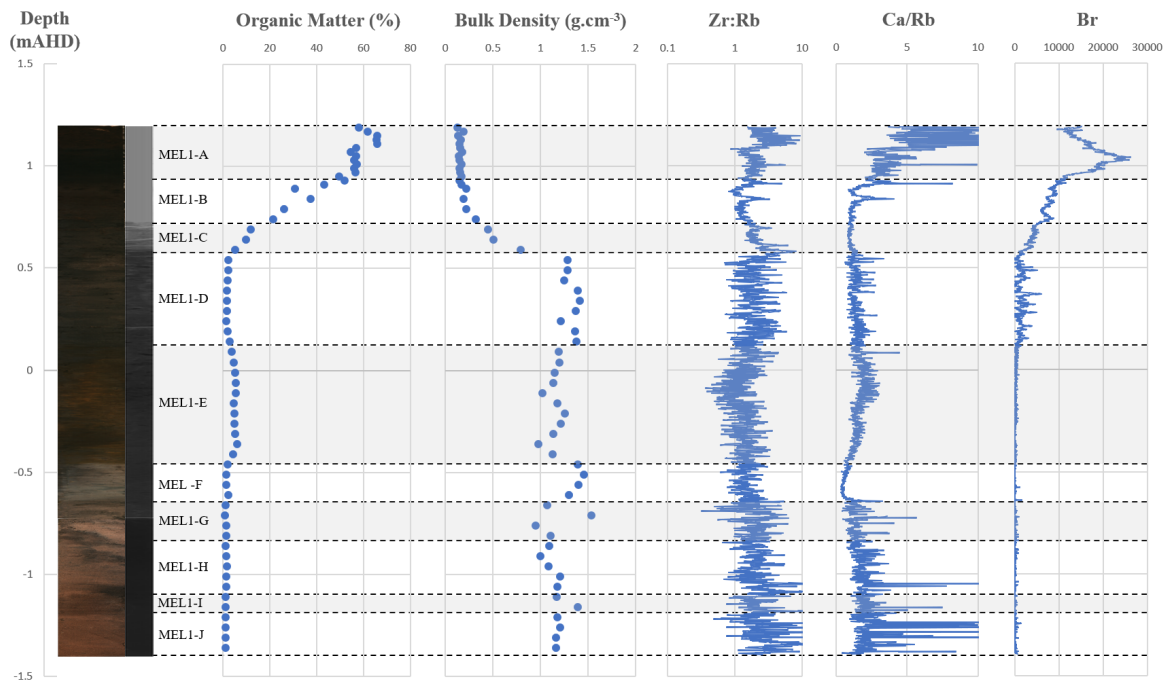


Figure 4.3: Core photo, radiograph, stratigraphic units, percentage organic matter, bulk density and elemental analysis (left to right) of the *Melaleuca* 1 core (MEL1).

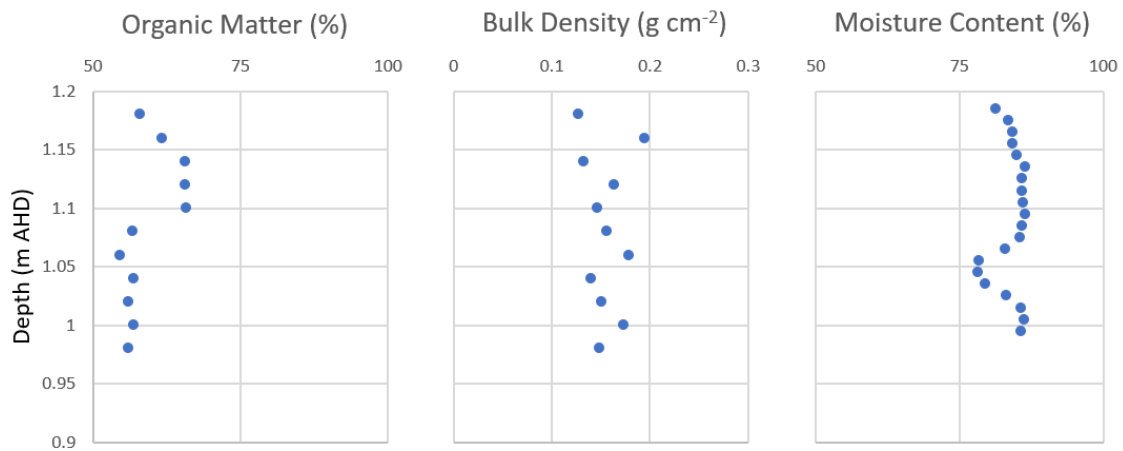


Figure 4.4: Percentage organic matter, bulk density and moisture content (left to right). Organic matter and bulk density data from the primary *Melaleuca* 1 core, while moisture content was collected separately using the Russian peat corer. 0 m AHD is approximately equivalent to mean sea level.

4.1.5 *Melaleuca* 2

MEL2 shows broad similarities in the surface organic horizon as MEL1 ranging from 57-65% (Figure 4.5). In contrast to MEL1, MEL2 organic horizon is the shallowest across the four cores, reaching 0.25 m below the surface (MAN-A to MAN-C). Beneath this, there is a sharp decline in organic matter leading into MEL2-B, where the gradient eases over MEL2-B to MEL-C as grain coarsens in the latter. MAN-D has a small rise

in percentage organic matter, with similar grain size and colouration to that of MAN-E, SM-G and MEL1-E. In contrast to MEL1, MEL2 sediment is predominately sands below MEL2-E. Poor preservation of organic material can be seen in occasional fine to moderate roots throughout the remainder of the core. MEL2-H has a break in the sand dominated sediments as this unit consists of silt and clay with no visible sands. Soil moisture in MEL2 declines after 10 cm, which is consistent with the trends observed in percentage organic matter (Figure 4.6).

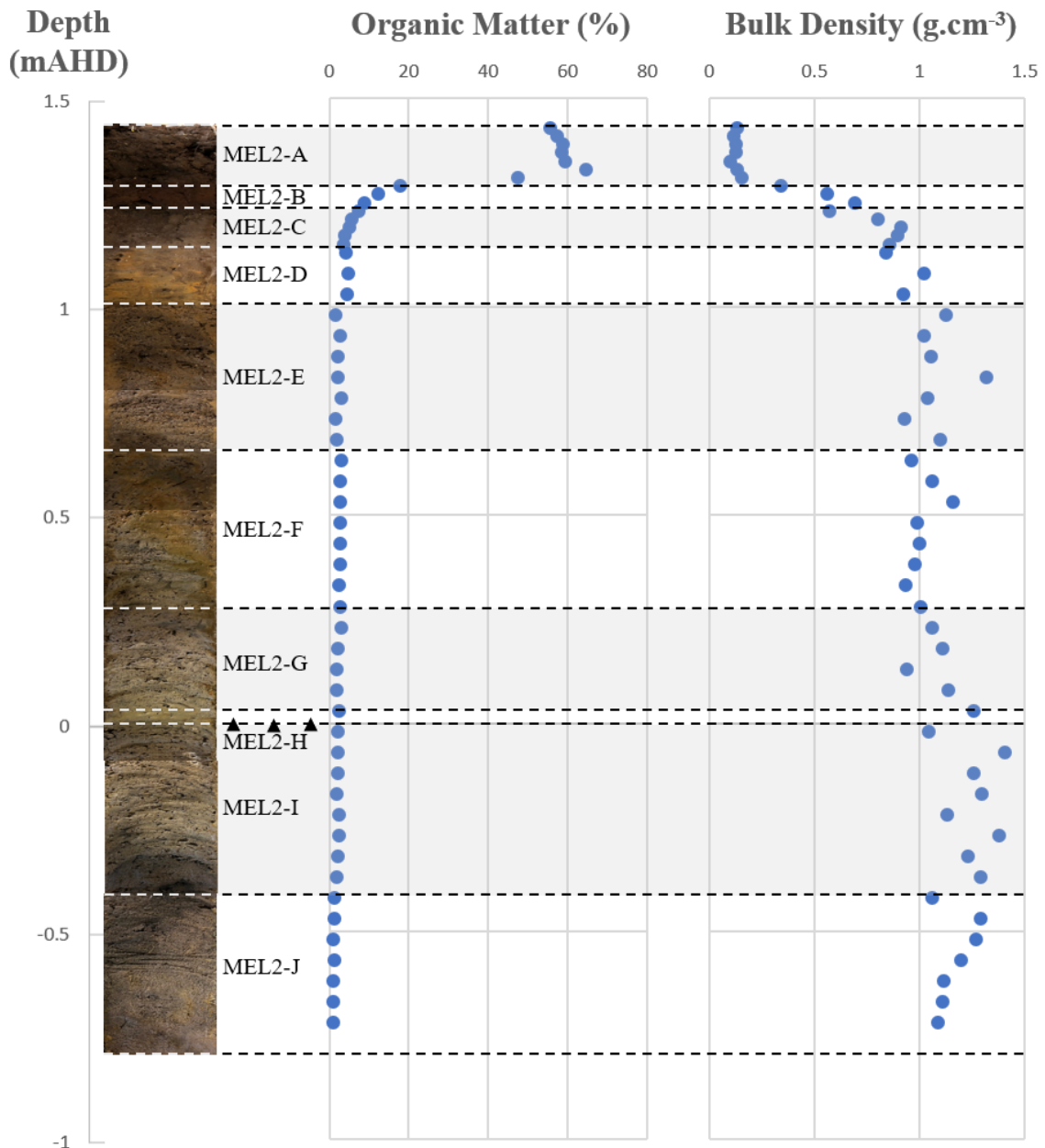


Figure 4.5: Core photo, stratigraphic units, percentage organic matter and bulk density (left to right) of the *Melaleuca 2* core (MEL2). 0 m AHD is approximately equivalent to mean sea level.

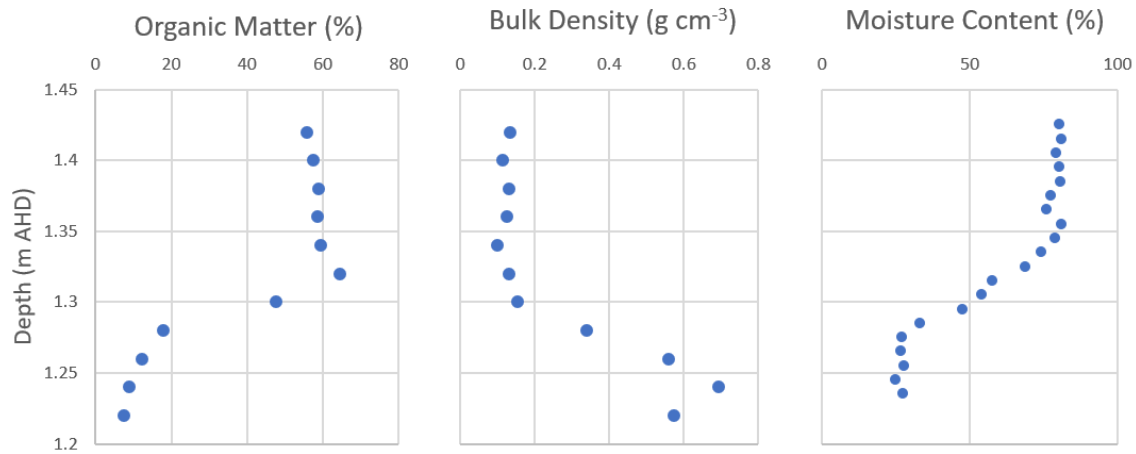


Figure 4.6: Percentage organic matter, bulk density and moisture content (left to right). Organic matter and bulk density data from the primary *Melaleuca* 2 core, while moisture content was collected separately using the Russian peat corer. 0 m AHD is approximately equivalent to mean sea level.

4.1.6 Intertidal-Supratidal Complex

When comparing the cores it can be seen that MAN has a comparatively low concentration of organic matter in the surface organic horizon, reaching a depth of 0.35 m below the surface (Table 3.1). The percentage organic matter in the surface sediments of the SM are greater than that found in MAN and extends 0.45 m below the surface. MEL1 contains the highest contribution of organic matter within the surface organic horizon, while also extending the deepest of all four cores (0.65 m below the surface). MEL2 is similar in percentage organic matter to MEL1, however it has the shallowest surface organic horizon of each core at 0.25 m AHD. Organic contribution beyond the surface horizon of MEL2 sharply declines for the remainder of the core. Across MAN, SM and MEL1 an increase in organic matter occurs approximately 0.8 m below the surface. The increase remained relatively stable ranging from 4-6% over the three cores until declining at approximately -0.5 m AHD. This drop-off was seen across all four cores and organic matter remains below 2%. Grain size comparisons across cores revealed that the surface mangrove sediments were consistent with the grain size that occurred in MEL1-E and the base of MEL1-D (Table 4.3). These consisted of an even mixing of sand and finer sediments. Comparisons can be made between the surface sediments of SM and the grain size of MEL1-C, consisting of predominantly finer sediments (Table 4.5).

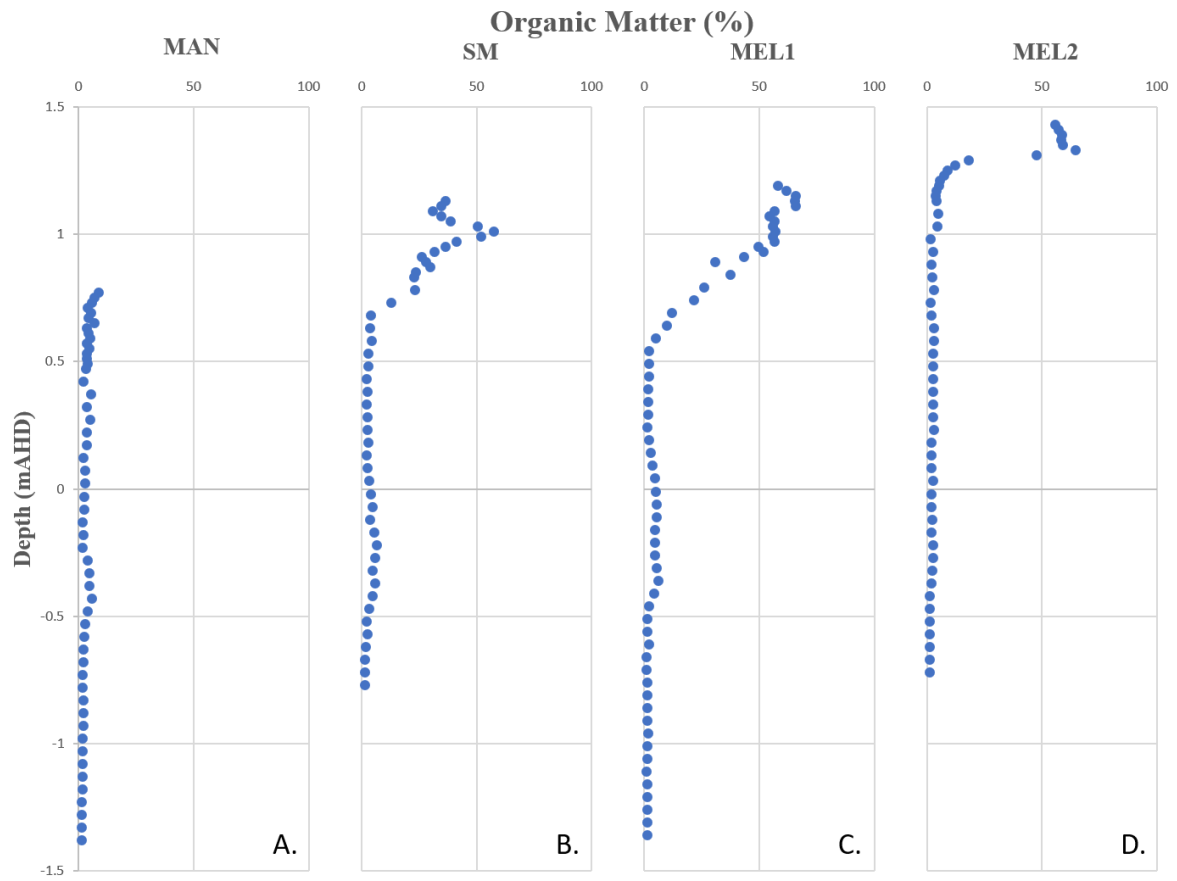


Figure 4.7: Percentage of organic matter downcore with respects to the Australian Height Datum (m AHD) across the four cores: A. Mangrove; B. Saltmarsh; C. *Melaleuca* 1; D. *Melaleuca* 2. 0 m AHD is approximately equivalent to mean sea level.

Table 4.3: Row by row comparison of similar grainsizes between the stratigraphic units through the profile of the *Melaleuca* 1 (MEL1) core and the surface 15 cm of the mangrove core (MAN). 0 m AHD is approximately equivalent to mean sea level.

| <i>Melaleuca</i> 1 grain size | | Mangrove Grain Size | |
|-------------------------------|---|---------------------|---|
| Depth (m AHD) | Grain Size Histogram | Depth (m AHD) | Grain Size Histogram |
| 0.35 | <p style="text-align: center;">GSa-8</p> <p style="text-align: center;">Grain Size (µm)</p> | 0.68 | <p style="text-align: center;">GSb-2</p> <p style="text-align: center;">Grain Size (µm)</p> |

Continues to Next Page ...

Melaleuca 1 grain size

Mangrove Grain Size

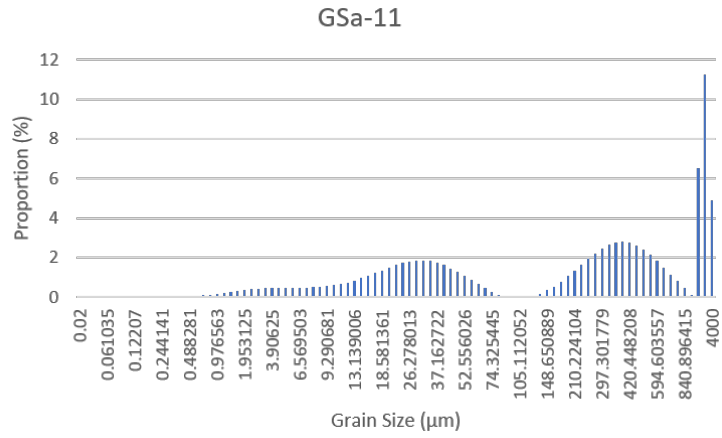
Depth
(m AHD)

Grain Size Histogram

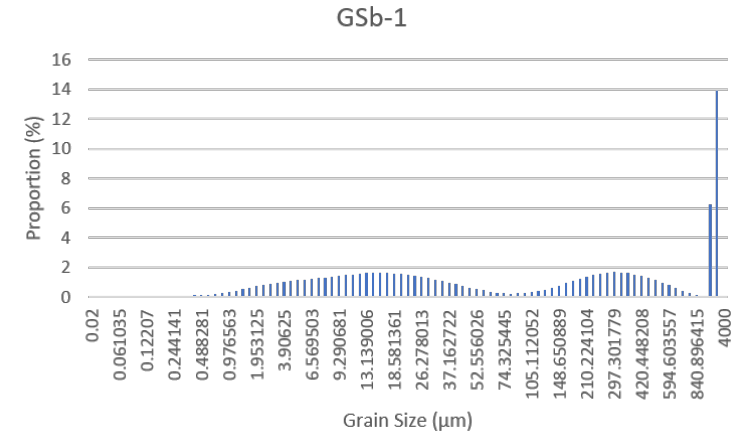
Depth
(m AHD)

Grain Size Histogram

-0.15



0.73



Continues to Next Page ...

Melaleuca 1 grain size

Mangrove Grain Size

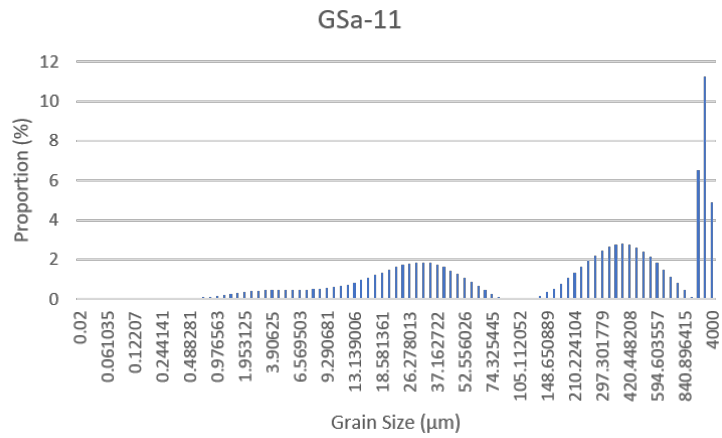
Depth
(m AHD)

Grain Size Histogram

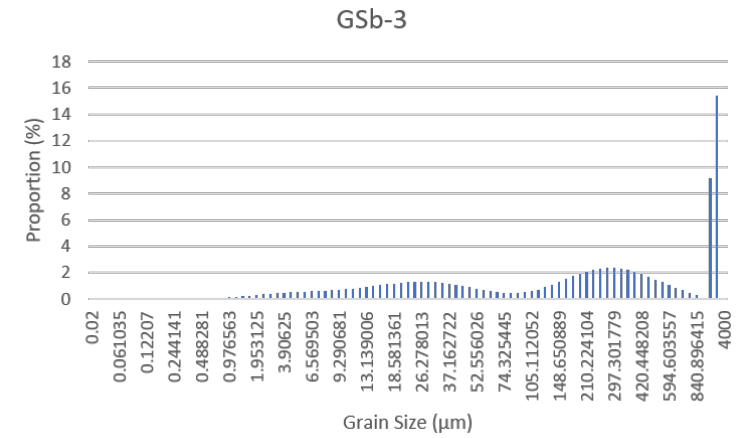
Depth
(m AHD)

Grain Size Histogram

-0.15



0.63



End of Table

Table 4.5: Row by row comparison of similar grain sizes between the stratigraphic units through the profile of the *Melaleuca* 1 (MEL1) core and the surface 15 cm of the saltmarsh core (SM). 0 m AHD is approximately equivalent to mean sea level.

| <i>Melaleuca</i> 1 Grain Size | | Saltmarsh Grain Size | |
|-------------------------------|---|----------------------|---|
| Depth (m AHD) | Grain Size Histogram | Depth (m AHD) | Grain Size Histogram |
| 0.74 | <p style="text-align: center;">GSa-5</p> <p style="text-align: center;">Grain Size (µm)</p> | 1.04 | <p style="text-align: center;">GSc-2</p> <p style="text-align: center;">Grain Size (µm)</p> |

Continues to Next Page ...

Melaleuca 1 Grain Size

Saltmarsh Grain Size

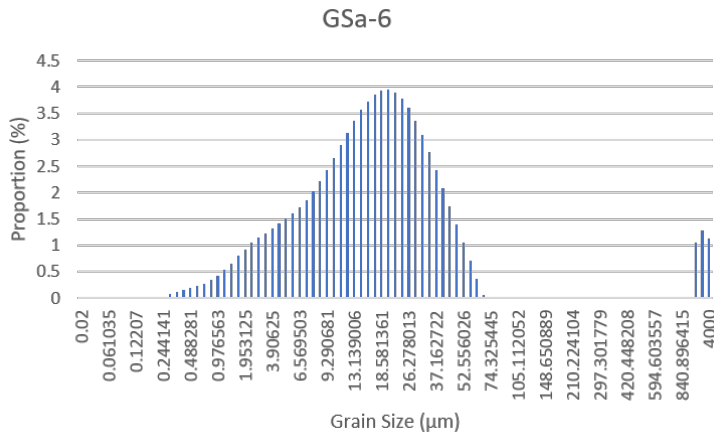
Depth
(m
AHD)

Grain Size Histogram

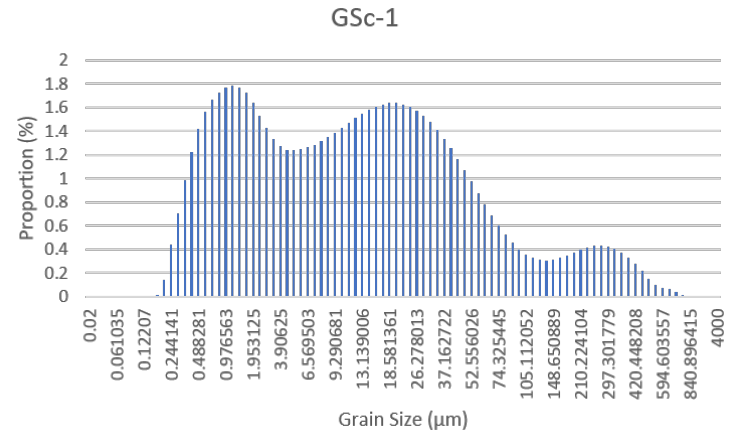
Depth
(m AHD)

Grain Size Histogram

0.59



1.09



Continues to Next Page ...

Melaleuca 1 Grain Size

Saltmarsh Grain Size

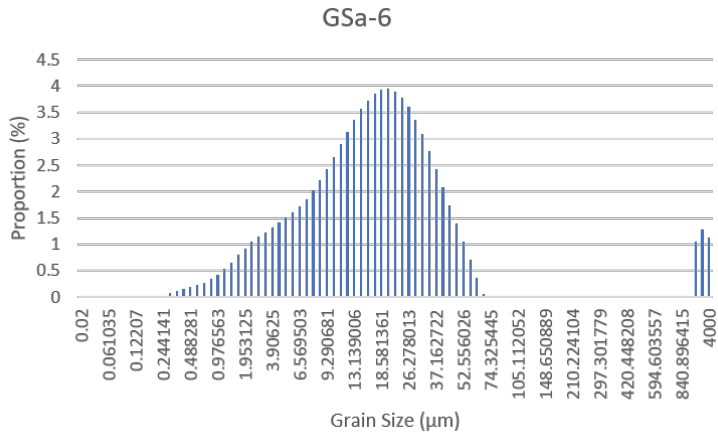
Depth
(m
AHD)

Grain Size Histogram

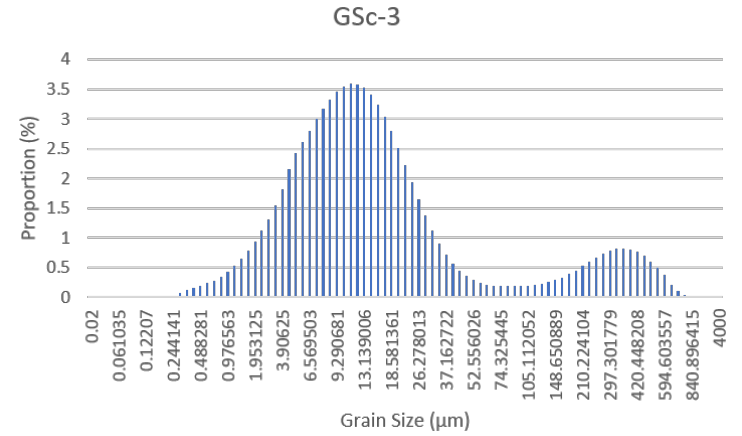
Depth
(m AHD)

Grain Size Histogram

0.59



0.99



End of Table

4.2 Photogrammetry

Mangroves in 1957 covered an area of 29204m², separated into five isolated regions (Figure 4.8 C and D; Figure 4.12 A; Table 4.7 A; Figure 4.10 C). Mangrove expanded at a relatively slow rate over with change between 1957 to 1987, expanding on average 0.8% per year over the 30 year period . Post 1987 the expansion rate of the mangroves increased over four fold to 2.7% from 1987 to 2010. This again increased to 4.76% per year between 2010 and 2020, with present day extents where mangrove cover an area of 89495m², 206.5% greater than its extent in 1957 (). Similar overall trends can be seen in the analysis of the transect with a total areal change of 193.5% (Figure 4.9 C and D; Figure 4.11 C; Figure 4.12 B; Table 4.7 A).

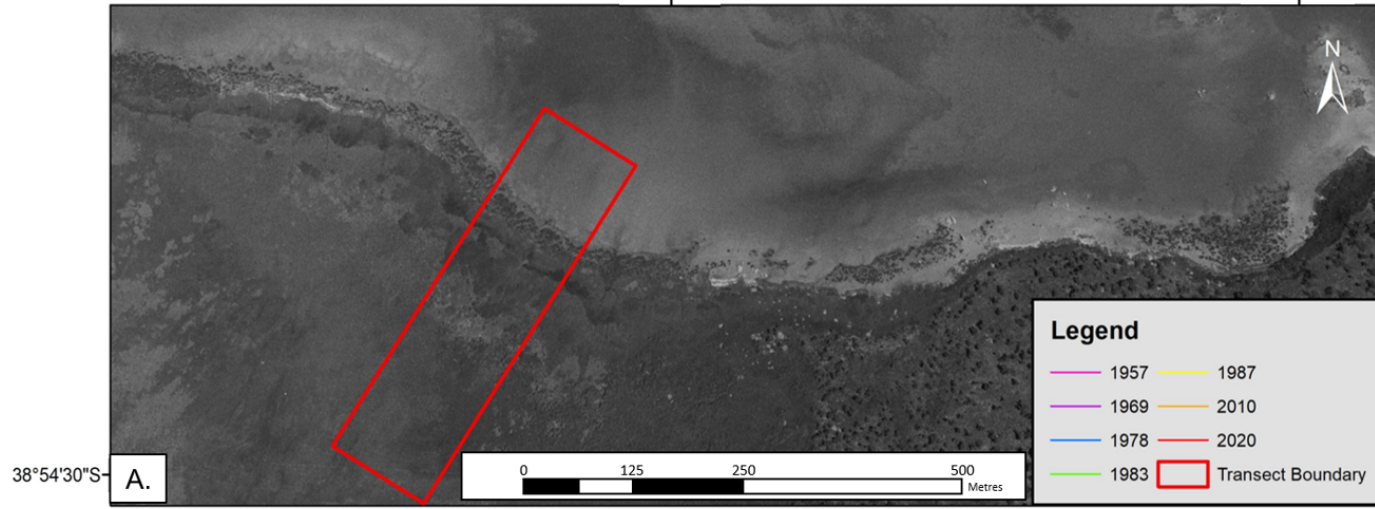
The coverage of bare ground experienced an overall increase by 99.5%, though did not see a pattern in its growth, differing from the mangrove expansion (Figure 4.8; Figure 4.10 D; Figure 4.12 A; Table 4.7 B). There are three periods where minor change over the site or the area decreased. Each of these changes correlate to expansion of other ecosystems. The changes that occur in 1978 and 2010 correspond to increase in the rate of mangrove expansion, while the changes between 1983 to 1987 follow an increase both mangrove and saltmarsh area. Bare ground in the transect was not present pre-1983. Post-1983 bare ground experienced a fivefold increase to area extent between 1983 to 2020 (Figure 4.9; Figure 4.11 D; Figure 4.12 B; Table 4.7 B).

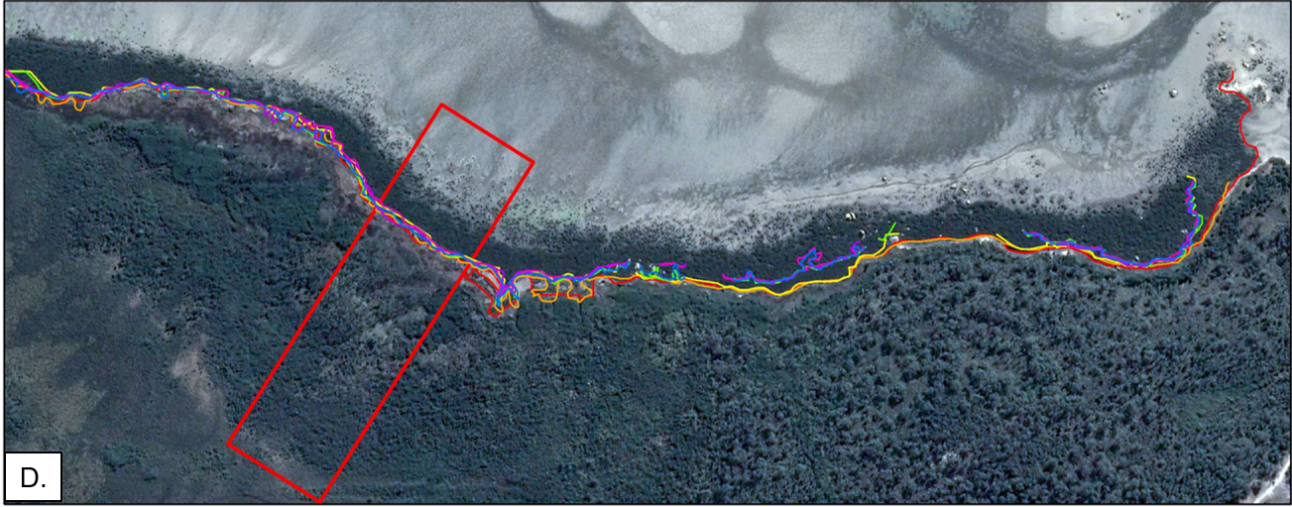
In contrast to the mangrove expansion both sea- and landward, saltmarsh experienced an overall landward retreat and decrease in extent. In 1957, saltmarsh formed one unit covering an area of 26613; an area of the mangrove at that time. Saltmarsh declined at a varying rate over the 1957 to 1983 before seeing a small increase of 4.2% in 1987 (Figure 4.8 E and F; Figure 4.10 E; Figure 4.12 A; Table 4.7 C). Saltmarsh extent further declined, becoming increasingly patchy as it experiences a total reduction in area of 52.3%. Similar overall trends can be seen along the transect with an overall decline of 61.3% (Figure 4.9 E and F; Figure 4.11 E; Figure 4.12 B; Table 4.7 C).

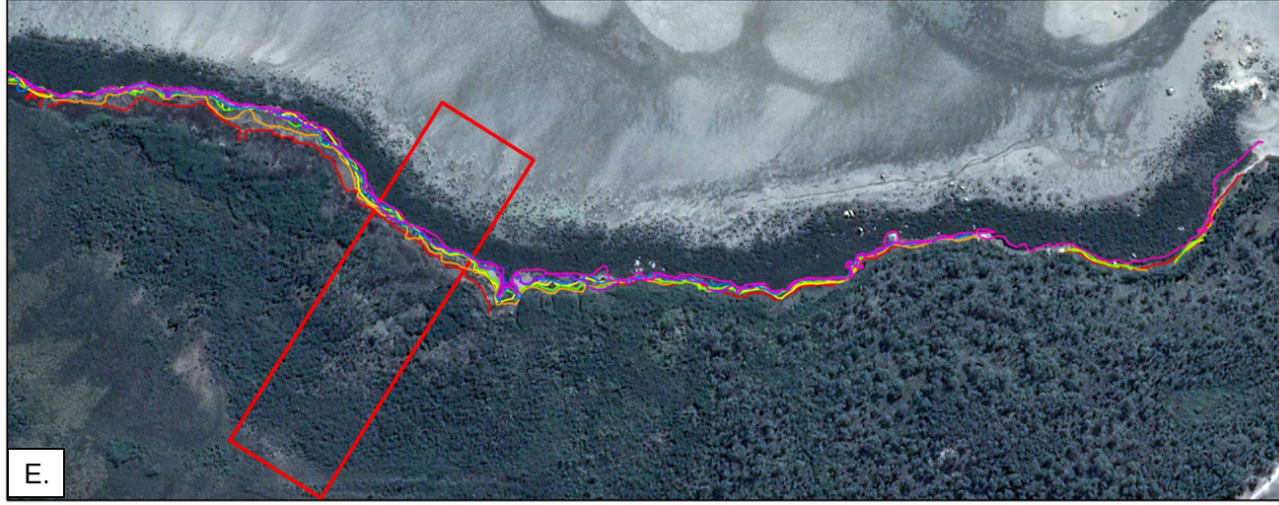
Rapid expansion of the MPS occurred across the embayment between 1957 to 2020, increasing coverage by 81.3% (Figure 4.8 G and H; Figure 4.10 F; Figure 4.12 A; Table 4.7 D). The predominately landward and western lateral (parallel to the foreshore) expansion of the MPS increased at an inverse rate to exponential increase of the mangrove communities. MPS expansion rates sharply decline post 1987, with 99% of the total change occurring between 1957 to 1987. During this declining expansion, MPS experienced spatial heterogeneous loss to the landward extent of the MPS from 1987 to 2020, which would have offset a portion of the total area change. The transect analysis experiences minor landwards retreat and a massive expansion, increasing MPS extent by 193.5% (Figure 4.9 G and H; Figure 4.11 F; Figure 4.12 B; Table 4.7 D).

146°18'0"E

146°18'30"E







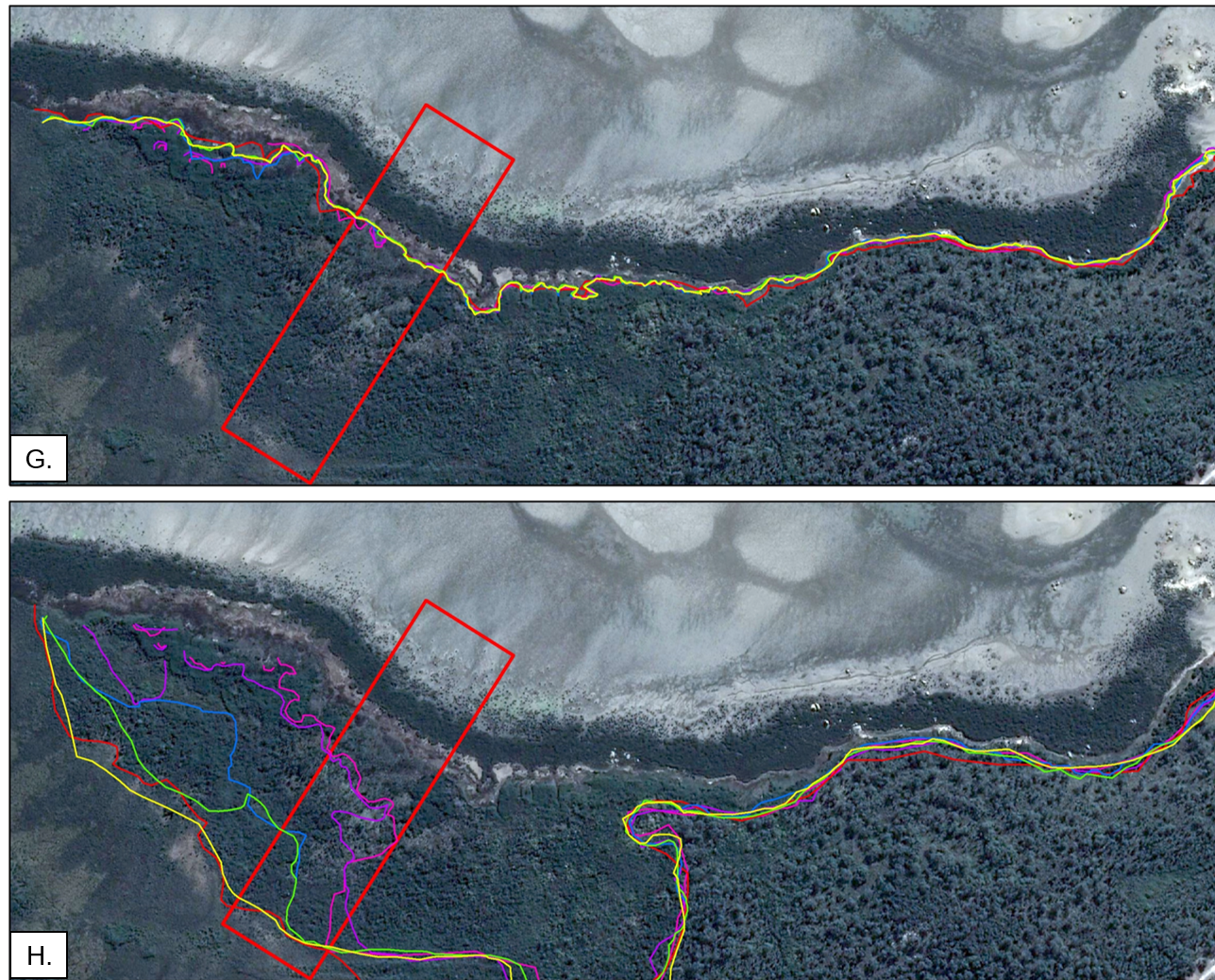


Figure 4.8: Time series analysis of the whole embayment area spanning from 1957 to 2020. (A) Reference map of Corner Inlet in 1957, (B) reference map of Corner Inlet in 2020 (C) digitised lines of mangrove seaward edge, (D) digitised lines of mangrove landward, (E) digitised lines of saltmarsh seaward edge, (F) digitised lines of intertidal vegetation landward edge, (G) digitised lines of *Melaleuca* seaward edge, and (H) digitised lines of *Melaleuca* landward edge.

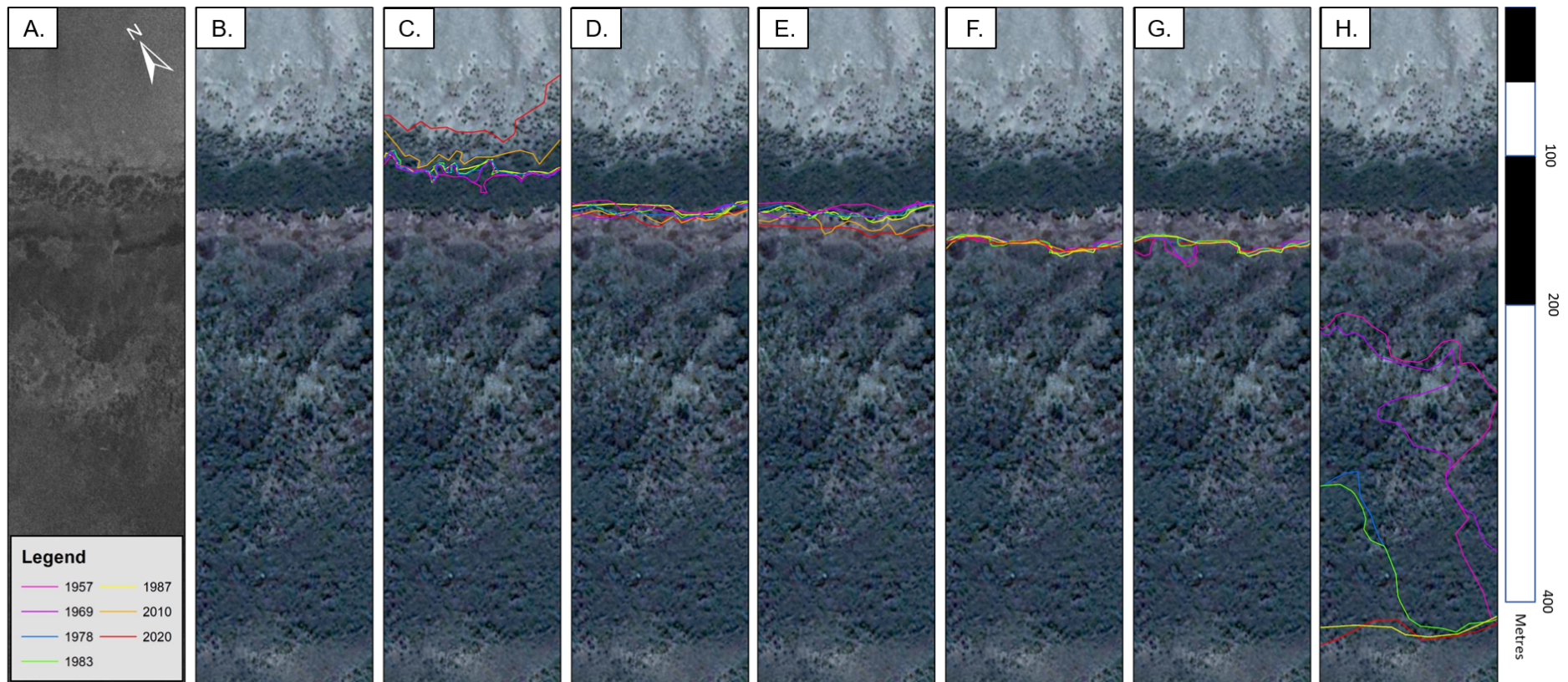
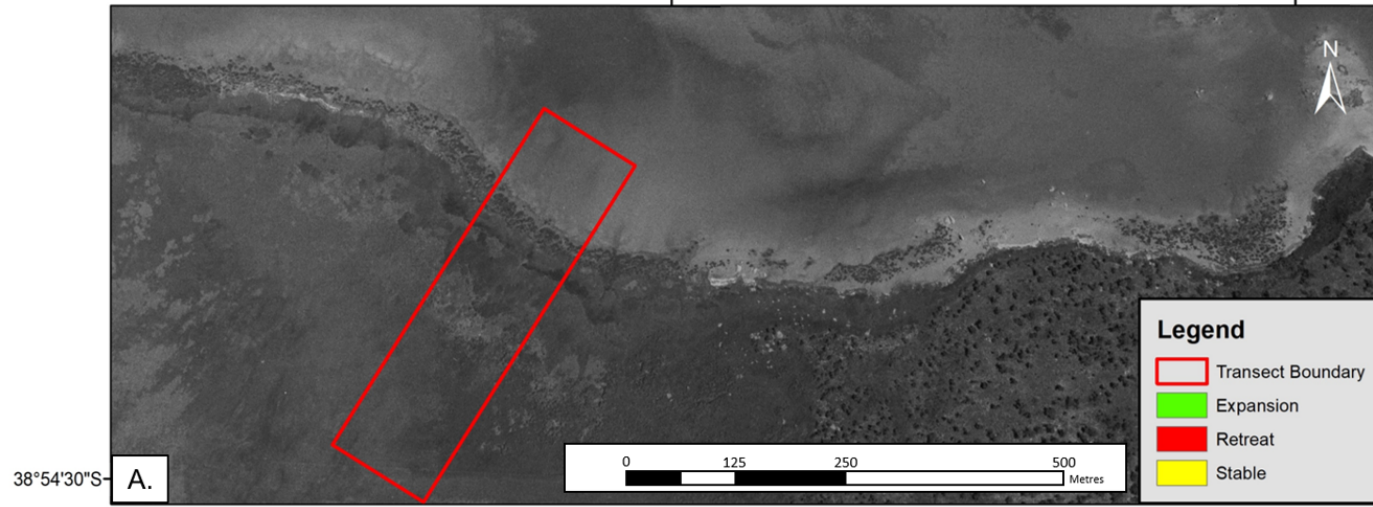
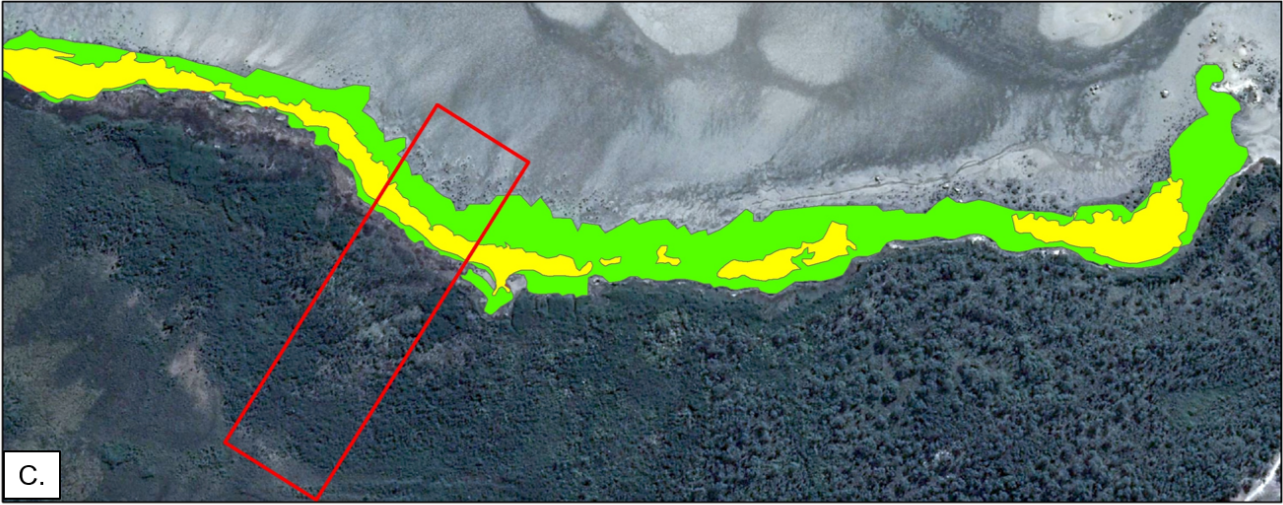


Figure 4.9: Time series analysis of the transect area spanning from 1957 to 2020. (A) Reference map of Corner Inlet in 1957, (B) reference map of Corner Inlet in 2020 (C) digitised lines of mangrove seaward edge, (D) digitised lines of mangrove landward, (E) digitised lines of saltmarsh seaward edge, (F) digitised lines of intertidal vegetation landward edge, (G) digitised lines of *Melaleuca* seaward edge, and (H) digitised lines of *Melaleuca* landward edge. The coordinates of the top right corner is $-38.904940^{\circ}\text{S}$ $146.299313^{\circ}\text{E}$.

146°18'0"E

146°18'30"E





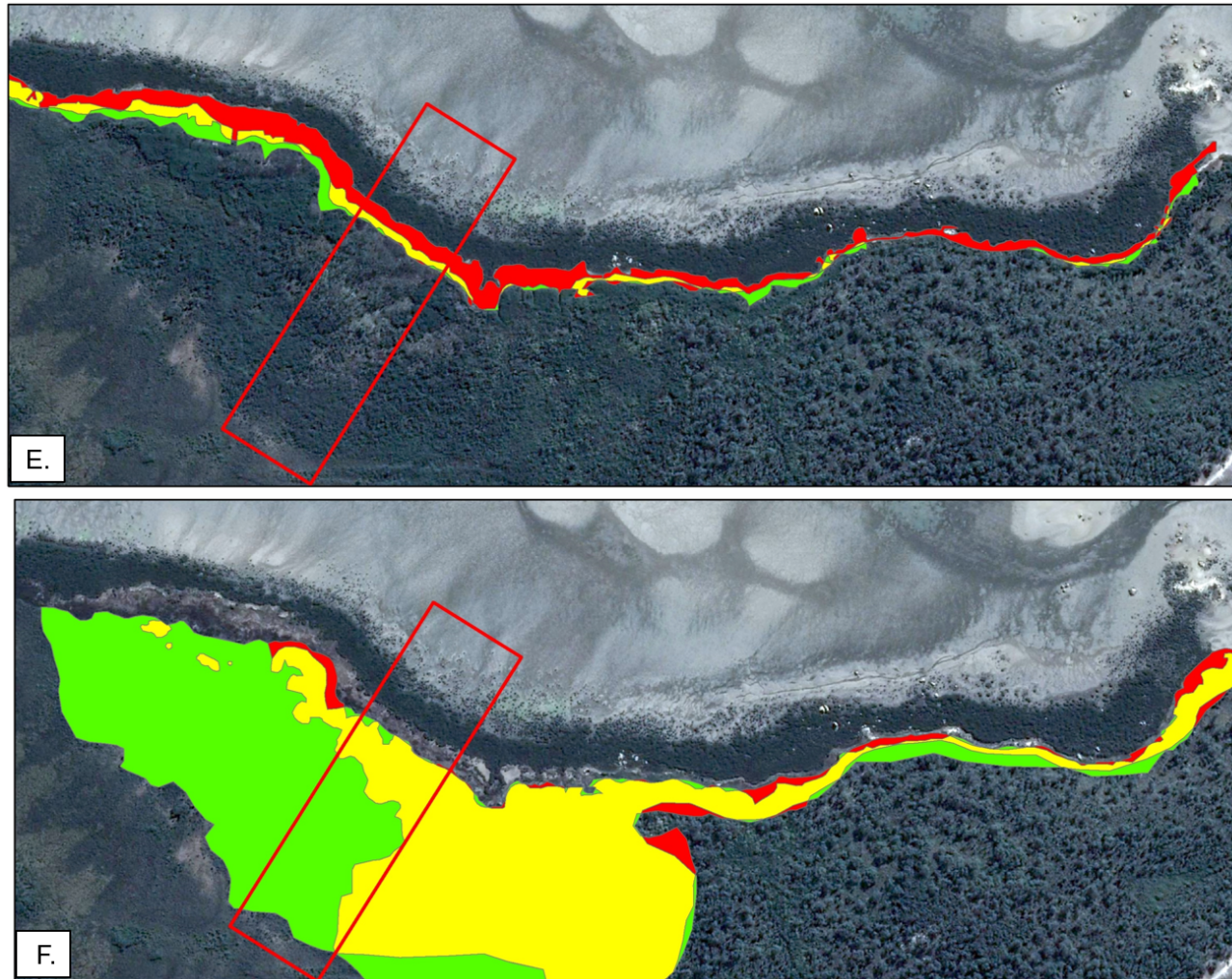


Figure 4.10: Changes in wetland vegetation distribution across the whole embayment from 1957 to 2020. (A) Reference map of Corner Inlet in 1957, (B) reference map of Corner Inlet in 2020, (C) changes in mangrove distribution, (D) changes in bare ground distribution, (E) changes in saltmarsh distribution, and (F) changes in *Melaleuca*. Green represents the area of growth; red represents the area of retreat; yellow represents the area that has remained stable.

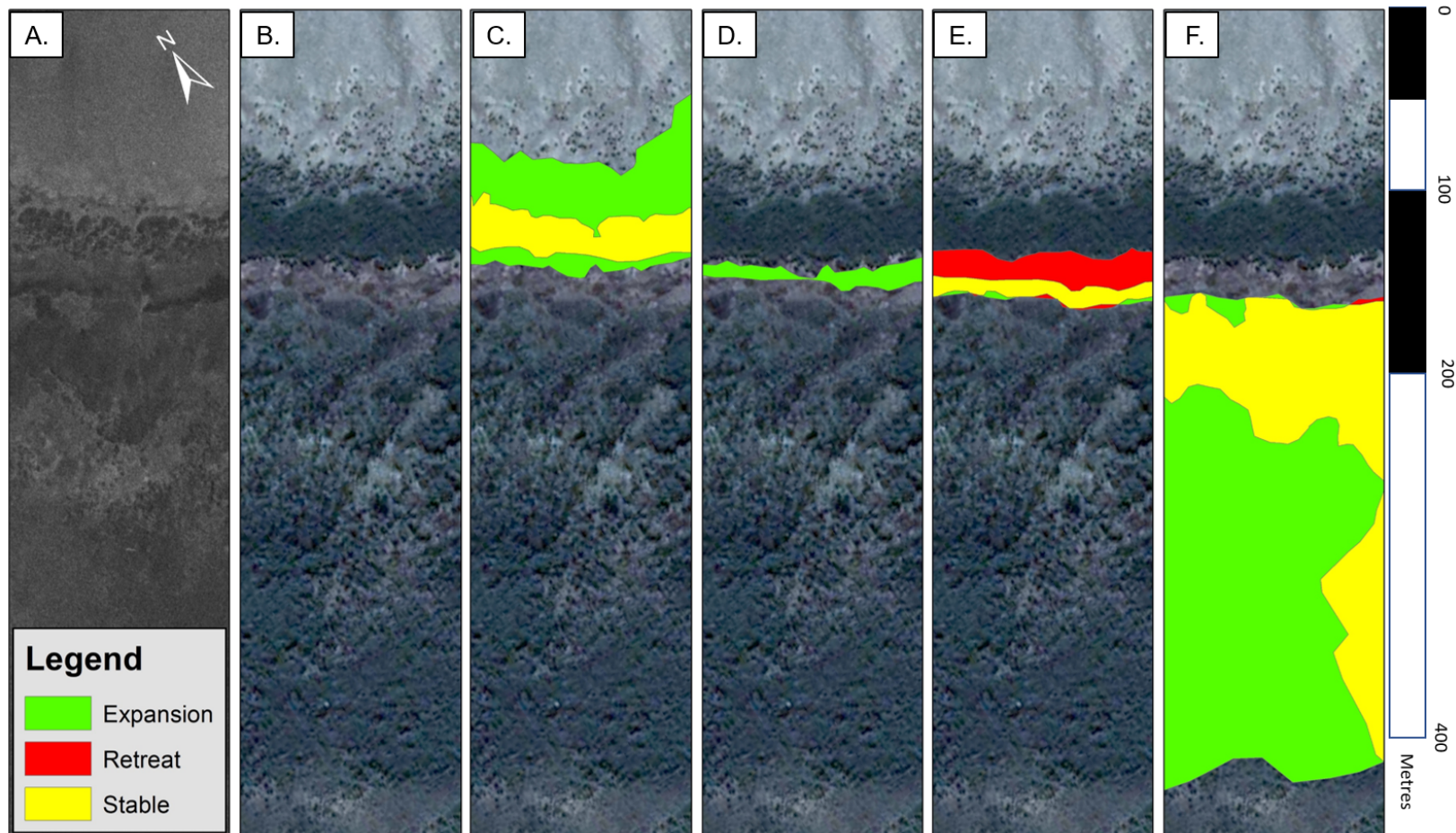


Figure 4.11: Changes in wetland vegetation distribution across the transect from 1957 to 2020. (A) Reference map of Corner Inlet in 1957, (B) reference map of Corner Inlet in 2020, (C) changes in mangrove distribution, (D) changes in bare ground distribution, (E) changes in saltmarsh distribution, and (F) changes in *Melaleuca*. Green represents the area of growth; red represents the area of retreat; yellow represents the area that has remained stable. The coordinates of the top right corner is $-38.904940^{\circ}\text{S}$ $146.299313^{\circ}\text{E}$.

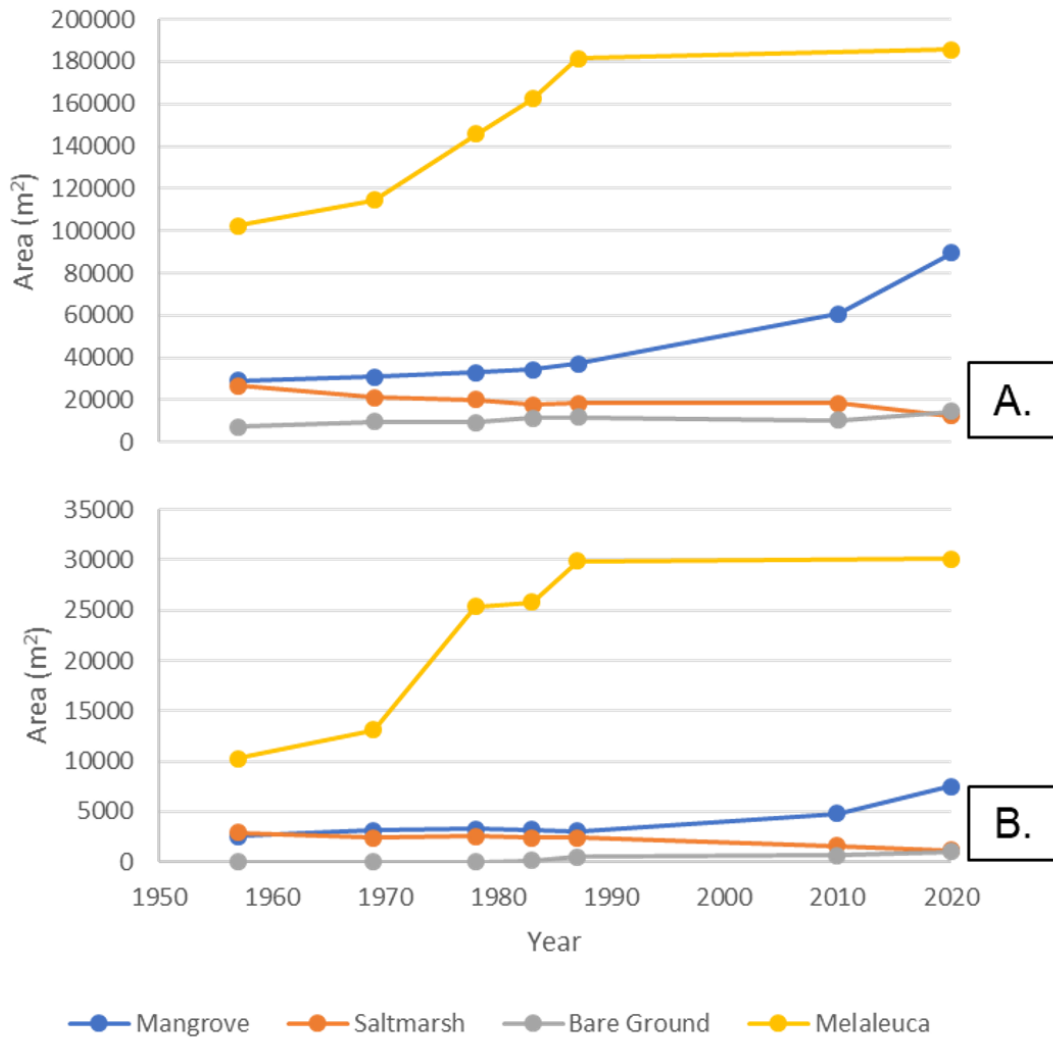


Figure 4.12: Wetland vegetation distribution changes across the (A) whole embayment and (B) transect from 1957 to 2020.

Table 4.7: Area coverage (m²) and percentage change of the wetland vegetation from 1957 to 2020. (A) Mangrove, (B) bare ground, (C) saltmarsh, and (D) *Melaleuca*.

| A. | Whole Embayment | | Transect | | |
|----|---------------------|------------------------|--------------|------------------------|--------------|
| | Year | Area (m ²) | Change (%) | Area (m ²) | Change (%) |
| | 1957 | 29203.7 | N/A | 2541.5 | N/A |
| | 1969 | 30886.0 | 5.8 | 3155.7 | 24.2 |
| | 1978 | 33072.9 | 7.1 | 3281.9 | 4.0 |
| | 1983 | 34452.3 | 4.2 | 3222.9 | -1.8 |
| | 1987 | 37211.2 | 8.0 | 3062.1 | -5.0 |
| | 2010 | 60628.0 | 62.9 | 4782.7 | 56.2 |
| | 2020 | 89495.3 | 47.6 | 7458.5 | 55.9 |
| | Total Change | 60291.6 | 206.5 | 4917.0 | 193.5 |

| B. | Whole Embayment | | Transect | | |
|----|---------------------|------------------------|-------------|------------------------|--------------|
| | Year | Area (m ²) | Change (%) | Area (m ²) | Change (%) |
| | 1957 | 7249.3 | N/A | 0.0 | N/A |
| | 1969 | 9723.4 | 34.1 | 0.0 | N/A |
| | 1978 | 9487.9 | -2.4 | 0.0 | N/A |
| | 1983 | 11405.6 | 20.2 | 163.2 | N/A |
| | 1987 | 11843.0 | 3.8 | 476.4 | 192.0 |
| | 2010 | 10530.8 | -11.1 | 659.0 | 38.3 |
| | 2020 | 14483.2 | 37.5 | 969.7 | 47.1 |
| | Total Change | 7233.9 | 99.8 | 806.5 | 494.3 |

| C. | Whole Embayment | | Transect | |
|---------------------|------------------------|--------------|------------------------|--------------|
| Year | Area (m ²) | Change (%) | Area (m ²) | Change (%) |
| 1957 | 26613.1 | N/A | 2887.1 | N/A |
| 1969 | 21263.6 | -20.1 | 2356.2 | -18.4 |
| 1978 | 20052.3 | -5.7 | 2522.2 | 7.0 |
| 1983 | 17798.1 | -11.2 | 2369.6 | -6.1 |
| 1987 | 18538.3 | 4.2 | 2379.0 | 0.4 |
| 2010 | 18403.7 | -0.7 | 1575.9 | -33.8 |
| 2020 | 12684.1 | -31.1 | 1116.8 | -29.1 |
| Total Change | -13929.0 | -52.3 | -1770.3 | -61.3 |

| D. | Whole Embayment | | Transect | |
|---------------------|------------------------|-------------|------------------------|--------------|
| Year | Area (m ²) | Change (%) | Area (m ²) | Change (%) |
| 1957 | 102366.6 | N/A | 10258.5 | N/A |
| 1969 | 114681.6 | 12.0 | 13131.1 | 28.0 |
| 1978 | 145873.7 | 27.2 | 25370.9 | 93.2 |
| 1983 | 162568.9 | 11.4 | 25794.0 | 1.7 |
| 1987 | 181386.6 | 11.6 | 29902.4 | 15.9 |
| 2020 | 185539.1 | 2.3 | 30108.3 | 0.7 |
| Total Change | 83172.4 | 81.2 | 19849.8 | 193.5 |

5 Discussion

5.1 Organic Contribution in Coastal Wetlands

Across the wetland gradient from mangrove to *Melaleuca*, an increase in organic contribution can be observed among surface units (Figure 4.7).

5.1.1 Organic Contribution in the Supratidal Zone

Both MEL1 and MEL2 exceeded the organic contribution of their intertidal counterparts, with up to 66% organic material in the surface horizon (Figure 4.3; Figure 4.5). MPS cores have a stable organic-rich surface, beneath which, organic matter declines. Organic matter experiences a slow decline in MEL-1 over the surface 0.65 m. Below this, a period of low organic contribution occurs until the preserved unit (MEL1-E); beneath which organic contribution returns to a stable low for the remainder of the profile. MEL-2 is unique amongst the cores, its surface organic matter sharply decreasing 0.1 m below the surface and experience a sub-surface preserved unit (MEL2-D) higher in absolute elevation (1.13 m AHD) than the other cores (-0.23 to 0.14 m AHD). Below this sandy mineral matter dominates the sediments.

Carbon concentration is primarily used to present the findings; however, this study prioritises its findings around biomass. Despite this, comparisons are still able to be made between this study and others. Tropical MPS have been found to have highly organic sediments containing 140 ± 40 (ranging 20–230) Mg C ha^{-1} in the surface 50 cm of the core (Adame *et al.*, 2019). The concentrations in this study were consistent with the average of Adame *et al.* (2019). MEL1 organic composition is consistent with the upper range of this core, while MEL2 sits around the mean findings from this study. The concentrations of this study are also consistent with sub-tropic MPS in Australia, with a organic composition greater than the mean of sub-tropical MPS ($104 \pm 16 \text{ t ha}^{-1}$) in the surface 30 cm (Tran and Dargusch, 2016). These high values are likely due to the high productivity and rate of litterfall from the forests. Finlayson *et al.* (1993) study of tropical MPS found that these forests produce approximately 700 g m^{-2} . The high productivity of MPS is evident from the organic-rich surface sediments of the MPS in this site (Figure 4.3; Figure 4.5). The aperiodic inundation of MPS results in the limitation of two substrate development processes that are potentially responsible for the organic-rich characteristics of the forests.

Firstly, the output of organic matter from the MPS is lowered due to a restricted mode of transport. This leads to a consistent build-up of surface-deposited organic material. However, inundation is required in part for organic preservation of the surface organic horizon. In a study of MPS disturbed by inundation, there was no significant impact observed on the carbon stocks of the stand understory, deadwood, roots, or soil (Tran and Dargusch, 2016). Leaf litter was the only factor found to impacted by inundation; with

inundated areas containing coarse to fine litter, while dry forests held little to no fine litter (Greenway, 1994; de Neiff *et al.*, 2006; Tran and Dargusch, 2016). This is supported by the differences observed in the surface organic horizon of MEL1 and MEL2 (Figure 4.3; Figure 4.5). Consistent high moisture content of MEL1 in the surface 20 cm aligns with a stable organic contribution (Figure 4.4). Soil moisture in MEL2 begins to decline below the surface 10 cm which correlates to the sharp decline in organic matter that occurs (Figure 4.6). This may also have been partially due to organic matters ability to absorb moisture. Nevertheless, a balance is required between areas in regards to inundation and soil moisture. Forests require sufficient inundation to accumulate and preserve fine litter and not experience excessive output of matter within wetland forests.

The second process is the lack of allochthonous sedimentation, which limits the input of mineral matter, giving a greater proportion of organic to mineral composition in the wetland (Figure 2.5; Kirwan and Mudd, 2012; Rogers *et al.*, 2019b). These two limiting factors within the supratidal forest can explain the organic-rich nature of MPS surface sediments. These findings suggest a potential placement for MPS on the Rogers *et al.* (2019b) conceptual model (Figure 2.5) of substrate accumulation, in which the figure considering regions above HAT. The inclusion of MPS and supratidal wetland forests based of this study only would hold severe limitations due to the extent of this study, and further research is required for a valid assessment. Despite this, the organic and mineral component within the MPS could be assessed and the substrate characterised by its high proportion of organic contribution.

5.1.2 Organic Contribution in the Intertidal Zone

Mangroves showed a predominantly mineral contribution, consisting of ~90-95% of sediment accumulated in the surface horizon (Figure 4.1). The organic matter throughout the profile of MAN slowly declines from organic peaks (MAN-A & MAN-C), with the latter being less organic-rich. Below these units, organic matter increases throughout MAN-E before decreasing and remaining consistently low. These findings are consistent within the range of south-eastern Australian mangrove communities (range = 2.5–34.3 kg C m⁻²; mean = 23.1 kg C m⁻²; Saintilan *et al.*, 2013). The mangroves of this study fall below the mean of both south-eastern Australian and global mangrove communities (mean = 25.5 kg C m⁻²; Siikamäki *et al.*, 2012; Donato *et al.*, 2011). Kelleway *et al.* (2016a) in a NSW study of temperate mangroves, found mangroves organic contribution higher than that of the mangroves within this study. Mangroves communities along the Hawkesbury River have shown variation in organics composition based on whether they are positioned in hypersaline and marine environments, or freshly accreted riverina bound communities (Saintilan, 1997). The mangroves of Corner Inlet exceeded the organic material stored in hypersaline and marine sand environments (mean = 5.21 kg m⁻², mean = 6.01 kg m⁻², respectively) and below the average for riverina flats (mean = 40 kg m⁻²) with a biomass of 34.7 kg m⁻².

Comparatively to the mangroves, the substrate composition of the saltmarsh community is organic-rich in the surface sediments (Figure 4.2). The difference in mineral accumulation between the mangrove and saltmarsh communities is likely associated to the differences in inundation frequency, depth, and duration. These variables restrict the input of allochthonous sediments, which are the primary driver for mineral accumulation in wetland communities (Alongi, 2009; Krauss *et al.*, 2010; Rogers *et al.*, 2019a). Organic concentration of saltmarsh communities in this study are higher than both marine and fluvial settings in a study of *Sarcocornia-Sporobolus* midmarsh wetlands by Kelleway *et al.*, 2017b. Saltmarsh organic contributions within this study were above average and within the expected range with respect to south-eastern Australian (range = 6.1–34.3 kg C m⁻²; mean = 19.1 kg C m⁻²; Saintilan *et al.*, 2013), and global (mean = 16.2 kg C m⁻²; Duarte *et al.*, 2013) values for saltmarsh communities. Productivity and biomass of saltmarsh vegetation have been shown to be less than that of mangroves (Clarke and Jacoby, 1994; Rogers *et al.*, 2019b). This however, does not correlate to the organic matter differences along the transect of this study.

5.2 Long-Term Shifts in Ecosystem Structure

An assessment of the stratigraphic and geochemical features throughout the profile allows for the paleo-reconstruction of the site on Corner Inlet. This gives insight into the long-term changes occurring over the wetland communities.

The paleo-reconstruction along the transect went as follows with respect to MEL1 (Figure 4.3):

- Marine sands and seagrass meadows vertically accreted until the approximate depth of the preserved unit (MEL-E) where mangrove became the prevailing wetland community.
- As the available accommodation space decreased in the mangrove community, it is likely that saltmarsh migrated accordingly.
- Saltmarsh proceeded to accumulate sediment, until eventually being overlaid by the fresh to brackish water herbaceous wetlands.
- Finally, the MPS that form the contemporary setting expanded into the herbaceous wetlands, which proceeded to migrate landward.

Between MEL1-G and MEL1-J there is a notable marine signature that steadily decline moving upwards in the strata shown through the high Ca/Rb values (Figure 4.3). The preservation of fine to medium roots embedded within sandy sediments is suggestive seagrass meadows (Lo Iocano *et al.*, 2008), in case of this study *Posidonia australis*. Macrofossils found in these units were identified as potential roots and rhizomes *Posidonia*

australis, commonly found within Corner Inlet (Figure 5.1). Similar units occur within MAN (MAN-F to MAN-G) and SM (SM-H) which are determined to likely be the same setting for deposition (Figure 4.1; Figure 4.2). The grey mix of sand and fine sediments of MEL-F correlates to a drop in marine influence (Ca/Rb). Here in MEL-F Ca/Rb was at its minimum, suggesting a higher contribution of terrestrial material relative to marine sediments.

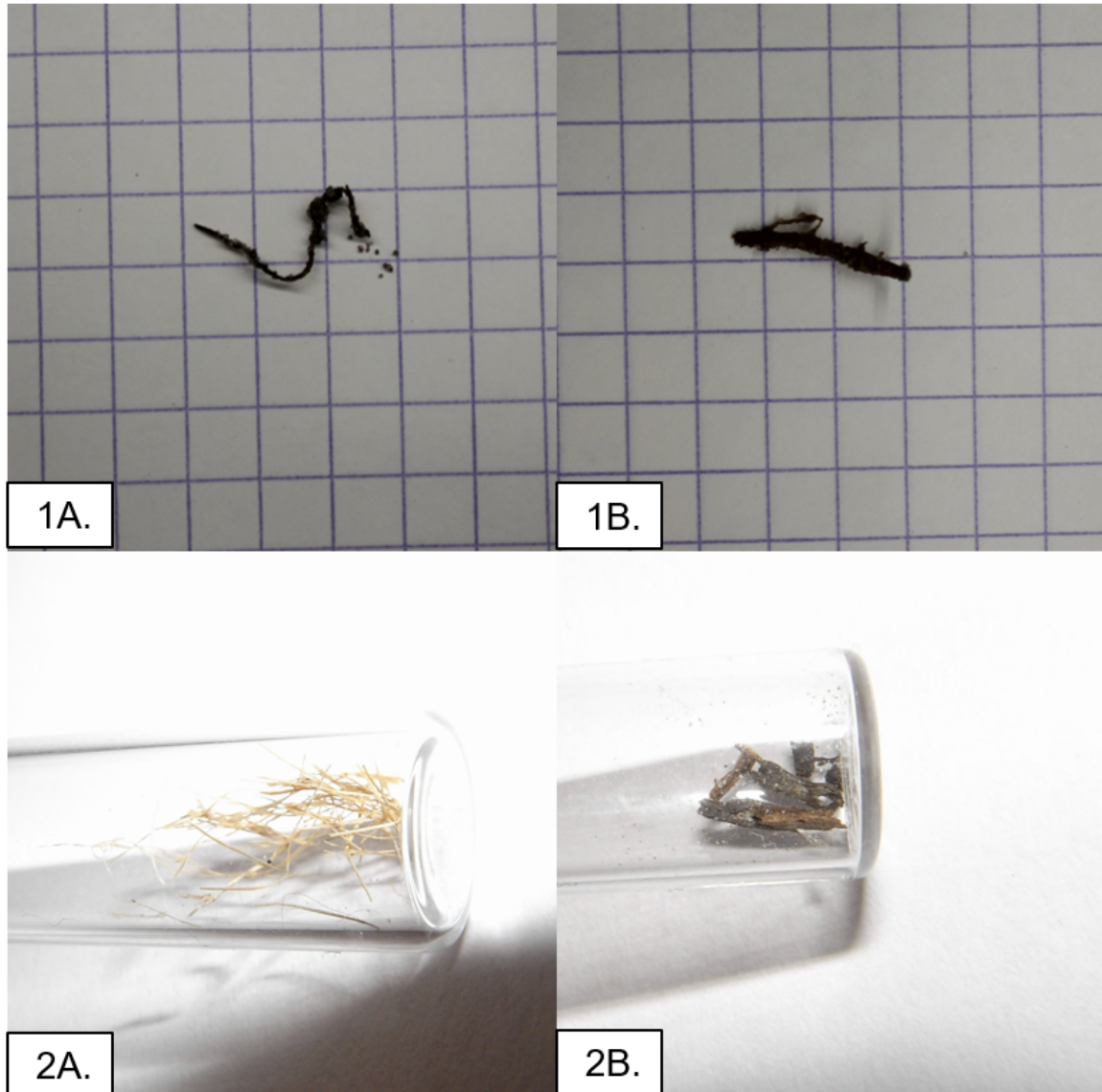


Figure 5.1: Comparison of *Posidonia australis* (A) root and (B) rhizome macrofossils. (1) Seagrass macrofossils collected from *Melaleuca 1* (MEL1). (2) reference photos of *Posidonia australis* macrofossil supplied by Oscar Serrano. Collected samples are (1A) MF-27, and (1B) MF-28. Background grid size for in (1) is 5 x 5 mm (Refer to Appendix B).

Above this unit is the preserved unit (MAN-E, SM-G and MEL1-E), which base is around -0.5 m ADH across MAN, SM and MEL1 (Figure 4.1; Figure 4.2; 4.3; Figure 4.7). This unit across MAN, SM and MEL1 occurs approximately 0.8 m below the contemporary

surface. The preservation in this layer is likely to be at least partly due to the soil structure present in the unit. The preserved unit sediments consist of primarily finer sediments which allow for tighter compaction of the soil. This acts as a physical barrier, as organic material becomes encapsulated by the inorganic silts and clays (Van Veen and Kuikman, 1990), which also trap water within and above the sediments.. Much of the preserved layer is below mean sea-level, increasing the duration this unit is inundated and thus preservation capacity (Rogers *et al.*, 2019c). The grain size of this unit roughly corresponded to the near surface samples collected from MAN (Figure 4.3; comparing GSa-11 to GSb-1 & 3). The bottom of MEL1-D has the closest grain size match for the MAN samples (comparing GSa-11 to GSb-2). Grain size comparisons and sedimentary characteristics suggest that the preserved unit across the cores are potentially the near surface sediments of the mangrove communities (Macphail *et al.*, 2010). The higher proportion of finer sediments shown in the grain size analysis and by a dip in the Zr/Rb ratio are consistent with the sediment accumulation that occurs within mangrove community. Mangroves have a high efficiency for trapping fine sediments within their pneumatophores (Victor *et al.*, 2004; Willemsen *et al.*, 2016). This is achieved by pneumatophores altering the hydrodynamics of the passing tides, effectively trapping 80% of suspended sediment, primarily silts and clays through flocculation of the finer sediments (Wolanski *et al.*, 1980; Wolanski *et al.*, 1992; Furukawa *et al.*, 1997). This is further supported by the marine signature (Ca:Rb) showing an increase in marine influence comparative to the adjacent stratigraphic units (MEL1-D and MEL1-F).

No clear comparison could be made for a saltmarsh boundary using the grain size analyses. The nearest grain size comparison to the surface grain size of the saltmarsh is GSa-4 & 6 (Figure 4.5). Saltmarsh accumulate primarily finer sediments which occur above GSa-7, suggesting saltmarsh occurred within in the overlying units. However, preserved detrital material found from 0-0.7 m AHD are larger than the roots and rhizomes of the dominant saltmarsh species of Corner Inlet. These samples are consistent with the larger rhizomes and roots of *Phragmites australis* or another fresh to brackish-water reed (Figure 5.2). This is more consistent with the herbaceous wetlands that exist beyond the MPS. Rhizomes are shallow growing material which indicate that they were deposited close to the surface. From this it can be distinguished that the herbaceous wetland community, at least in part, was present along MEL1. It is possible that the MPS expanded into the herbaceous wetland present between 0-0.7 m AHD, followed by a shift in the vegetation communities at some point beyond 0.7 m AHD, where MPS becomes the overlying wetland community. Though changes to the environmental factors such as salinity levels likely changed, which resulted in the retreat of the herbaceous wetlands. Long-term changes observed across the transect correlate to the expect gradual infilling of estuaries (Roy *et al.*, 2001). As a result, the wetland communities have experienced a mostly seawards migration with surface sediments (above 0.7 m AHD) indicating a shift in environmental conditions.

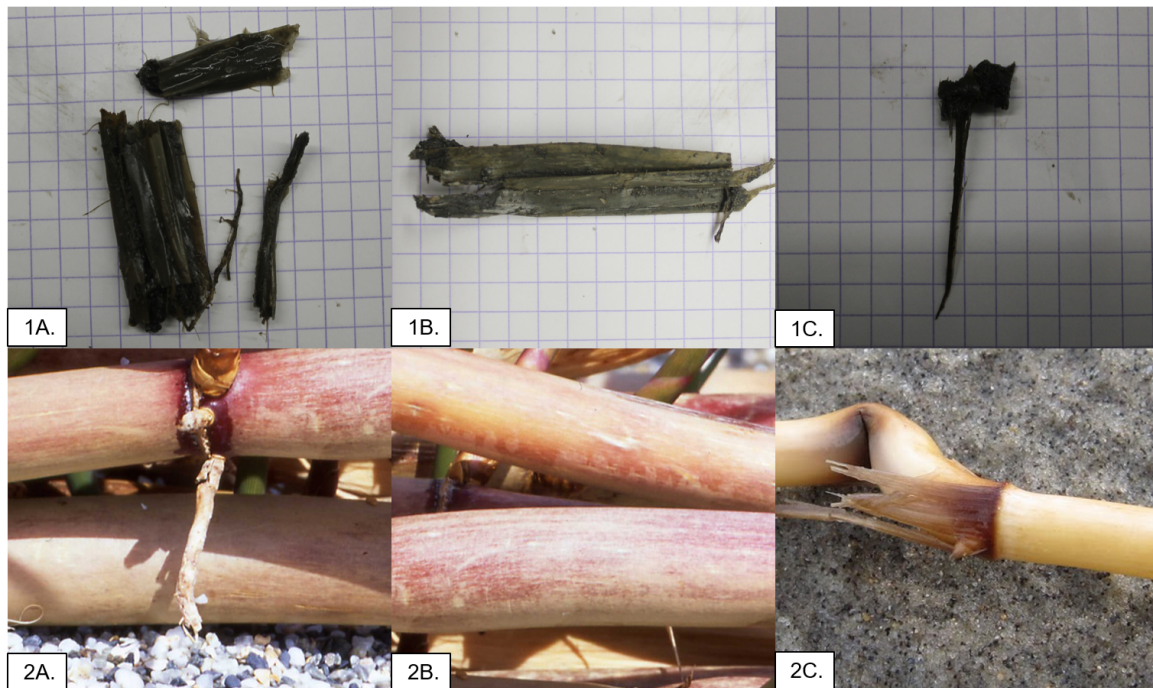


Figure 5.2: Comparison of *Phragmites australis* roots, rhizome and nodes. (1) Root and rhizome macrofossils collected from *Melaleuca* 1 (MEL1). (2) Living root and rhizome of *Phragmites australis*. (A) Roots and rhizome casing, (B) rhizome casing, and (C) node. Collected samples are (1A) MF-7, (1B) MF-6, and (1C) MF-1. Background grid size for in (1) is 5 x 5 mm (Refer to Appendix B).

5.3 Short-Term Shifts in Ecosystem Structure

In contrast to the vegetation shifts occurring in Corner Inlet over longer time scales, interpretation of aerial photographs demonstrated that between 1957 to 2020 the extent of mangroves increased by 206.5% and saltmarsh communities decreased by 52.3% along the study site (Figure 4.10; Figure 4.8; Figure 4.12; Table 4.7). The changes that occur in these intertidal communities follow a trend that is near ubiquitous across estuaries in south eastern Australia (Saintilan and Williams, 1999a; Saintilan and Wilton, 2001; Rogers *et al.*, 2006) and other temperate coastlines including New Zealand (Burns and Ogden, 1985; Morrisey *et al.*, 2003; Lovelock *et al.*, 2009; Debra *et al.*, 2010).

Varying influences have been found to cause the mangrove transgression occurring across the estuaries of south-east Australia. Hypothesised drivers include:

- Changes in temperature (Saintilan *et al.*, 2014; Whitt *et al.*, 2020).
- Increased sedimentation regimes (Saintilan and Williams, 1999a).
- Changes to the water chemistry of the estuary through increased freshwater and nutrients (Saintilan and Wilton, 2001).
- Saltmarsh compaction during drought conditions (Rogers *et al.*, 2006).

- Altered tidal regimes (Saintilan and Williams, 1999a).

Whitt *et al.* (2020) hypothesised that the cause of the marine transgression within Western Port Bay, a nearby Victorian estuary was due to the impacts of changes in temperature. Under a temperature driven expansion of mangroves, it might be expected that the saltmarsh would see a similar rate of loss as a result of competition between the saltmarsh and mangrove. The saltmarsh zone appears to have retreated prior to the arrival of the mangrove, leaving patches of bare ground that the mangrove proceeds to grow within (Figure 4.10; Figure 4.8; Figure 4.12; Table 4.7 A and B). Under a rising sea-level, changes in the abiotic and biotic contributions within the environment may have caused an early retreat in the saltmarsh community. The landward retreat observed in some areas of MPS is also supportive of this hypothesis. That is, there is no obvious reason why temperature changes would lead to a *Melaleuca* retreat at its seaward edge. However, it is likely that the increased stress of an increased RSL would result in a landward retreat of the MPS. The exponential increase in mangrove growth correlates to an increase in *Melaleuca* dieback between 1987-2020, which may suggest a common cause in these two vegetation changes. Dieback of *Melaleuca* observed in Northern Australia were suggested to have occurred as a result of SLR which caused in increased salinity, combined with the effects of feral ungulate damage (Bowman *et al.*, 2010; Sloane *et al.*, 2019). This demonstrates the impacts of introducing environmental stressors into a *Melaleuca* community.

Seaward and lateral changes account for the largest increase in coverage along the study site (Figure 4.10 C; Figure 4.11 C Figure 4.8 C and D; Figure 4.9 C and D). These changes are likely due to increased sedimentation rates causing greater rates of vertically accretion, increasing surface elevation to that suitable for mangrove development (Williams and Meehan, 2004; Roper *et al.*, 2011). Although there is no local data on sedimentation rates, the high mineral contribution within the mangrove core supports that there is sufficient mineral supply to allow for the mangrove expansion through these means. Natural cliffing has formed around the MPS which may explain the origins of a portion of the accumulated sediment (Figure 5.3). Areas where natural cliffing has occurred coincide with historic breaks in the mangrove communities. One possible explanation for this is that these exposed areas were eroded by inundation and subsequently deposited along the foreshore. This would also explain the initial lateral expansion of the mangroves between 1957- 2010: sediment accumulated, building the foundations for mangrove development. The largest and most well defined cliffing occurs along the eastern most break in the mangroves between 1987-2010, which was the last large lateral expansion (Figure 5.4). The majority of seaward expansion occurs after the lateral infilling of mangroves. The exponential change to coverage within the mangrove communities suggests that environmental conditions were altered around the 1980s. This coincides with the La Nina event that occurred between April 1988 and July 1989 (BOM, 2020). This period experienced high rainfall events in the highest decile, with strong effects on the south-east half of Australia. Large flood

events, including several flash floods across the Gippsland region which were preceded by two dry periods in the Gippsland area: The 1987 to 1988 El Nino; and the break that occurred during the La Nina event. These climatic events cause large runoff events and potentially alter sedimentation rates in the estuary as a result (McLaughlin *et al.*, 2003; Istanbuluoglu and Bras, 2006; Eslami-Andargoli *et al.*, 2010). The fine silt and clay sediment deposited in the upper reaches of Corner Inlet's tributaries may have been removed during this period (Dickson *et al.*, 2013). This change in sediment load would explain the large-scale expansion between 1987-2020. The non-linear acceleration in SLR over this time might also explain the non-linear mangrove expansion. Rising sea-levels have been shown to increase sediment loading in coastal wetlands and is another potential contributor to this hypothesised sediment movement (Morris *et al.*, 2002). The effect of mangrove communities on hydrodynamics and sediment accumulation naturally encourage sedimentation, while also reducing erosion rates (Furukawa *et al.*, 1997). The seaward and lateral changes may be attributed solely to this process or a combination of some of the aforementioned explanations.



Figure 5.3: Natural cliffing along the *Melaleuca* seaward edge. Image taken from within the outline boundary of Figure 5.4



Figure 5.4: Lateral expansion of the mangrove community that occurred between (A) 1987 and (B) 2010.

Extensive landward and lateral change occurred for the MPS, encroaching into the herbaceous wetlands of Corner Inlet (Figure 4.10 F; Figure 4.11 F Figure 4.8 G and H; Figure 4.9 G and H) . This interaction was suggested as far back as the 1960s as a result of increasing salinity causing a dieback and replacement of the *Phragmites australis* communities with MPS (Bird, 1961). However, salinity is unlikely to be the only factor driving changes between these communities. A similar study on short-term changes between herbaceous wetlands and MPS in the Gippsland region of south-east Australia found a 72% expansion of MPS and decline of 26% in the herbaceous wetlands (Boon *et al.*, 2008). Boon *et al.* (2008) suggests that a combination of salinity and inundation contributed to changes in microtopographical relief in the area. This would be further complimented by preservation capacity of *Melaleuca* spp. via the essential oils in their leaves (Bailey *et al.*, 2003). *Phragmites australis* has been found to have a lower tolerance than *Melaleuca* to increasing accumulation rates of organic matter (Morris *et al.*, 2008). MPS high productivity likely stressed the organic sensitive *Phragmites australis* resulting in its retreat.

Changes to the seaward extent of the MPS occur at a much slower rate than that of intertidal communities (Figure 4.8 G; Figure 4.9 G; Figure 4.10 E and F; Figure 4.11 E and F). This is potentially due the high rates in which MPS accumulate sediment. Higher

rates of vertical accumulation would assist in maintaining the elevation of the MPS with respects to a rising sea-level. This equilibrium is observed across 1957 to 1987, where little variation in *Melaleuca* extent occurs. This trend did not continue post 1987 with a majority of *Melaleuca* decline occurring between 1987-2020. The non-linear increase in MPS correlates to the exponential increase observed in the mangrove extent. These findings suggest that post 1987 rate of change in RSL has begun to exceed the rate in which the MPS can accumulate sediment, resulting in the spatial heterogeneity that has occurred in recent decades.

The comparatively slow retreat of the MPS acts as a landward boundary for the saltmarsh community, restricting the retreat of saltmarsh as a result of RSL. If the rate of change within the wetland communities continues, then saltmarsh will potentially see a localised extinction of the endangered community in this region of Corner Inlet. Saltmarsh decline and mangrove expansions can be attributed to each community's ability to vertically accrete sediment. Rogers *et al.* (2006) found saltmarsh to have a low capacity for vertical accretion comparatively to mangroves. This suggests that mangroves have a greater ability to respond to changes in SLR. Vertical accumulation of organic material in the MPS and intertidal wetlands is insufficient in maintaining elevation in Corner Inlet. Therefore, supply of mineral material will act as the limiting factor in the future resilience of the intertidal-supratidal complex to SLR.

5.4 Limitations and Further Research

The major limitation present in this study involved the spatial scale in which it covers. This study would have benefited from a larger scale assessment of the region using multiple transects for the analysis and increased spatial extent. A smaller scale assessment was chosen to allow for a higher resolution spatial analysis, while focusing on the same area the stratigraphic analysis took place to effectively compare the findings. Within the stratigraphic analysis the proportion of living root material to preserved organic matter within the surface organic horizon was difficult to delineate. This produces problems quantifying the organic preservation capacity of the wetlands surface sediments. Minor human error within the LOI, BD, grain size and spatial analyses potentially occurred. COVID-19 travel restrictions prevented the collection and download of salinity and water level logger data. This led to the data collected to be limited to single point in time (i.e. at installation of the loggers). This produced data that could be used as minor insight into the conditions of site. Resources for macrofossil identification are difficult to come by within literature and other available texts, while specimens collected may not be diagnostic for the identification of specific taxa.

Within the analysis of historic aerial photography several limitations arose based on image resolution and clarity. Imagery for 2010 and 2020 were sourced from Google Earth Pro and captured using CNES/Airbus. Due to this, the resolution of the image provided

presented a large limitation in assessing finer details. This combined with colouration of the photography, in particularly showing the contrast between juvenile mangroves and water in the 2010 image, and saltmarsh to bare ground in the 2020 image created error within digitised boundaries. Similar issues in contrast and resolution occurred in the photos from 1957-1969. Low contrast in the black and white aerial photograph made 1957 difficult to assess all boundaries, excluding mangrove. The boundary for saltmarsh and mangroves in 1969 was unclear due to little contrast. The uncertainty across imagery resulted in operator error during the digitisation process of vegetation delineation. Rate of change for the MPS was restricted by the unclear landward extent of the forest combined with limitation to georeferencing the inland vegetation. As a result, the area change was limited to a static and arbitrary landward boundary in the whole site and transect analyses. The final limitation of the spatial analysis came with addressing the spatial heterogeneity of the MPS. An overall rate of change was assessed for *Melaleuca*, despite a majority of change being localised to zones within the embayment.

Further research into the role of organic matter in MPS should be undertaken to develop the gaps within current literature. This would create a greater pool of information surrounding supratidal wetland forests of the temperate regions of Australia. As a result, the valid addition of MPS to the Rogers *et al.* (2019b) conceptual diagram could be developed to show the processes driving substrate development above HAT for wetland communities. Increasing the extent of the geospatial analysis to an estuary wide scale would allow for a deeper understanding of the recent changes and potential trajectory of Corner Inlets wetland communities. Extending this to the northern boundary of the embayment would potentially show a very different result being located at the mouth of many river systems draining into Corner Inlet. Addressing both above- and belowground biomass would further highlight the potential of supratidal wetland forests as carbon stores and their role within the carbon cycle. Develop our understanding of their importance would provide further rationale for the protection and conservation of these valued communities. Radiocarbon dating of macrofossils and bulk sediment samples within the core would generate an aspect of time through the profile and provide insight into the rate the estuary and wetlands are changing. The inclusion of other analyses that aid in distinguishing changes in environmental setting would allow for an improved reconstruction of the wetlands.

6 Conclusion

Organic material contribution within surface organic horizons were found to increase with elevation across the intertidal-supratidal gradient. Mangrove ecosystems were predominately low in organic matter when compared to saltmarsh, while the MPS had the highest organic contributions. This is a result of decreasing inundation with increasing elevation, limiting the overall mineral input. The high productivity MPS and low mineral input from tidal inundation resulted the proportionally organic-rich soil. Limits to the capacity of organic matter preservation were found surrounding MPS position. Correlations between soil moisture and organic composition were observed as the landward extent of the forest showed a shallow organic horizon and low sub-surface organic preservation, while the hydrated soils of the seaward *Melaleuca* demonstrated greater potential for preservation. Conversely, organic matter preservation may be resulting in higher water retention. Long-term changes within the estuary's wetlands follow the trends of subsequent infilling associated with estuarine evolution. That is, the wetland communities of the site have migrated seaward over the course of the Holocene, as indicated by the shifts in the stratigraphic record, marine influence and detrital remnants throughout the profile of the cores. In contrast to this, changes in vegetation distribution in recent years has predominantly seen a landwards retreat. Mangrove was found to be encroaching on the saltmarsh communities along with localised dieback of the MPS. Together these changes may be indicative of an increasing rate of SLR that exceeds vertical sediment accumulation, influence wetland community distribution. The landward retreat of MPS and related rise in sea-level may result in the belowground disruption of preserved organic matter. This may lead to alterations in the global carbon cycle with large proportion of organic matter sequestered in these forests to be remineralised into CO², having further implications on anthropogenic climate change.

Further research into organic matter contributions in temperate MPS and other supratidal wetland forests beyond a site-specific study would highlight their importance across temperate regions. An assessment addressing the above and belowground components would determine the role of MPS in organic preservation and total biomass. Increasing the spatial extent of the study would better present the estuary scale shifts in the wetland communities of Corner Inlet. This would enhance the understanding of the short-term changes occurring, while the addition of radiocarbon dating, and other analyses would improve the understand of the long-term changes that have occurred.

This study has highlighted the potential importance of temperate MPS as effective ecosystems in biomass accumulation and preservation, presenting the role MPS play in the global carbon cycle as a carbon sink. It was also able to identify the ubiquitous trend of temperate mangroves expansion and encroachment towards saltmarsh occurring in recent years, while presenting some of the first evidence for the retreat of seaward *Melaleuca* margins in temperate Australia.

References

- ABARES, (2016). 'Australian Bureau of Agricultural and Resource Economics and Sciences. Department of Agriculture and Water Resources. Australian Government. Australian forest profiles: Melaleuca.' Tech. rep.
- Adam, P., (1993). *Saltmarsh ecology*. Cambridge University Press.
- Adame, M. F., Reef, R., Wong, V. N., Balcombe, S. R., Turschwell, M. P., Kavehei, E., Rodríguez, D. C., Kelleway, J. J., Masque, P. and Ronan, M., (2019). 'Carbon and Nitrogen Sequestration of Melaleuca Floodplain Wetlands in Tropical Australia.' *Ecosystems*. ISSN 14350629. doi:10.1007/s10021-019-00414-5.
- Allen, J. R., (2000). 'Morphodynamics of Holocene salt marshes: A review sketch from the Atlantic and Southern North Sea coasts of Europe.' *Quaternary Science Reviews*, vol. 19(12), pp. 1155–1231. ISSN 02773791. doi:10.1016/S0277-3791(99)00034-7.
- Alongi, D., (2009). *The energetics of mangrove forests*. Springer Science & Business Media.
- Alongi, D. M., (2002). 'Present state and future of the world's mangrove forests.' *Environmental Conservation*, vol. 29(3), pp. 331–349. ISSN 03768929. doi:10.1017/S0376892902000231.
- Alongi, D. M., (2014). 'Carbon Cycling and Storage in Mangrove Forests.' *Annual Review of Marine Science*, vol. 6(1), pp. 195–219. ISSN 1941-1405. doi:10.1146/annurev-marine-010213-135020.
- Bailey, P., Watkins, S., Morris, K. and Boon, P., (2003). 'Do Melaleuca ericifolia SM. leaves suppress organic matter decay in freshwater wetlands?' *Archiv für Hydrobiologie*, vol. 156(2), pp. 225–240.
- Baker, C., Thompson, J. R. and Simpson, M., (2009). 'Hydrological dynamics I: surface waters, flood and sediment dynamics.' In: 'The Wetlands Handbook,' pp. 120–168.
- Barlow, B. A., (1988). 'Patterns of differentiation in tropical species of Melaleuca L.(Myrtaceae).'
- Bird, E., (1961). 'The Coastal Barriers of East Gippsland , Australia.' *Royal, The Society, Geographical Geographers, British*.
- Bird, E., (1993). *The coast of Victoria: the shaping of scenery*. Melbourne University Press.
- BOM, (2020). 'Bureau of Meteorology - Climate statistics for Australian locations.' Tech. rep.

- Boon, P., Keith, D. and Raulings, E., (2016). 'Vegetation of coastal floodplains and wetlands in south-eastern Australia.' *Vegetation of Australia's Riverine Landscapes*, CSIRO Publishing, Collingwood, VIC, pp. 145–176.
- Boon, P., Raulings, E., Roach, M. and Morris, K., (2008). 'Vegetation changes over a four decade period in Dowd Morass, a brackish-water wetland of the Gippsland Lakes, South-Eastern Australia.' *Proceedings of the Royal Society of Victoria*, vol. 120(2), pp. 403–418.
- Bowkett, L. A. and Kirkpatrick, J. B., (2003). 'Ecology and conservation of remnant *Melaleuca ericifolia* stands in the Tamar Valley, Tasmania.' *Australian Journal of Botany*, vol. 51(4), pp. 405–413. ISSN 00671924. doi:10.1071/BT02071.
- Bowman, D. M., Prior, L. D. and De Little, S. C., (2010). 'Retreating *Melaleuca* swamp forests in Kakadu National Park: Evidence of synergistic effects of climate change and past feral buffalo impacts.' *Austral Ecology*, vol. 35(8), pp. 898–905. ISSN 14429985. doi:10.1111/j.1442-9993.2009.02096.x.
- Boyd, J. and Banzhaf, S., (2007). 'What are ecosystem services? The need for standardized environmental accounting units.' *Ecological Economics*, vol. 63(2-3), pp. 616–626. ISSN 09218009. doi:10.1016/j.ecolecon.2007.01.002.
- Boyd, R., (1992). 'Classification of clastic coastal depositional environments.' vol. 80, pp. 139–150.
- Buckney, R. T., (1987). 'Three decades of habitat change: Kooragang Island.' *New South Wales*, pp. 227–232.
- Burns, B. R. and Ogden, J., (1985). 'The demography of the temperate mangrove [*Avicennia marina* (Forsk.) Vierh.] at its southern limit in New Zealand.' *Australian Journal of Ecology*, vol. 10(2), pp. 125–133. ISSN 14429993. doi:10.1111/j.1442-9993.1985.tb00874.x.
- Chafer, C. J., (1998). 'A Spatio-temporal analysis of estuarine vegetation change in the Minnamurra River 1938-1997.'
- Chmura, G. L., Anisfeld, S. C., Cahoon, D. R. and Lynch, J. C., (2003). 'Global carbon sequestration in tidal, saline wetland soils.' *Global Biogeochemical Cycles*, vol. 17(4), pp. n/a–n/a. ISSN 0886-6236. doi:10.1029/2002gb001917.
- Clarke, P. and Benson, D., (2010). 'The natural vegetation of Homebush Bay - Two hundred years of changes.' doi:10.31646/wa.121.

- Clarke, P. J. and Jacoby, C. A., (1994). 'Biomass and above-ground productivity of salt-marsh plants in south-eastern Australia.' *Marine and Freshwater Research*, vol. 45(8), pp. 1521–1528. ISSN 13231650. doi:10.1071/MF9941521.
- Cooper, J. A., (2001). 'Geomorphological variability among microtidal estuaries from the wave-dominated South African coast.' *Geomorphology*, vol. 40(1-2), pp. 99–122. ISSN 0169555X. doi:10.1016/S0169-555X(01)00039-3.
- Cooper, J. A. G., (1993). 'Sedimentation in a river dominated estuary.' *Sedimentology*, vol. 40(5), pp. 979–1017. ISSN 13653091. doi:10.1111/j.1365-3091.1993.tb01372.x.
- Crowley, G. M. and Gagan, M. K., (1995). 'Holocene evolution of coastal wetlands in wet-tropical northeastern Australia.' *Holocene*, vol. 5(4), pp. 385–399. ISSN 09596836. doi:10.1177/095968369500500401.
- Dalrymple, R. W., Knight, R. J., Zaitlin, B. A. and Middleton, G. V., (1990). 'Dynamics and facies model of a macrotidal sand-bar complex, Cobequid Bay—Salmon River Estuary (Bay of Fundy).' *Sedimentology*, vol. 37(4), pp. 577–612. ISSN 13653091. doi:10.1111/j.1365-3091.1990.tb00624.x.
- Dalrymple, R. W., Zaitlin, B. A. and Boyd, R., (1992). 'Estuarine facies models : conceptual basis and stratigraphic implications.' *Journal of Sedimentary Petrology*, vol. 62(6), pp. 1130–1146. ISSN 00224472. doi:10.1306/D4267A69-2B26-11D7-8648000102C1865D.
- de Groot, R., Brander, L., van der Ploeg, S., Costanza, R., Bernard, F., Braat, L., Christie, M., Crossman, N., Ghermandi, A., Hein, L., Hussain, S., Kumar, P., McVittie, A., Portela, R., Rodriguez, L. C., ten Brink, P. and van Beukering, P., (2012). 'Global estimates of the value of ecosystems and their services in monetary units.' *Ecosystem Services*, vol. 1(1), pp. 50–61. ISSN 22120416. doi:10.1016/j.ecoser.2012.07.005.
URL: <http://dx.doi.org/10.1016/j.ecoser.2012.07.005>
- de Neiff, A., Neiff, J. and Casco, S., (2006). 'Leaf litter decomposition in three wetland types of the Paraná River floodplain.' *Wetlands*, vol. 26(2), pp. 558–566. ISSN 0277-5212. doi:10.1672/0277-5212(2006)26[558:LLDITW]2.0.CO;2.
- Debra, J., Terry, R. and Penelope, J., (2010). 'Expansion Dynamics of Monospecific, Temperate Mangroves and Sedimentation i...: EBSCOhost.'
- Del Grosso, S., Parton, W., Stohlgren, T., Zheng, D., Bachelet, D., Prince, S., Hibbard, K. and Olson, R., (2010). 'Global potential net primary production predicted from vegetation class, precipitation, and temperature: Comment.' *Ecology*, vol. 91(3), pp. 921–923. ISSN 00129658. doi:10.1890/08-2018.1.

- DeLaune, R. D. and White, J. R., (2012). 'Will coastal wetlands continue to sequester carbon in response to an increase in global sea level?: A case study of the rapidly subsiding Mississippi river deltaic plain.' *Climatic Change*, vol. 110(1-2), pp. 297–314. ISSN 01650009. doi:10.1007/s10584-011-0089-6.
- Dickson, M., Park, G. and Roberts, A., (2013). 'Corner Inlet Water Quality Improvement Plan 2013. West Gippsland Catchment Management Authority.'
- Dise, N. B., (2009). 'Biogeochemical Dynamics III: The Critical Role of Carbon in Wetlands.' In: 'The Wetlands Handbook,' p. 249.
- Dixon, R. K., Brown, S., Houghton, R. A., Solomon, A. M., Trexler, M. C. and Wisniewski, J., (1994). 'Carbon pools and flux of global forest ecosystems.' *Science*, vol. 263(5144), pp. 185–190. ISSN 00368075. doi:10.1126/science.263.5144.185.
- Donato, D. C., Kauffman, J. B., Murdiyarso, D., Kurnianto, S., Stidham, M. and Kanninen, M., (2011). 'Mangroves among the most carbon-rich forests in the tropics.' *Nature Geoscience*, vol. 4(5), pp. 293–297. ISSN 17520894. doi:10.1038/ngeo1123.
- Duarte, C. M., Losada, I. J., Hendriks, I. E., Mazarrasa, I. and Marbà, N., (2013). 'The role of coastal plant communities for climate change mitigation and adaptation.' *Nature Climate Change*, vol. 3(11), pp. 961–968. ISSN 1758678X. doi:10.1038/nclimate1970.
- Eskert, C. G., (2002). 'The loss of sex in clonal plants.' In: 'Ecology and evolutionary biology of clonal plants,' pp. 279–298.
- Eslami-Andargoli, L., Dale, P. E., Sipe, N. and Chaseling, J., (2010). 'Local and landscape effects on spatial patterns of mangrove forest during wetter and drier periods: Moreton Bay, Southeast Queensland, Australia.' *Estuarine, Coastal and Shelf Science*, vol. 89(1), pp. 53–61. ISSN 02727714. doi:10.1016/j.ecss.2010.05.011.
URL: <http://dx.doi.org/10.1016/j.ecss.2010.05.011>
- Finlayson, C., Cowie, I. and Bailey, B., (1993). 'Biomass and litter dynamics in a Melaleuca forest on a seasonally inundated floodplain in tropical, northern Australia.' *Wetlands Ecology and Management*, vol. 2(4), pp. 177–188.
- French, J., (2006). 'Tidal marsh sedimentation and resilience to environmental change: Exploratory modelling of tidal, sea-level and sediment supply forcing in predominantly allochthonous systems.' *Marine Geology*, vol. 235(1-4 SPEC. ISS.), pp. 119–136. ISSN 00253227. doi:10.1016/j.margeo.2006.10.009.
- Friess, D. A., Krauss, K. W., Horstman, E. M., Balke, T., Bouma, T. J., Galli, D. and Webb, E. L., (2012). 'Are all intertidal wetlands naturally created equal? Bottlenecks, thresholds

- and knowledge gaps to mangrove and saltmarsh ecosystems.’ *Biological Reviews*, vol. 87(2), pp. 346–366. ISSN 14647931. doi:10.1111/j.1469-185X.2011.00198.x.
- Furukawa, K., Wolanski, E. and Mueller, H., (1997). ‘Currents and sediment transport in mangrove forests.’ *Estuarine, Coastal and Shelf Science*, vol. 44(3), pp. 301–310. ISSN 02727714. doi:10.1006/ecss.1996.0120.
- Galloway, R. W., (1982). ‘Distribution and physiographic patterns of Australian mangroves.’ In: ‘Mangrove ecosystems in Australia: Structure, function and management,’ pp. 31–54.
- Gilmour, W., (2014). ‘Corner Inlet Dynamic Storm Tide Modelling Assessment.’ (June).
- Giri, C., Ochieng, E., Tieszen, L. L., Zhu, Z., Singh, A., Loveland, T., Masek, J. and Duke, N., (2011). ‘Status and distribution of mangrove forests of the world using earth observation satellite data.’ *Global Ecology and Biogeography*, vol. 20(1), pp. 154–159. ISSN 1466822X. doi:10.1111/j.1466-8238.2010.00584.x.
- Gray, A. B., Pasternack, G. B. and Watson, E. B., (2010). ‘Hydrogen peroxide treatment effects on the particle size distribution of alluvial and marsh sediments.’ *Holocene*, vol. 20(2), pp. 293–301. ISSN 09596836. doi:10.1177/0959683609350390.
- Greenway, M., (1994). ‘Litter accession and accumulation in a melaleuca quinquenervia (Cav.) s.t. blake wetland in South-Eastern Queensland.’ *Marine and Freshwater Research*, vol. 45(8), pp. 1509–1519. ISSN 13231650. doi:10.1071/MF9941509.
- Harris, P., Heap, A., Bryce, S., Porter-Smith, R., Ryan, D. and Heggie, D., (2002). ‘Classification of Australian Clastic Coastal Depositional Environments Based Upon a Quantitative Analysis of Wave, Tidal, and River Power.’ *Journal of Sedimentary Research*, vol. 72(6), pp. 858–870. ISSN 1527-1404. doi:10.1306/040902720858.
- Heap, A. D., Bryce, S. and Ryan, D. A., (2004). ‘Facies evolution of Holocene estuaries and deltas: A large-sample statistical study from Australia.’ *Sedimentary Geology*, vol. 168(1-2), pp. 1–17. ISSN 00370738. doi:10.1016/j.sedgeo.2004.01.016.
- Heiri, O., Lotter, A. F. and Lemcke, G., (2001). ‘Loss on ignition as a method for estimating organic and carbonate content in sediments: Reproducibility and comparability of results.’ *Journal of Paleolimnology*, vol. 25(1), pp. 101–110. ISSN 09212728. doi:10.1023/A:1008119611481.
- Hodgkin, E. P. and Hesp, P., (1998). ‘Estuaries to salt lakes: Holocene transformation of the estuarine ecosystems of south-western Australia.’ *Marine and Freshwater Research*, vol. 49(3), pp. 183–201. ISSN 13231650. doi:10.1071/MF96109.

- Hodgkin, E. P. and Kendrick, G. W., (1984). 'The changing aquatic environment 7000 BP to 1983 in the estuaries of south western Australia.' *Estuarine Environments of the Southern Hemisphere*, pp. 85–95.
- Howard, J., Hoyt, S., Isensee, K., Pidgeon, E. and Telszewski, M., (2014). 'Coastal Blue Carbon.' *National Wetlands Newsletter*.
- Hughes, M., Swetnam, T. and Diaz, H., (2010). *Developments in Paleoenvironmental Research, ed. Smol JP*. ISBN 9789400778160.
- Istanbulluoglu, E. and Bras, R. L., (2006). 'On the dynamics of soil moisture, vegetation, and erosion: Implications of climate variability and change.' *Water Resources Research*, vol. 42(6), pp. 1–17. ISSN 00431397. doi:10.1029/2005WR004113.
- Janzen, H. H., (2004). 'Carbon cycling in earth systems - A soil science perspective.' *Agriculture, Ecosystems and Environment*, vol. 104(3), pp. 399–417. ISSN 01678809. doi:10.1016/j.agee.2004.01.040.
- Jeanes, J. A., (1996). 'Myrtaceae.' In: 'Flora of Victoria Volume 3, Dicotyledons Winteraceae to Myrtaceae,' pp. 942–1044.
- Jupiter, S. D., Potts, D. C., Phinn, S. R. and Duke, N. C., (2007). 'Natural and anthropogenic changes to mangrove distributions in the Pioneer River Estuary (QLD, Australia).' *Wetlands Ecology and Management*, vol. 15(1), pp. 51–62. ISSN 09234861. doi:10.1007/s11273-006-9011-9.
- Kelleway, J. J., Cavanaugh, K., Rogers, K., Feller, I. C., Ens, E., Doughty, C. and Saintilan, N., (2017a). 'Review of the ecosystem service implications of mangrove encroachment into salt marshes.' *Global Change Biology*, vol. 23(10), pp. 3967–3983. ISSN 13652486. doi:10.1111/gcb.13727.
- Kelleway, J. J., Mazumder, D., Baldock, J. A. and Saintilan, N., (2018). 'Carbon isotope fractionation in the mangrove *Avicennia marina* has implications for food web and blue carbon research.' *Estuarine, Coastal and Shelf Science*. ISSN 02727714. doi:10.1016/j.ecss.2018.03.011.
- Kelleway, J. J., Saintilan, N., Macreadie, P. I., Baldock, J. A., Heijnen, H., Zawadzki, A., Gadd, P., Jacobsen, G. and Ralph, P. J., (2017b). 'Geochemical analyses reveal the importance of environmental history for blue carbon sequestration.' *Journal of Geophysical Research: Biogeosciences*, vol. 122(7), pp. 1789–1805. ISSN 21698961. doi:10.1002/2017JG003775.

- Kelleway, J. J., Saintilan, N., Macreadie, P. I. and Ralph, P. J., (2016a). ‘Sedimentary Factors are Key Predictors of Carbon Storage in SE Australian Saltmarshes.’ *Ecosystems*, vol. 19(5), pp. 865–880. ISSN 14350629. doi:10.1007/s10021-016-9972-3.
- Kelleway, J. J., Saintilan, N., Macreadie, P. I., Skilbeck, C. G., Zawadzki, A. and Ralph, P. J., (2016b). ‘Seventy years of continuous encroachment substantially increases ‘blue carbon’ capacity as mangroves replace intertidal salt marshes.’ *Global Change Biology*, vol. 22(3), pp. 1097–1109. ISSN 13652486. doi:10.1111/gcb.13158.
- Kirk, G., (2004). *The biogeochemistry of submerged soils*. John Wiley & Sons.
- Kirwan, M. L. and Blum, L. K., (2011). ‘Enhanced decomposition offsets enhanced productivity and soil carbon accumulation in coastal wetlands responding to climate change.’ *Biogeosciences*, vol. 8(4), pp. 987–993. ISSN 17264170. doi:10.5194/bg-8-987-2011.
- Kirwan, M. L., Kirwan, J. L. and Copenheaver, C. A., (2007). ‘Dynamics of an estuarine forest and its response to rising sea level.’ *Journal of Coastal Research*, vol. 23(2), pp. 457–463. ISSN 07490208. doi:10.2112/04-0211.1.
- Kirwan, M. L. and Megonigal, J. P., (2013). ‘Tidal wetland stability in the face of human impacts and sea-level rise.’ doi:10.1038/nature12856.
- Kirwan, M. L. and Mudd, S. M., (2012). ‘Response of salt-marsh carbon accumulation to climate change.’ *Nature*, vol. 489(7417), pp. 550–553. ISSN 00280836. doi:10.1038/nature11440.
- Krauss, K. W., Cahoon, D. R., Allen, J. A., Ewel, K. C., Lynch, J. C. and Cormier, N., (2010). ‘Surface elevation change and susceptibility of different mangrove zones to sea-level rise on Pacific high islands of Micronesia.’ *Ecosystems*, vol. 13(1), pp. 129–143. ISSN 14329840. doi:10.1007/s10021-009-9307-8.
- Krauss, K. W., Mckee, K. L., Lovelock, C. E., Cahoon, D. R., Saintilan, N., Reef, R. and Chen, L., (2014). ‘How mangrove forests adjust to rising sea level.’ *New Phytologist*, vol. 202(1), pp. 19–34. ISSN 0028646X. doi:10.1111/nph.12605.
- Ladiges, P. Y., Foord, P. C. and Willis, R. J., (1981). ‘Salinity and waterlogging tolerance of some populations of *Melaleuca ericifolia* Smith.’ *Australian Journal of Ecology*, vol. 6(2), pp. 203–215. ISSN 14429993. doi:10.1111/j.1442-9993.1981.tb01291.x.
- Lal, R., (2005). ‘Forest soils and carbon sequestration.’ *Forest Ecology and Management*, vol. 220(1-3), pp. 242–258. ISSN 03781127. doi:10.1016/j.foreco.2005.08.015.

- Lambeck, K. and Bard, E., (2000). 'Sea-level change along the French Mediterranean coast for the past 30000 years.' *Earth and Planetary Science Letters*, vol. 175(3-4), pp. 203–222. ISSN 0012821X. doi:10.1016/s0012-821x(99)00289-7.
- Lambeck, K. and Chappell, J., (2001). 'Sea level change through the last glacial cycle.' *Science*, vol. 292(5517), pp. 679–686. ISSN 00368075. doi:10.1126/science.1059549.
- Lo Iocano, C., Mateo, M. A., Gràcia, E., Guasch, L., Carbonell, R., Serrano, L., Serrano, O. and Dañobeitia, J., (2008). 'Very high-resolution seismo-acoustic imaging of seagrass meadows (Mediterranean Sea): Implications for carbon sink estimates.' *Geophysical Research Letters*, vol. 35(18), pp. 1–5. ISSN 00948276. doi:10.1029/2008GL034773.
- Lovelock, C. E., Ball, M. C., Martin, K. C. and Feller, I. C., (2009). 'Nutrient enrichment increases mortality of mangroves.' *PLoS ONE*, vol. 4(5), pp. 4–7. ISSN 19326203. doi:10.1371/journal.pone.0005600.
- Macphail, R. I., Allen, M. J., Crowther, J., Cruise, G. M. and Whittaker, J. E., (2010). 'Marine inundation: Effects on archaeological features, materials, sediments and soils.' *Quaternary International*, vol. 214(1-2), pp. 44–55. ISSN 10406182. doi:10.1016/j.quaint.2009.10.020.
URL: <http://dx.doi.org/10.1016/j.quaint.2009.10.020>
- Marion, C., Anthony, E. J. and Trentesaux, A., (2009). 'Short-term (2 yrs) estuarine mudflat and saltmarsh sedimentation: High-resolution data from ultrasonic altimetry, rod surface-elevation table, and filter traps.' *Estuarine, Coastal and Shelf Science*, vol. 83(4), pp. 475–484. ISSN 02727714. doi:10.1016/j.ecss.2009.03.039.
URL: <http://dx.doi.org/10.1016/j.ecss.2009.03.039>
- McLaughlin, C. J., Smith, C. A., Buddemeier, R. W., Bartley, J. D. and Maxwell, B. A., (2003). 'Rivers, runoff, and reefs.' *Global and Planetary Change*, vol. 39(1-2), pp. 191–199. ISSN 09218181. doi:10.1016/S0921-8181(03)00024-9.
- McLeod, E., Chmura, G. L., Bouillon, S., Salm, R., Björk, M., Duarte, C. M., Lovelock, C. E., Schlesinger, W. H. and Silliman, B. R., (2011). 'A blueprint for blue carbon: Toward an improved understanding of the role of vegetated coastal habitats in sequestering CO₂.' *Frontiers in Ecology and the Environment*, vol. 9(10), pp. 552–560. ISSN 15409295. doi:10.1890/110004.
- McSweeney, S. L., Kennedy, D. M. and Rutherford, I. D., (2018). 'The daily-scale entrance dynamics of intermittently open/closed estuaries.' *Earth Surface Processes and Landforms*, vol. 43(4), pp. 791–807. ISSN 10969837. doi:10.1002/esp.4280.
- MEA, (2005). 'Ecosystems and human well-being.' Tech. rep., United States of America: Island press.

- Mitsch, W. J. and Gossilink, J. G., (2000). ‘The value of wetlands: Importance of scale and landscape setting.’ *Ecological Economics*, vol. 35(1), pp. 25–33. ISSN 09218009. doi:10.1016/S0921-8009(00)00165-8.
- Morris, J. T., Barber, D. C., Callaway, J. C., Chambers, R., Hagen, S. C., Hopkinson, C. S., Johnson, B. J., Megonigal, P., Neubauer, S. C., Troxler, T. and Wigand, C., (2016). ‘Contributions of organic and inorganic matter to sediment volume and accretion in tidal wetlands at steady state.’ *Earth’s Future*, vol. 4(4), pp. 110–121. ISSN 23284277. doi:10.1002/2015EF000334.
- Morris, J. T., Sundareshwar, P. V., Nietch, C. T., Kjerfve, B. and Cahoon, D. R., (2002). ‘Responses of coastal wetlands to rising sea level.’ *Ecology*, vol. 83(10), pp. 2869–2877. ISSN 00129658. doi:10.1890/0012-9658(2002)083[2869:ROCWTR]2.0.CO;2.
- Morris, K., Boon, P. I., Raulings, E. J. and White, S. D., (2008). ‘Floristic shifts in wetlands: The effects of environmental variables on the interaction between *Phragmites australis* (Common Reed) and *Melaleuca ericifolia* (Swamp Paperbark).’ *Marine and Freshwater Research*, vol. 59(3), pp. 187–204. ISSN 13231650. doi:10.1071/MF07072.
- Morrisey, D. J., Skilleter, G. A., Ellis, J. I., Burns, B. R., Kemp, C. E. and Burt, K., (2003). ‘Differences in benthic fauna and sediment among mangrove (*Avicennia marina* var. *australasica*) stands of different ages in New Zealand.’ *Estuarine, Coastal and Shelf Science*, vol. 56(3-4), pp. 581–592. ISSN 02727714. doi:10.1016/S0272-7714(02)00208-1.
- Nixon, S. W., (1980). ‘Between coastal marshes and coastal waters—a review of twenty years of speculation and research on the role of salt marshes in estuarine productivity and water chemistry.’ In: ‘Estuarine and wetland processes,’ pp. 437–525.
- Oppenheimer, M., Glavovic, B., Hinkel, J., van de Wal, R., Magnan, A., Abd-Elgawad, A., Cai, R., Cifuentes-Jara, M., Deconto, R., Ghosh, T. and Hay, J., (2019). ‘Sea level rise and implications for low lying islands, coasts and communities.’
- Osland, M. J., Day, R. H., Hall, C. T., Brumfield, M. D., Dugas, J. L. and Jones, W. R., (2017). ‘Mangrove expansion and contraction at a poleward range limit: Climate extremes and land-ocean temperature gradients.’ *Ecology*, vol. 98(1), pp. 125–137. ISSN 00129658. doi:10.1002/ecy.1625.
- Osland, M. J., Enwright, N., Day, R. H. and Doyle, T. W., (2013). ‘Winter climate change and coastal wetland foundation species: Salt marshes vs. mangrove forests in the southeastern United States.’ *Global Change Biology*, vol. 19(5), pp. 1482–1494. ISSN 13541013. doi:10.1111/gcb.12126.

- Pennings, S. C., Grant, M. B. and Bertness, M. D., (2005). 'Plant zonation in low-latitude salt marshes: Disentangling the roles of flooding, salinity and competition.' *Journal of Ecology*, vol. 93(1), pp. 159–167. ISSN 00220477. doi:10.1111/j.1365-2745.2004.00959.x.
- Perillo, G., Wolanski, E., Cahoon, D. R. and Hopkinson, C. S., (2018). *Coastal wetlands: an integrated ecosystem approach*. Elsevier.
- Pester, M., Knorr, K. H., Friedrich, M. W., Wagner, M. and Loy, A., (2012). 'Sulfate-reducing microorganisms in wetlands - fameless actors in carbon cycling and climate change.' *Frontiers in Microbiology*, vol. 3(FEB), pp. 1–19. ISSN 1664302X. doi:10.3389/fmicb.2012.00072.
- Raulings, E. J., Boon, P. I., Bailey, P. C., Roache, M. C., Morris, K. and Robinson, R., (2007). 'Rehabilitation of Swamp Paperbark (*Melaleuca ericifolia*) wetlands in south-eastern Australia: Effects of hydrology, microtopography, plant age and planting technique on the success of community-based revegetation trials.' *Wetlands Ecology and Management*, vol. 15(3), pp. 175–188. ISSN 09234861. doi:10.1007/s11273-006-9022-6.
- Reed, D. J., (1995). 'The response of coastal marshes to sea-level rise: Survival or submergence?' *Earth Surface Processes and Landforms*, vol. 20(1), pp. 39–48. ISSN 10969837. doi:10.1002/esp.3290200105.
- Robinson, R. W., Boon, P. I. and Bailey, P., (2006). 'Germination characteristics of *Melaleuca ericifolia* Sm. (swamp paperbark) and their implications for the rehabilitation of coastal wetlands.' *Marine and Freshwater Research*, vol. 57(7), pp. 703–711. ISSN 13231650. doi:10.1071/MF06006.
- Rogers, K., Kelleway, J. J., Saintilan, N., Megonigal, J. P., Adams, J. B., Holmquist, J. R., Lu, M., Schile-Beers, L., Zawadzki, A., Mazumder, D. and Woodroffe, C. D., (2019a). 'Wetland carbon storage controlled by millennial-scale variation in relative sea-level rise.' *Nature*, vol. 567(7746), pp. 91–95. ISSN 14764687. doi:10.1038/s41586-019-0951-7. **URL:** <http://dx.doi.org/10.1038/s41586-019-0951-7>
- Rogers, K., Kelleway, J. J., Saintilan, N., Megonigal, J. P., Adams, J. B., Holmquist, J. R., Lu, M., Schile-Beers, L., Zawadzki, A., Mazumder, D. and Woodroffe, C. D., (2019b). 'Wetland carbon storage controlled by millennial-scale variation in relative sea-level rise.' *Nature*, vol. 567(7746), pp. 91–95. ISSN 14764687. doi:10.1038/s41586-019-0951-7. **URL:** <http://dx.doi.org/10.1038/s41586-019-0951-7>
- Rogers, K., Macreadie, P. I., Kelleway, J. J. and Saintilan, N., (2019c). 'Blue carbon

- in coastal landscapes: a spatial framework for assessment of stocks and additionality.' *Sustainability Science*. ISSN 18624057. doi:10.1007/s11625-018-0575-0.
- Rogers, K. and Saintilan, N., (2008). 'Relationships between surface elevation and groundwater in mangrove forests of southeast Australia.' *Journal of Coastal Research*, vol. 24, pp. 63–69.
- Rogers, K., Saintilan, N. and Heijnis, H., (2005). 'Mangrove encroachment of salt marsh in Western Port Bay, Victoria: The role of sedimentation, subsidence, and sea level rise.' *Estuaries*, vol. 28(4), pp. 551–559. ISSN 01608347. doi:10.1007/BF02696066.
- Rogers, K., Wilton, K. and Saintilan, N., (2006). 'Vegetation change and surface elevation dynamics in estuarine wetlands of southeast Australia.' *Estuarine, Coastal and Shelf Science*, vol. 66(3-4), pp. 559–589.
- Roper, T., Creese, B., Scanes, P., Stephens, K., Williams, R., Dela-Cruz, J., Coade, G., Coates, B. and Fraser, M., (2011). 'Assessing the condition of estuaries and coastal lake ecosystems in NSW.'
- Rothwell, R. G., Hoogakker, B., Thomson, J., Croudace, I. W. and Frenz, M., (2006). 'Turbidite emplacement on the southern Balearic Abyssal Plain (western Mediterranean Sea) during Marine Isotope Stages 1-3: An application of ITRAX XRF scanning of sediment cores to lithostratigraphic analysis.' *Geological Society Special Publication*, vol. 267(Haschke 2006), pp. 79–98. ISSN 03058719. doi:10.1144/GSL.SP.2006.267.01.06.
- Roy, P. S., (1984). 'New South Wales estuaries: their origin and evolution.' *Coastal geomorphology in Australia*.
- Roy, P. S., (1994). 'Holocene estuary evolution—stratigraphic studies from southeastern Australia.'
- Roy, P. S., Williams, R. J., Jones, A. R., Yassini, I., Gibbs, P. J., Coates, B., West, R. J., Scanes, P. R., Hudson, J. P. and Nichol, S., (2001). 'Structure and function of south-east Australian estuaries.' *Estuarine, Coastal and Shelf Science*, vol. 53(3), pp. 351–384. ISSN 02727714. doi:10.1006/ecss.2001.0796.
- Rozaimi, M., Lavery, P. S., Serrano, O. and Kyrwood, D., (2016). 'Long-term carbon storage and its recent loss in an estuarine *Posidonia australis* meadow (Albany, Western Australia).' *Estuarine, Coastal and Shelf Science*, vol. 171, pp. 58–65. ISSN 02727714. doi:10.1016/j.ecss.2016.01.001.
- URL:** <http://dx.doi.org/10.1016/j.ecss.2016.01.001>

- Saintilan, N., (1997). 'Above-and below-ground biomasses of two species of mangrove on the Hawkesbury River estuary, New South Wales.' *Marine and Freshwater Research*, vol. 48(2), pp. 147–152.
- Saintilan, N., (2009). 'Distribution of Australian saltmarsh plants.' In: 'Australian saltmarsh ecology,' p. 23.
- Saintilan, N. and Hashimoto, T. R., (1999). 'Mangrove-saltmarsh dynamics on a bay-head delta in the Hawkesbury River estuary, New South Wales, Australia.' In: 'Diversity and Function in Mangrove Ecosystems,' pp. 95–102. Springer, Dordrecht.
- Saintilan, N., Rogers, K., Kelleway, J. J., Ens, E. and Sloane, D. R., (2018). 'Climate Change Impacts on the Coastal Wetlands of Australia.' *Wetlands*, pp. 1–10. ISSN 19436246. doi:10.1007/s13157-018-1016-7.
- Saintilan, N., Rogers, K., Mazumder, D. and Woodroffe, C., (2013). 'Allochthonous and autochthonous contributions to carbon accumulation and carbon store in southeastern Australian coastal wetlands.' *Estuarine, Coastal and Shelf Science*, vol. 128, pp. 84–92. ISSN 02727714. doi:10.1016/j.ecss.2013.05.010.
- Saintilan, N. and Williams, R. J., (1999a). 'Mangrove transgression into saltmarsh environments in south-east Australia.' *Global Ecology and Biogeography*, vol. 8(2), pp. 117–124. ISSN 1466822X. doi:10.1046/j.1365-2699.1999.00133.x.
- Saintilan, N. and Williams, R. J., (1999b). 'Mangrove transgression into saltmarsh environments in south-east Australia.' *Global Ecology and Biogeography*, vol. 8(2), pp. 117–124. ISSN 1466822X. doi:10.1046/j.1365-2699.1999.00133.x.
- Saintilan, N., Wilson, N. C., Rogers, K. and Rajkaran, A., (2014). 'Mangrove expansion and salt marsh decline at mangrove poleward limits.' pp. 147–157. doi:10.1111/gcb.12341.
- Saintilan, N. and Wilton, K., (2001). 'Changes in the distribution of mangroves and saltmarshes in Jervis Bay, Australia.' *Wetlands Ecology and Management*, vol. 9(5), pp. 409–420. ISSN 09234861. doi:10.1023/A:1012073018996.
- Salter, J., Morris, K., Bailey, P. C. and Boon, P. I., (2007). 'Interactive effects of salinity and water depth on the growth of *Melaleuca ericifolia* Sm. (Swamp paperbark) seedlings.' *Aquatic Botany*, vol. 86(3), pp. 213–222. ISSN 03043770. doi:10.1016/j.aquabot.2006.10.002.
- Salter, J., Morris, K., Read, J. and Boon, P. I., (2010). 'Understanding the potential effects of water regime and salinity on recruitment of *Melaleuca ericifolia* Sm.' *Aquatic Botany*, vol. 93(3), pp. 200–206.

- Schieder, N. W., Walters, D. C. and Kirwan, M. L., (2018). 'Massive Upland to Wetland Conversion Compensated for Historical Marsh Loss in Chesapeake Bay, USA.' *Estuaries and Coasts*, vol. 41(4), pp. 940–951. ISSN 15592731. doi:10.1007/s12237-017-0336-9.
- Siikamäki, J., Sanchirico, J. N. and Jardine, S. L., (2012). 'Global economic potential for reducing carbon dioxide emissions from mangrove loss.' *Proceedings of the National Academy of Sciences of the United States of America*, vol. 109(36), pp. 14 369–14 374. ISSN 00278424. doi:10.1073/pnas.1200519109.
- Sloane, D. R., Ens, E., Wunungmurra, J., Falk, A., Marika, G., Maymuru, M., Towler, G. and Preece, D., (2019). 'Western and Indigenous knowledge converge to explain Melaleuca forest dieback on Aboriginal land in northern Australia.' *Marine and Freshwater Research*, vol. 70(1), pp. 125–139. ISSN 13231650. doi:10.1071/MF18009.
- Sloss, C. R., Jones, B. G., McClennen, C. E., de Carli, J. and Price, D. M., (2006). 'The geomorphological evolution of a wave-dominated barrier estuary: Burrill Lake, New South Wales, Australia.' *Sedimentary Geology*, vol. 187(3-4), pp. 229–249. ISSN 00370738. doi:10.1016/j.sedgeo.2005.12.029.
- Sloss, C. R., Jones, B. G., Murray-Wallace, C. V. and McClennen, C. E., (2005). 'Holocene Sea Level Fluctuations and the Sedimentary Evolution of a Barrier Estuary: Lake Illawarra, New South Wales, Australia.' *Journal of Coastal Research*, vol. 215, pp. 943–959. ISSN 0749-0208. doi:10.2112/03-0110.1.
- Sohn, J., McElhinny, C., Grove, S., Hilbig, E. and Bauhus, J., (2013). 'A simplified inventory approach for estimating carbon in coarse woody debris in high-biomass forests.' *Papers and Proceedings of the Royal Society of Tasmania*, vol. 147, pp. 15–24. ISSN 00804703. doi:10.26749/rstpp.147.15.
- Spalding, M., (2010). *World atlas of mangroves*. Routledge.
- Tran, D. B. and Dargusch, P., (2016). 'Melaleuca forests in Australia have globally significant carbon stocks.' *Forest Ecology and Management*, vol. 375, pp. 230–237. ISSN 03781127. doi:10.1016/j.foreco.2016.05.028.
URL: <http://dx.doi.org/10.1016/j.foreco.2016.05.028>
- Tran, D. B., Dargusch, P., Herbohn, J. and Moss, P., (2013a). 'Interventions to better manage the carbon stocks in australian melaleuca forests.' *Land Use Policy*, vol. 35, pp. 417–420. ISSN 02648377. doi:10.1016/j.landusepol.2013.04.018.
URL: <http://dx.doi.org/10.1016/j.landusepol.2013.04.018>
- Tran, D. B., Dargusch, P., Moss, P. and Hoang, T. V., (2013b). 'An assessment of potential responses of Melaleuca genus to global climate change.' *Mitigation and*

- Adaptation Strategies for Global Change*, vol. 18(6), pp. 851–867. ISSN 13812386. doi:10.1007/s11027-012-9394-2.
- Trettin, C. C. and Jurgensen, M. F., (2002). ‘Carbon cycling in wetland forest soils.’ In: ‘The Potential of U.S. Forest Soils to Sequester Carbon and Mitigate the Greenhouse Effect,’ ISBN 9781420032277. doi:10.1201/9781420032277-19.
- Van Veen, J. and Kuikman, P., (1990). ‘Soil structural aspects of decomposition of organic matter by micro-organisms.’ *Biogeochemistry*, vol. 11(3), pp. 213–233.
- Victor, S., Golbuu, Y., Wolanski, E. and Richmond, R. H., (2004). ‘Fine sediment trapping in two mangrove-fringed estuaries exposed to contrasting land-use intensity, Palau, Micronesia.’ *Wetlands Ecology and Management*, vol. 12(4), pp. 277–283. ISSN 09234861. doi:10.1007/s11273-005-8319-1.
- Victoria. Department of Sustainability and Environment., (2012). *A field guide to Victorian wetland ecological vegetation classes for the index of wetland condition*. ISBN 9781742874166.
- Walther, G.-r., Post, E., Convey, P., Menzel, A., Parmesan, C., Beebee, T. J. C., Fromentin, J.-m., I. O. H.-g. and Bairlein, F., (2002). ‘Ecological response to recent climate change.’ *Nature*, vol. 416, pp. 389–395.
- Wang, Q. and Li, Y., (2011). ‘Optimizing the weight loss-on-ignition methodology to quantify organic and carbonate carbon of sediments from diverse sources.’ pp. 241–257. doi:10.1007/s10661-010-1454-z.
- West, S., Jansen, J. H. and Stuut, J. B., (2004). ‘Surface water conditions in the Northern Benguela Region (SE Atlantic) during the last 450 ky reconstructed from assemblages of planktonic foraminifera.’ *Marine Micropaleontology*, vol. 51(3-4), pp. 321–344. ISSN 03778398. doi:10.1016/j.marmicro.2004.01.004.
- West Gippsland Catchment Management Authority, V., (2014). ‘West Gippsland Waterway Strategy.’ Tech. rep.
- Whitt, A. A., Coleman, R., Lovelock, C. E., Gillies, C., Ierodiaconou, D., Liyanapathirana, M. and Macreadie, P. I., (2020). ‘March of the mangroves: Drivers of encroachment into southern temperate saltmarsh.’ *Estuarine, Coastal and Shelf Science*, p. 106776. ISSN 02727714. doi:10.1016/j.ecss.2020.106776.
URL: <https://doi.org/10.1016/j.ecss.2020.106776>
- Willemsen, P. W., Horstman, E. M., Borsje, B. W., Friess, D. A. and Dohmen-Janssen, C. M., (2016). ‘Sensitivity of the sediment trapping capacity of an estuarine mangrove forest.’ *Geomorphology*, vol. 273, pp. 189–201. ISSN 0169555X. doi:10.1016/j.

geomorph.2016.07.038.

URL: <http://dx.doi.org/10.1016/j.geomorph.2016.07.038>

- Williams, A. R., (1984). 'Changes in Melaleuca forest density on the Magela floodplain, Northern Territory, between 1950 and 1975.' *Australian Journal of Ecology*, vol. 9(3), pp. 199–202. ISSN 14429993. doi:10.1111/j.1442-9993.1984.tb01357.x.
- Williams, R. J. and Meehan, A. J., (2004). 'Focusing management needs at the sub-catchment level via assessments of change in the cover of estuarine vegetation, Port Hacking, NSW, Australia.' *Wetlands Ecology and Management*, vol. 12(5), pp. 499–518. ISSN 09234861. doi:10.1007/s11273-005-3948-y.
- Williams, R. J., Watford, F. A. and Balashov, V., (1999). 'Kooragang Wetland Rehabilitation Project: Changes in wetland fish habitats of the lower Hunter River. NSW Fisheries Office of Conservation.' *Fisheries Research Institute, Cronulla*.
- Williamson, G. J., Boggs, G. S. and Bowman, D. M. J. S., (2011). 'Late 20th century mangrove encroachment in the coastal Australian monsoon tropics parallels the regional increase in woody biomass.' *Regional Environmental Change*, vol. 11(1), pp. 19–27. ISSN 14363798. doi:10.1007/s10113-010-0109-5.
- Winning, G., (1990). 'Lake Macquarie littoral habitats study.' *Prepared for Lake Macquarie City Council, by Shortland Wetlands Centre*.
- Wolanski, E., Jones, M. and Bunt, J. S., (1980). 'Hydrodynamics of a Tidal Creek-Mangrove Swamp System.' *Marine and Freshwater Research*, vol. 31(4), pp. 431–450. ISSN 13231650. doi:10.1071/MF9800431.
- Wolanski, E., Mazda, Y. and Ridd, P., (1992). 'Mangrove hydrodynamics.' *Tropical mangrove ecosystems. coastal and estuarine studies*, vol. 41.
- Wolters, S., Zeiler, M. and Bungenstock, F., (2010). 'Early Holocene environmental history of sunken landscapes: Pollen, plant macrofossil and geochemical analyses from the Borkum Riffgrund, southern North Sea.' *International Journal of Earth Sciences*, vol. 99(8), pp. 1707–1719. ISSN 14373254. doi:10.1007/s00531-009-0477-6.
- Woodroffe, C. D., (1993). 'Late quaternary evolution of coastal and lowland riverine plains of Southeast Asia and northern Australia: an overview.' *Sedimentary Geology*, vol. 83(3-4), pp. 163–175. ISSN 00370738. doi:10.1016/0037-0738(93)90010-3.
- Woodroffe, C. D., (2002). *Coasts: form, process and evolution*. Cambridge University Press.

- Woodroffe, C. D., Rogers, K., Mckee, K. L., Lovelock, C. E., Mendelssohn, I. A. and Saintilan, N., (2016). 'Mangrove Sedimentation and Response to Relative Sea-Level Rise.' *Annual Review of Marine Science*, vol. 8, pp. 243–266. doi:10.1146/annurev-marine-122414-034025.
- Zaitlin, B. A., Dalrymple, R. W. and Boyd, R., (1994). 'The stratigraphic organization of incised-valley systems associated with relative sea-level change.'
- Zhao, Q., Bai, J., Liu, P., Gao, H. and Wang, J., (2015). 'Decomposition and carbon and nitrogen dynamics of phragmites australis litter as affected by flooding periods in coastal wetlands.' *Clean - Soil, Air, Water*, vol. 43(3), pp. 441–445. ISSN 18630669. doi:10.1002/clen.201300823.
- Ziegler, M., Lourens, L. J., Tuenter, E. and Reichert, G.-J., (2009). 'Anomalously high Arabian Sea productivity conditions during MIS 13.' *Climate of the Past Discussions*, vol. 5(4), pp. 1989–2018. ISSN 1814-9359. doi:10.5194/cpd-5-1989-2009.

Appendices

A Summary of Stratigraphic Units

The following tables provide the details of the stratigraphic units of MAN, SM, MEL1, and MEL2.

Table A.1: Stratigraphic units of mangrove core (MAN) consisting of depth range in m ADH, colouration, organic content, and grain size. 0 m AHD is approximately equivalent to mean sea level.

| Stratigraphic Unit | Depth Range (m AHD) | Colouration | Organic Content | Grain Size |
|--------------------|---------------------|----------------|---|---|
| MAN-A | 0.50 - 0.77 | Very dark grey | Organic-rich, fine roots (1mm), dead seagrass rack | Fine to very fine sediments |
| MAN-B | 0.38 - 0.50 | Dark grey | Organic matter present, less roots than A, mangrove root (1-2 cm) | Sands with fine sediments mixing |
| MAN-C | 0.32 - 0.38 | Dark grey | Organic matter present, coarse root (1 cm) at 0.35 m AHD | Sands with fine sediments mixing, fining down to predominantly fine sediment with some sand |

Continue to Next Page ...

| Stratigraphic Unit | Depth Range (m AHD) | Colouration | Organic Content | Grain Size |
|--------------------|---------------------|--|------------------------|--|
| MAN-D | -0.19 - 0.32 | Dark grey | Organic matter present | Predominantly fine sediment with some sand. Shell fragments (carbonates present) |
| MAN-E | -0.50 - -0.19 | Dark grey mottled with yellowish brown. Transitions to light grey from dark grey below -0.44 m AHD | Organic matter present | Predominantly fine sediment with very little sand |
| MAN-F | -1.04 - -0.50 | Light grey with lenses of dark grey | Low organic matter | Sandy |
| MAN-G | -1.40 - -1.04 | Light greyish brown | Low organic matter | Sandy |
| End of Table | | | | |

Table A.3: Stratigraphic units of saltmarsh core (SM) consisting of depth range in m ADH, colouration, organic content, grain size, and additional information. 0 m AHD is approximately equivalent to mean sea level.

| Stratigraphic Unit | Depth Range (m AHD) | Colouration | Organic Content | Grain Size |
|--------------------|---------------------|-------------------------|---|--------------------------------|
| SM-A | 1.07 -1.13 | Strong brown | Organic-rich, fine roots to coarse roots (up to 5mm) | Very fine sediment |
| SM-B | 1.01 - 1.07 | Dark brown | Organic-rich, fine roots to coarse roots (up to 5mm) | Very fine sediment |
| SM-C | 0.94 - 1.01 | Very dark brown | Organic-rich, fine roots to medium roots (up to 2mm) | Very fine sediment |
| SM-D | 0.82 - 0.94 | Dark greyish brown | Organic-rich, fine roots (up to 1mm) | Very fine sediment |
| SM-E | 0.73 - 0.82 | Very dark greyish brown | Organic-rich, fine roots (up to 1mm), roots coarsen at the bottom (4mm) | Very fine sediment |
| SM-F | 0.05 - 0.73 | Dark grey | Organic presents | Sand with fine sediment mixing |

Continue to Next Page ...

| Stratigraphic Unit | Depth Range (m AHD) | Colouration | Organic Content | Grain Size |
|--------------------|---------------------|--|--|---|
| SM-G | -0.47 - 0.05 | Dark grey mottled with yellowish brown | Organic-rich, long medium roots (3mm). | Predominantly fine with sandy sediment mixing. Coarsens downwards below -0.29 m AHD |
| SM-H | 0.78 - -0.47 | Grey mottled with dary grey. Transitions to light brownish grey from grey below -0.6 m AHD | Low organic matter | Sandy |
| End of Table | | | | |

Table A.5: Stratigraphic units of *Melaleuca* 1 core (MEL1) consisting of depth range in m ADH, colouration, organic content, grain size, and additional information. 0 m AHD is approximately equivalent to mean sea level.

| Stratigraphic Unit | Depth Range (m AHD) | Colouration | Organic Content | Grain Size |
|--------------------|---------------------|---|---|---------------------------------|
| MEL1-A | 0.94 - 1.19 | Black | Organic-rich, fine to coarse roots (up to 4mm) | Fine sediment |
| MEL1-B | 0.75 - 0.95 | Black | Organic-rich, fine roots | Fine sediment |
| MEL1-C | 0.58 - 0.75 | Dark brown | Organic-rich, very fine to fine roots (up to 1mm), roots and rhizomes | Fine sediment |
| MEL1-D | 0.13 - 0.58 | Dark grey | Some organics present, preserved roots, plus >2 cm wide rhizome | Fine sediment mixed with sands |
| MEL1-E | -0.47 - 0.13 | Dark grey mottled with yellowish brown | Organic-rich, few preserved roots | Fine sediment with some sand |
| MEL1-F | -0.64 - -0.47 | Grey | Low organic, little preservation | Sandy with fine sediment mixing |
| MEL1-G | -0.84 - -0.64 | Reddish grey mottled with dark reddish grey | Low organic, little preservation | Sandy |

Continue to Next Page ...

| Stratigraphic Unit | Depth Range (m AHD) | Colouration | Organic Content | Grain Size |
|--------------------|---------------------|--|----------------------------------|------------|
| MEL1-H | -1.10 - -0.84 | Reddish grey mottled with dark reddish grey | Low organic, little preservation | Sandy |
| MEL1-I | -1.19 - -1.10 | Dusty red some mottling with dark reddish grey | Low organic, little preservation | Sandy |
| MEL1-J | -1.42 - -1.19 | Weak red | Low organic, little preservation | Sandy |
| End of Table | | | | |

Table A.7: Stratigraphic units of *Melaleuca* 2 core (MEL2) consisting of depth range in m ADH, colouration, organic content, grain size, and additional information. 0 m AHD is approximately equivalent to mean sea level.

| Stratigraphic Unit | Depth Range (m AHD) | Colouration | Organic Content | Grain Size |
|--------------------|---------------------|--|---|-------------------------------------|
| MEL2-A | 1.31 - 1.43 | Very dark brown | Organic -rich, fine roots | Fine sediment |
| MEL2-B | 1.25 - 1.31 | Dark brown | Organic-rich, fine roots | Fine sediment |
| MEL2-C | 1.16 - 1.25 | Very dark brown | Organic-rich, fine roots | Fine sediment with some sand mixing |
| MEL2-D | 1.02 - 1.16 | Dark greyish brown mottle with yellowish brown | Organic-rich, fine roots | Fine sediment |
| MEL2-E | 0.67 - 1.02 | Dark grey | Low organic matter, some fine roots | Sandy |
| MEL2-F | 0.28 - 0.67 | Dark grey | Low organic matter, some fine roots | Sandy |
| MEL2-G | 0.04 - 0.28 | Grey | Low organic matter, poorly preserved fine roots | Sandy |
| MEL2-H | 0.01 - 0.04 | Grey | Low organic matter | Very fine sediment |
| MEL2-I | -0.40 - 0.01 | Grey | Low organic matter | Sandy |

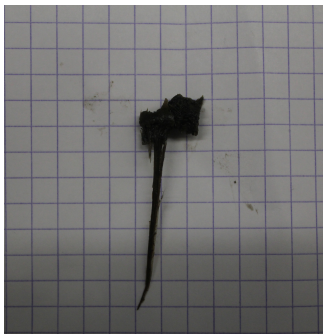

Continue to Next Page ...

| Stratigraphic Unit | Depth Range (m AHD) | Colouration | Organic Content | Grain Size |
|--------------------|---------------------|-------------|---|------------|
| MEL2-J | -0.82 - -0.40 | Light Brown | Low organic matter, poorly preserved fine roots | Sandy |
| End of Table | | | | |



B Table of Macrofossil

The following table presents the macrofossils found throughout the profile of MEL1



Table B.1: Macrofossils collected throughout the profile of *Melaleuca* 1. Macrofossils are given a sample ID, photo, depth range (0 m AHD is approximately equivalent to mean sea level) description and identification where possible. Background grid size for scaling is 5 x 5 mm.

| Sample ID | Photo | Start Depth (m AHD) | End Depth (m AHD) | Description | Identification |
|-----------|---|---------------------|-------------------|---------------------------------------|----------------------------------|
| MF-1 |  | 67.06 | 65.76 | Vegetation node, hard, well preserved | <i>Phragmites australis</i> node |
| MF-2 |  | 67.06 | 64.46 | Coarse casing of a root or rhizome | |



Continue to next page ...

| Sample ID | Photo | Start Depth (m AHD) | End Depth (m AHD) | Description | Identification |
|-----------|--|---------------------|-------------------|---|--|
| MF-3 |  | 65.76 | 63.16 | Dense very fine roots and long coarse roots | |
| MF-4 |  | 57.97 | 56.67 | Wide rhizome and medium-fine root/rhizome | Wide rhizome - <i>Phragmites australis</i> |



Continue to next page ...

| Sample ID | Photo | Start Depth (m AHD) | End Depth (m AHD) | Description | Identification |
|-----------|--|---------------------|-------------------|-------------------------------|-----------------------------|
| MF-5 |  | 56.67 | 55.37 | Well preserved woody fragment | |
| MF-6 |  | 55.37 | 52.78 | Long and wide rhizome | <i>Phragmites australis</i> |



Continue to next page ...

| Sample ID | Photo | Start Depth (m AHD) | End Depth (m AHD) | Description | Identification |
|-----------|--|---------------------|-------------------|-----------------|-----------------------------|
| MF-7 |  | 52.78 | 44.99 | | <i>Phragmites australis</i> |
| MF-8 |  | 51.48 | 50.18 | Medium rhizomes | |



Continue to next page ...

| Sample ID | Photo | Start Depth (m AHD) | End Depth (m AHD) | Description | Identification |
|-----------|--|---------------------|-------------------|-----------------------------------|-----------------------------|
| MF-9 |  | 44.99 | 43.69 | Potential seed pod | |
| MF-10 |  | 44.99 | 43.69 | Rhizome and dense very fine roots | <i>Phragmites australis</i> |



Continue to next page ...

| Sample ID | Photo | Start Depth (m AHD) | End Depth (m AHD) | Description | Identification |
|-----------|--|---------------------|-------------------|--------------------------------------|----------------|
| MF-11 |  | 41.09 | 34.60 | Collection of long rhizome | |
| MF-12 |  | 35.90 | 33.30 | Collection of long rhizome and roots | |

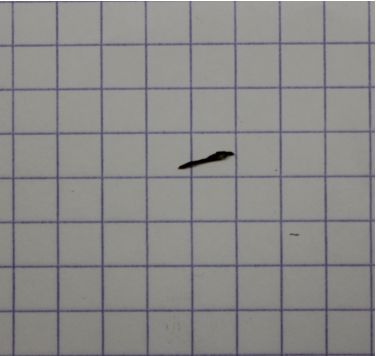

Continue to next page ...

| Sample ID | Photo | Start Depth (m AHD) | End Depth (m AHD) | Description | Identification |
|-----------|--|---------------------|-------------------|--------------------------------------|----------------|
| MF-13 |  | 33.30 | 21.61 | Collection of long rhizome and roots | |
| MF-14 |  | 7.33 | 7.33 | Fine root | |



Continue to next page ...

| Sample ID | Photo | Start Depth (m AHD) | End Depth (m AHD) | Description | Identification |
|-----------|--|---------------------|-------------------|-------------|----------------|
| MF-15 |  | 6.03 | 4.73 | Root casing | |
| MF-16 |  | 3.43 | 2.13 | Fine roots | |



Continue to next page ...

| Sample ID | Photo | Start Depth (m AHD) | End Depth (m AHD) | Description | Identification |
|-----------|--|---------------------|-------------------|----------------|----------------|
| MF-17 |  | -4.36 | -6.31 | Very fine root | |
| MF-18 |  | -7.60 | -10.85 | Fine root | |



Continue to next page ...

| Sample ID | Photo | Start Depth (m AHD) | End Depth (m AHD) | Description | Identification |
|-----------|--|---------------------|-------------------|----------------|----------------|
| MF-19 |  | -21.24 | -26.43 | Long fine root | |
| MF-20 |  | -21.24 | -22.54 | Medium root | |



Continue to next page ...

| Sample ID | Photo | Start Depth (m AHD) | End Depth (m AHD) | Description | Identification |
|-----------|--|---------------------|-------------------|-------------|----------------|
| MF-21 |  | -36.82 | -39.42 | Medium root | |
| MF-22 |  | -40.72 | -42.01 | Medium root | |


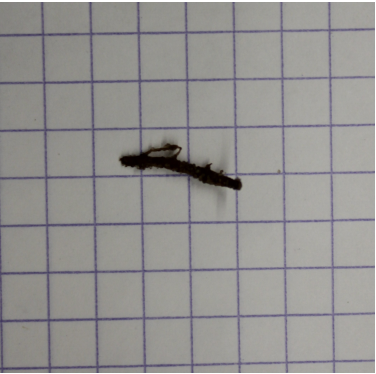
Continue to next page ...

| Sample ID | Photo | Start Depth (m AHD) | End Depth (m AHD) | Description | Identification |
|-----------|--|---------------------|-------------------|-------------------------|----------------|
| MF-23 |  | -42.01 | -44.61 | Medium root | |
| MF-24 |  | -58.90 | -60.19 | Fine and very fine root | |

Continue to next page ...

| Sample ID | Photo | Start Depth (m AHD) | End Depth (m AHD) | Description | Identification |
|-----------|--|---------------------|-------------------|--------------|----------------|
| MF-25 |  | -83.57 | -88.76 | Long rhizome | |
| MF-26 |  | -87.46 | -93.96 | Long rhizome | |

Continue to next page ...

| Sample ID | Photo | Start Depth (m AHD) | End Depth (m AHD) | Description | Identification |
|-----------|--|---------------------|-------------------|---------------------------------------|----------------------------|
| MF-27 |  | -108.24 | -109.54 | Very fine root | <i>Posidonia australis</i> |
| MF-28 |  | -125.12 | -126.42 | Very fine casing of a root or rhizome | <i>Posidonia australis</i> |

End of Table

C ITRAX Reference Profiles

The following figure refers to the geochemical profiles from the high-resolution core logging used in this study.

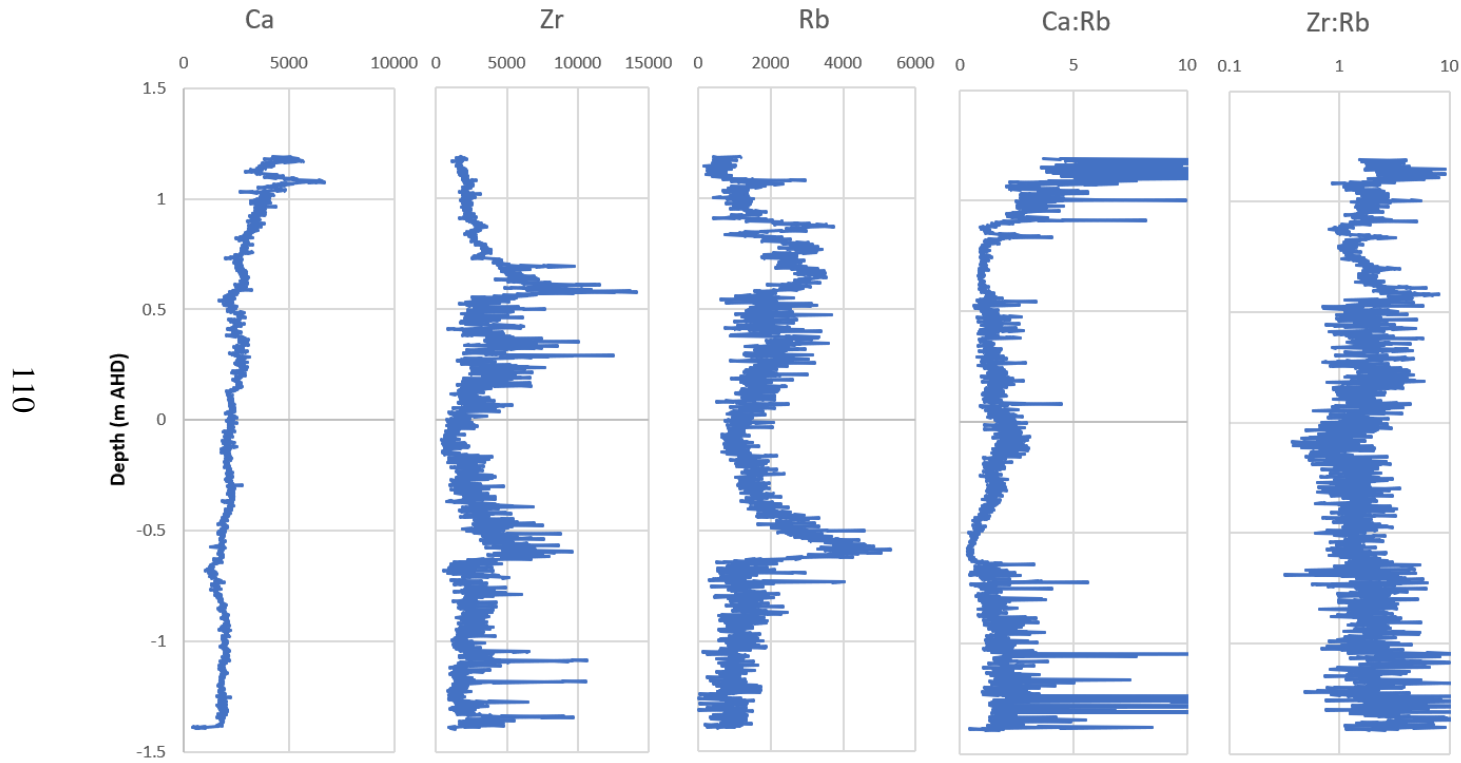


Figure C.1: Micro-XRF data collected from *Melaleuca 1*. Ca is environmental proxy for marine influences. Zr is a proxy for coarser sediment grain size. Rb is used as a proxy for terrestrial influence and finer sediment grain sizes. High values Ca/Rb concentrations indicate greater marine influence. High Zr/Rb concentrations are a proxy for coarser grain size. 0 m AHD is approximately equivalent to mean sea level.

D Data Tables

The following tables present the data values collected from the LOI and BD analysis of MAN, SM, ME1, and MEL2. Moisture content data for MEL1 and MEL2 is also presented in this appendix.

Table D.1: Results of the bulk density and loss-on-ignition analysis of mangrove core (MAN). Samples are presented with an ID, depth range (0 m AHD is approximately equivalent to mean sea level), bulk density (given in g cm^{-3}) and percentage organic matter.

| Sample ID | Start Depth (m AHD) | End Depth (m AHD) | Bulk Density (g cm^{-3}) | Organic Matter (%) |
|-----------|---------------------|-------------------|-------------------------------------|--------------------|
| MAN-1 | 0.77 | 0.75 | 0.35 | 8.87 |
| MAN-2 | 0.75 | 0.73 | 0.61 | 6.93 |
| MAN-3 | 0.73 | 0.71 | 0.75 | 5.76 |
| MAN-4 | 0.71 | 0.69 | 0.77 | 4.06 |
| MAN-5 | 0.69 | 0.67 | 0.61 | 5.59 |
| MAN-6 | 0.67 | 0.65 | 0.67 | 4.44 |
| MAN-7 | 0.65 | 0.63 | 0.54 | 7.00 |
| MAN-8 | 0.63 | 0.61 | 0.64 | 3.47 |
| MAN-9 | 0.61 | 0.59 | 0.60 | 4.24 |
| MAN-10 | 0.59 | 0.57 | 0.65 | 5.12 |
| MAN-11 | 0.57 | 0.55 | 0.67 | 3.56 |
| MAN-12 | 0.55 | 0.53 | 0.75 | 4.58 |
| MAN-13 | 0.53 | 0.51 | 0.70 | 3.67 |
| MAN-14 | 0.51 | 0.49 | 0.79 | 3.77 |
| MAN-15 | 0.49 | 0.47 | 0.91 | 3.86 |
| MAN-16 | 0.47 | 0.45 | 0.80 | 3.13 |
| MAN-17 | 0.42 | 0.4 | 1.14 | 2.08 |
| MAN-18 | 0.37 | 0.35 | 0.60 | 5.56 |
| MAN-19 | 0.32 | 0.3 | 0.76 | 3.73 |

Continue to next page ...

| Sample ID | Start Depth (m AHD) | End Depth (m AHD) | Bulk Density (g cm ⁻³) | Organic Matter (%) |
|-----------|---------------------|-------------------|------------------------------------|--------------------|
| MAN-20 | 0.27 | 0.25 | 0.70 | 5.24 |
| MAN-21 | 0.22 | 0.2 | 0.88 | 3.77 |
| MAN-22 | 0.17 | 0.15 | 1.07 | 3.63 |
| MAN-23 | 0.12 | 0.1 | 1.13 | 2.22 |
| MAN-24 | 0.07 | 0.05 | 1.01 | 2.99 |
| MAN-25 | 0.02 | 0 | 1.00 | 2.99 |
| MAN-26 | -0.03 | -0.05 | 1.14 | 2.68 |
| MAN-27 | -0.08 | -0.1 | 1.19 | 2.50 |
| MAN-28 | -0.13 | -0.15 | 1.33 | 1.64 |
| MAN-29 | -0.18 | -0.2 | 1.40 | 1.96 |
| MAN-30 | -0.23 | -0.25 | 1.40 | 1.68 |
| MAN-31 | -0.28 | -0.3 | 1.07 | 3.99 |
| MAN-32 | -0.33 | -0.35 | 1.06 | 4.77 |
| MAN-33 | -0.38 | -0.4 | 1.09 | 4.85 |
| MAN-34 | -0.43 | -0.45 | 1.07 | 5.76 |
| MAN-35 | -0.48 | -0.5 | 1.30 | 3.99 |
| MAN-36 | -0.53 | -0.55 | 1.25 | 3.06 |
| MAN-37 | -0.58 | -0.6 | 1.51 | 2.65 |
| MAN-38 | -0.63 | -0.65 | 1.26 | 2.30 |
| MAN-39 | -0.68 | -0.7 | 1.61 | 1.96 |
| MAN-40 | -0.73 | -0.75 | 1.60 | 1.76 |
| MAN-41 | -0.78 | -0.8 | 1.53 | 1.95 |
| MAN-42 | -0.83 | -0.85 | 1.32 | 2.22 |
| MAN-43 | -0.88 | -0.9 | 1.41 | 2.02 |
| MAN-44 | -0.93 | -0.95 | 1.47 | 2.20 |
| MAN-45 | -0.98 | -1 | 1.52 | 1.91 |

Continue to next page ...

| Sample ID | Start Depth (m AHD) | End Depth (m AHD) | Bulk Density (g cm ⁻³) | Organic Matter (%) |
|--------------|---------------------|-------------------|------------------------------------|--------------------|
| MAN-46 | -1.03 | -1.05 | 1.45 | 1.95 |
| MAN-47 | -1.08 | -1.1 | 1.43 | 1.87 |
| MAN-48 | -1.13 | -1.15 | 1.44 | 1.84 |
| MAN-49 | -1.18 | -1.2 | 1.48 | 1.77 |
| MAN-50 | -1.23 | -1.25 | 1.38 | 1.48 |
| MAN-51 | -1.28 | -1.3 | 1.38 | 1.41 |
| MAN-52 | -1.33 | -1.35 | 1.50 | 1.36 |
| End of Table | | | | |

Table D.3: Results of the bulk density and loss-on-ignition analysis of saltmarsh core (SM). Samples are presented with an ID, depth range (0 m AHD is approximately equivalent to mean sea level), bulk density (given in g cm^{-3}) and percentage organic matter.

| Sample ID | Start Depth (m AHD) | End Depth (m AHD) | Bulk Density (g cm^{-3}) | Organic Matter (%) |
|-----------|---------------------|-------------------|-------------------------------------|--------------------|
| SM-1 | 1.13 | 1.11 | 0.17 | 36.25 |
| SM-2 | 1.11 | 1.09 | 0.22 | 34.71 |
| SM-3 | 1.09 | 1.07 | 0.26 | 30.91 |
| SM-4 | 1.07 | 1.05 | 0.17 | 34.62 |
| SM-5 | 1.05 | 1.03 | 0.16 | 38.55 |
| SM-6 | 1.03 | 1.01 | 0.14 | 50.36 |
| SM-7 | 1.01 | 0.99 | 0.15 | 57.62 |
| SM-8 | 0.99 | 0.97 | 0.22 | 51.77 |
| SM-9 | 0.97 | 0.95 | 0.21 | 41.37 |
| SM-10 | 0.95 | 0.93 | 0.21 | 36.25 |
| SM-11 | 0.93 | 0.91 | 0.25 | 31.66 |
| SM-12 | 0.91 | 0.89 | 0.23 | 26.18 |
| SM-13 | 0.89 | 0.87 | 0.21 | 28.05 |
| SM-14 | 0.87 | 0.85 | 0.17 | 29.78 |
| SM-15 | 0.85 | 0.83 | 0.21 | 23.69 |
| SM-16 | 0.83 | 0.81 | 0.22 | 22.66 |
| SM-17 | 0.78 | 0.76 | 0.24 | 23.19 |
| SM-18 | 0.73 | 0.71 | 0.36 | 12.96 |
| SM-19 | 0.68 | 0.66 | 0.82 | 3.97 |
| SM-20 | 0.63 | 0.61 | 0.82 | 3.60 |
| SM-21 | 0.58 | 0.56 | 0.49 | 4.25 |
| SM-22 | 0.53 | 0.51 | 1.12 | 2.93 |
| SM-23 | 0.48 | 0.46 | 1.19 | 3.02 |

Continue to next page ...

| Sample ID | Start Depth (m AHD) | End Depth (m AHD) | Bulk Density (g cm ⁻³) | Organic Matter (%) |
|-----------|---------------------|-------------------|------------------------------------|--------------------|
| SM-24 | 0.43 | 0.41 | 0.99 | 2.01 |
| SM-25 | 0.38 | 0.36 | 1.16 | 2.56 |
| SM-26 | 0.33 | 0.31 | 1.21 | 2.14 |
| SM-27 | 0.28 | 0.26 | 1.22 | 2.53 |
| SM-28 | 0.23 | 0.21 | 1.11 | 2.54 |
| SM-29 | 0.18 | 0.16 | 1.14 | 2.85 |
| SM-30 | 0.13 | 0.11 | 1.24 | 2.28 |
| SM-31 | 0.08 | 0.06 | 1.32 | 2.63 |
| SM-32 | 0.03 | 0.01 | 1.25 | 3.33 |
| SM-33 | -0.02 | -0.04 | 1.01 | 4.03 |
| SM-34 | -0.07 | -0.09 | 0.91 | 4.70 |
| SM-35 | -0.12 | -0.14 | 0.96 | 3.75 |
| SM-36 | -0.17 | -0.19 | 0.74 | 5.42 |
| SM-37 | -0.22 | -0.24 | 0.77 | 6.68 |
| SM-38 | -0.27 | -0.29 | 0.88 | 5.90 |
| SM-39 | -0.32 | -0.34 | 0.92 | 4.78 |
| SM-40 | -0.37 | -0.39 | 0.80 | 5.81 |
| SM-41 | -0.42 | -0.44 | 0.87 | 4.72 |
| SM-42 | -0.47 | -0.49 | 1.08 | 3.33 |
| SM-43 | -0.52 | -0.54 | 1.23 | 2.02 |
| SM-44 | -0.57 | -0.59 | 1.21 | 2.36 |
| SM-45 | -0.62 | -0.64 | 1.35 | 1.74 |
| SM-46 | -0.67 | -0.69 | 1.36 | 1.57 |
| SM-47 | -0.72 | -0.74 | 1.29 | 1.42 |
| SM-48 | -0.77 | -0.79 | 1.29 | 1.36 |

Continue to next page ...

| Sample ID | Start Depth (m AHD) | End Depth (m AHD) | Bulk Density (g cm ⁻³) | Organic Matter (%) |
|-----------|---------------------|-------------------|------------------------------------|--------------------|
|-----------|---------------------|-------------------|------------------------------------|--------------------|

End of Table

Table D.5: Results of the bulk density and loss-on-ignition analysis of *Melaleuca* 1 core (MEL1). Samples are presented with an ID, depth range (0 m AHD is approximately equivalent to mean sea level), bulk density (given in g cm^{-2}) and percentage organic matter.

| Sample ID | Start Depth (m AHD) | End Depth (m AHD) | Bulk Density (g cm^{-3}) | Organic Matter (%) |
|-----------|---------------------|-------------------|-------------------------------------|--------------------|
| MEL1-1 | 1.19 | 1.17 | 0.13 | 58.04 |
| MEL1-2 | 1.17 | 1.15 | 0.19 | 61.76 |
| MEL1-3 | 1.15 | 1.13 | 0.13 | 65.70 |
| MEL1-4 | 1.13 | 1.11 | 0.16 | 65.65 |
| MEL1-5 | 1.11 | 1.09 | 0.15 | 65.87 |
| MEL1-6 | 1.09 | 1.07 | 0.16 | 56.70 |
| MEL1-7 | 1.07 | 1.05 | 0.18 | 54.49 |
| MEL1-8 | 1.05 | 1.03 | 0.14 | 56.82 |
| MEL1-9 | 1.03 | 1.01 | 0.15 | 56.05 |
| MEL1-10 | 1.01 | 0.99 | 0.17 | 56.97 |
| MEL1-11 | 0.99 | 0.97 | 0.15 | 55.94 |
| MEL1-12 | 0.97 | 0.95 | 0.16 | 56.47 |
| MEL1-13 | 0.95 | 0.93 | 0.17 | 49.60 |
| MEL1-14 | 0.93 | 0.91 | 0.15 | 51.76 |
| MEL1-15 | 0.91 | 0.89 | 0.17 | 43.26 |
| MEL1-16 | 0.89 | 0.87 | 0.22 | 30.68 |
| MEL1-17 | 0.84 | 0.82 | 0.19 | 37.50 |
| MEL1-18 | 0.79 | 0.77 | 0.22 | 26.15 |
| MEL1-19 | 0.74 | 0.72 | 0.32 | 21.41 |
| MEL1-20 | 0.69 | 0.67 | 0.45 | 11.88 |
| MEL1-21 | 0.64 | 0.62 | 0.51 | 9.84 |
| MEL1-22 | 0.59 | 0.57 | 0.79 | 5.05 |
| MEL1-23 | 0.54 | 0.52 | 1.29 | 2.21 |

Continue to next page ...

| Sample ID | Start Depth (m AHD) | End Depth (m AHD) | Bulk Density (g cm ⁻³) | Organic Matter (%) |
|-----------|---------------------|-------------------|------------------------------------|--------------------|
| MEL1-24 | 0.49 | 0.47 | 1.28 | 2.17 |
| MEL1-25 | 0.44 | 0.42 | 1.25 | 1.93 |
| MEL1-26 | 0.39 | 0.37 | 1.39 | 1.63 |
| MEL1-27 | 0.34 | 0.32 | 1.42 | 1.74 |
| MEL1-28 | 0.29 | 0.27 | 1.37 | 1.60 |
| MEL1-29 | 0.24 | 0.22 | 1.22 | 1.37 |
| MEL1-30 | 0.19 | 0.17 | 1.36 | 2.05 |
| MEL1-31 | 0.14 | 0.12 | 1.37 | 2.77 |
| MEL1-32 | 0.09 | 0.07 | 1.19 | 3.64 |
| MEL1-33 | 0.04 | 0.02 | 1.20 | 4.50 |
| MEL1-34 | -0.01 | -0.03 | 1.15 | 5.04 |
| MEL1-35 | -0.06 | -0.08 | 1.14 | 5.48 |
| MEL1-36 | -0.11 | -0.13 | 1.02 | 5.46 |
| MEL1-37 | -0.16 | -0.18 | 1.18 | 4.60 |
| MEL1-38 | -0.21 | -0.23 | 1.25 | 4.80 |
| MEL1-39 | -0.26 | -0.28 | 1.21 | 4.79 |
| MEL1-40 | -0.31 | -0.33 | 1.14 | 5.28 |
| MEL1-41 | -0.36 | -0.38 | 0.97 | 5.95 |
| MEL1-42 | -0.41 | -0.43 | 1.13 | 4.17 |
| MEL1-43 | -0.46 | -0.48 | 1.39 | 1.90 |
| MEL1-44 | -0.51 | -0.53 | 1.46 | 1.36 |
| MEL1-45 | -0.56 | -0.58 | 1.40 | 1.44 |
| MEL1-46 | -0.61 | -0.63 | 1.30 | 2.14 |
| MEL1-47 | -0.66 | -0.68 | 1.07 | 1.11 |
| MEL1-48 | -0.71 | -0.73 | 1.53 | 0.92 |
| MEL1-49 | -0.76 | -0.78 | 0.95 | 1.33 |

Continue to next page ...

| Sample ID | Start Depth (m AHD) | End Depth (m AHD) | Bulk Density (g cm ⁻³) | Organic Matter (%) |
|--------------|---------------------|-------------------|------------------------------------|--------------------|
| MEL1-50 | -0.81 | -0.83 | 1.10 | 1.42 |
| MEL1-51 | -0.86 | -0.88 | 1.09 | 1.15 |
| MEL1-52 | -0.91 | -0.93 | 1.00 | 1.31 |
| MEL1-53 | -0.96 | -0.98 | 1.08 | 1.60 |
| MEL1-54 | -1.01 | -1.03 | 1.21 | 1.45 |
| MEL1-55 | -1.06 | -1.08 | 1.18 | 1.38 |
| MEL1-56 | -1.11 | -1.13 | 1.17 | 1.12 |
| MEL1-57 | -1.16 | -1.18 | 1.39 | 1.15 |
| MEL1-58 | -1.21 | -1.23 | 1.17 | 1.23 |
| MEL1-59 | -1.26 | -1.28 | 1.20 | 1.18 |
| MEL1-60 | -1.31 | -1.33 | 1.16 | 1.14 |
| MEL1-61 | -1.36 | -1.38 | 1.16 | 1.23 |
| End of Table | | | | |

Table D.7: Results of the soil moisture analysis of *Melaleuca* 1. Samples are presented with an ID, depth range (0 m AHD is approximately equivalent to mean sea level), and percentage moisture content.

| Sample ID | Start Depth (m AHD) | End Depth (m AHD) | Moisture Content (%) |
|-----------|---------------------|-------------------|----------------------|
| MEL1-1 | 1.19 | 1.18 | 81.38 |
| MEL1-2 | 1.18 | 1.17 | 83.50 |
| MEL1-3 | 1.17 | 1.16 | 84.20 |
| MEL1-4 | 1.16 | 1.15 | 84.19 |
| MEL1-5 | 1.15 | 1.14 | 85.01 |
| MEL1-6 | 1.14 | 1.13 | 86.40 |
| MEL1-7 | 1.13 | 1.12 | 85.81 |
| MEL1-8 | 1.12 | 1.11 | 85.83 |
| MEL1-9 | 1.11 | 1.1 | 86.07 |
| MEL1-10 | 1.1 | 1.09 | 86.36 |
| MEL1-11 | 1.09 | 1.08 | 85.94 |
| MEL1-12 | 1.08 | 1.07 | 85.43 |
| MEL1-13 | 1.07 | 1.06 | 83.01 |
| MEL1-14 | 1.06 | 1.05 | 78.32 |
| MEL1-15 | 1.05 | 1.04 | 78.16 |
| MEL1-16 | 1.04 | 1.03 | 79.54 |
| MEL1-17 | 1.03 | 1.02 | 83.19 |
| MEL1-18 | 1.02 | 1.01 | 85.63 |
| MEL1-19 | 1.01 | 1 | 86.16 |
| MEL1-20 | 1 | 0.99 | 85.68 |

Table D.9: Results of the bulk density and loss-on-ignition analysis of *Melaleuca* 2 core (MEL2). Samples are presented with an ID, depth range (0 m AHD is approximately equivalent to mean sea level), bulk density (given in g cm^{-3}) and percentage organic matter.

| Sample ID | Start Depth (m AHD) | End Depth (m AHD) | Bulk Density (g cm^{-3}) | Organic Matter (%) |
|-----------|---------------------|-------------------|-------------------------------------|--------------------|
| MEL2-1 | 1.43 | 1.41 | 0.13 | 55.68 |
| MEL2-2 | 1.41 | 1.39 | 0.12 | 57.38 |
| MEL2-3 | 1.39 | 1.37 | 0.13 | 58.78 |
| MEL2-4 | 1.37 | 1.35 | 0.12 | 58.47 |
| MEL2-5 | 1.35 | 1.33 | 0.10 | 59.26 |
| MEL2-6 | 1.33 | 1.31 | 0.13 | 64.57 |
| MEL2-7 | 1.31 | 1.29 | 0.15 | 47.54 |
| MEL2-8 | 1.29 | 1.27 | 0.34 | 17.98 |
| MEL2-9 | 1.27 | 1.25 | 0.56 | 12.40 |
| MEL2-10 | 1.25 | 1.23 | 0.69 | 8.90 |
| MEL2-11 | 1.23 | 1.21 | 0.57 | 7.45 |
| MEL2-12 | 1.21 | 1.19 | 0.80 | 5.63 |
| MEL2-13 | 1.19 | 1.17 | 0.91 | 5.13 |
| MEL2-14 | 1.17 | 1.15 | 0.89 | 4.06 |
| MEL2-15 | 1.15 | 1.13 | 0.86 | 3.69 |
| MEL2-16 | 1.13 | 1.11 | 0.84 | 4.15 |
| MEL2-17 | 1.08 | 1.06 | 1.02 | 4.78 |
| MEL2-18 | 1.03 | 1.01 | 0.92 | 4.43 |
| MEL2-19 | 0.98 | 0.96 | 1.13 | 1.71 |
| MEL2-20 | 0.93 | 0.91 | 1.02 | 2.68 |
| MEL2-21 | 0.88 | 0.86 | 1.06 | 2.04 |
| MEL2-22 | 0.83 | 0.81 | 1.32 | 2.18 |
| MEL2-23 | 0.78 | 0.76 | 1.04 | 3.04 |

Continue to next page ...

| Sample ID | Start Depth (m AHD) | End Depth (m AHD) | Bulk Density (g cm ⁻³) | Organic Matter (%) |
|-----------|---------------------|-------------------|------------------------------------|--------------------|
| MEL2-24 | 0.73 | 0.71 | 0.93 | 1.51 |
| MEL2-25 | 0.68 | 0.66 | 1.10 | 1.91 |
| MEL2-26 | 0.63 | 0.61 | 0.96 | 3.12 |
| MEL2-27 | 0.58 | 0.56 | 1.06 | 2.90 |
| MEL2-28 | 0.53 | 0.51 | 1.16 | 2.65 |
| MEL2-29 | 0.48 | 0.46 | 0.99 | 2.71 |
| MEL2-30 | 0.43 | 0.41 | 1.00 | 2.71 |
| MEL2-31 | 0.38 | 0.36 | 0.98 | 2.82 |
| MEL2-32 | 0.33 | 0.31 | 0.93 | 2.49 |
| MEL2-33 | 0.28 | 0.26 | 1.00 | 2.75 |
| MEL2-34 | 0.23 | 0.21 | 1.06 | 2.95 |
| MEL2-35 | 0.18 | 0.16 | 1.11 | 2.09 |
| MEL2-36 | 0.13 | 0.11 | 0.94 | 1.80 |
| MEL2-37 | 0.08 | 0.06 | 1.14 | 1.81 |
| MEL2-38 | 0.03 | 0.01 | 1.26 | 2.55 |
| MEL2-39 | -0.02 | -0.04 | 1.04 | 2.06 |
| MEL2-40 | -0.07 | -0.09 | 1.40 | 2.06 |
| MEL2-41 | -0.12 | -0.14 | 1.26 | 2.15 |
| MEL2-42 | -0.17 | -0.19 | 1.30 | 1.77 |
| MEL2-43 | -0.22 | -0.24 | 1.13 | 2.54 |
| MEL2-44 | -0.27 | -0.29 | 1.38 | 2.58 |
| MEL2-45 | -0.32 | -0.34 | 1.23 | 2.19 |
| MEL2-46 | -0.37 | -0.39 | 1.29 | 1.91 |
| MEL2-47 | -0.42 | -0.44 | 1.06 | 1.36 |
| MEL2-48 | -0.47 | -0.49 | 1.29 | 1.20 |
| MEL2-49 | -0.52 | -0.54 | 1.27 | 1.09 |

Continue to next page ...

| Sample ID | Start Depth (m AHD) | End Depth (m AHD) | Bulk Density (g cm ⁻³) | Organic Matter (%) |
|-----------|---------------------|-------------------|------------------------------------|--------------------|
| MEL2-50 | -0.57 | -0.59 | 1.19 | 1.31 |
| MEL2-51 | -0.62 | -0.64 | 1.11 | 1.10 |
| MEL2-52 | -0.67 | -0.69 | 1.11 | 1.10 |
| MEL2-53 | -0.72 | -0.74 | 1.09 | 1.14 |

End of Table

Table D.11: Results of the soil moisture analysis of *Melaleuca 2*. Samples are presented with an ID, depth range (0 m AHD is approximately equivalent to mean sea level), and percentage moisture content.

| Sample ID | Start Depth (m AHD) | End Depth (m AHD) | Moisture Content (%) |
|-----------|---------------------|-------------------|----------------------|
| MEL2-1 | 1.43 | 1.42 | 80.25 |
| MEL2-2 | 1.42 | 1.41 | 81.06 |
| MEL2-3 | 1.41 | 1.4 | 79.16 |
| MEL2-4 | 1.4 | 1.39 | 80.41 |
| MEL2-5 | 1.39 | 1.38 | 80.61 |
| MEL2-6 | 1.38 | 1.37 | 77.55 |
| MEL2-7 | 1.37 | 1.36 | 76.17 |
| MEL2-8 | 1.36 | 1.35 | 81.07 |
| MEL2-9 | 1.35 | 1.34 | 78.90 |
| MEL2-10 | 1.34 | 1.33 | 74.33 |
| MEL2-11 | 1.33 | 1.32 | 68.77 |
| MEL2-12 | 1.32 | 1.31 | 57.72 |
| MEL2-13 | 1.31 | 1.3 | 54.13 |
| MEL2-14 | 1.3 | 1.29 | 47.75 |
| MEL2-15 | 1.29 | 1.28 | 33.22 |
| MEL2-16 | 1.28 | 1.27 | 27.17 |
| MEL2-17 | 1.27 | 1.26 | 26.66 |
| MEL2-18 | 1.26 | 1.25 | 27.63 |
| MEL2-19 | 1.25 | 1.24 | 24.98 |

E Grain Size Histograms

The following tables present the grain size histograms developed as part of the grain size analysis.

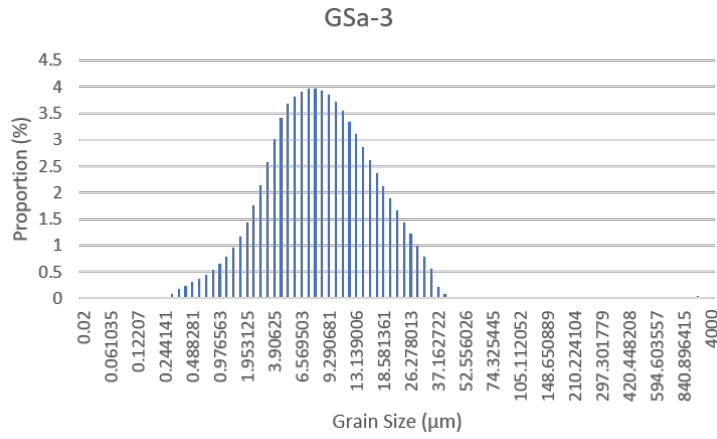
Table E.1: Results of the grain size analysis of *Melaleuca* 1 core (MEL1). Sample are presented with a grain size histogram and depth range (0 m AHD is approximately equivalent to mean sea level).

| Grain Size Histogram | Depth (m AHD) |
|---|---------------|
| <p>GSa-1</p> <p style="text-align: center;">Grain Size (µm)</p> | 1.06 |
| <p>GSa-2</p> <p style="text-align: center;">Grain Size (µm)</p> | 0.96 |

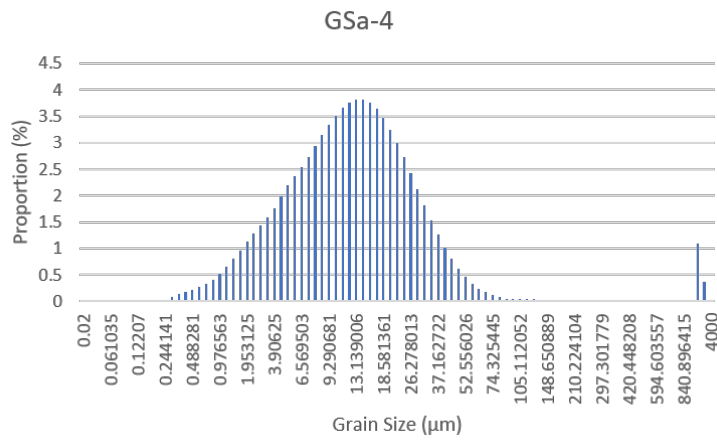
Continue to Next Page ...

Grain Size Histogram

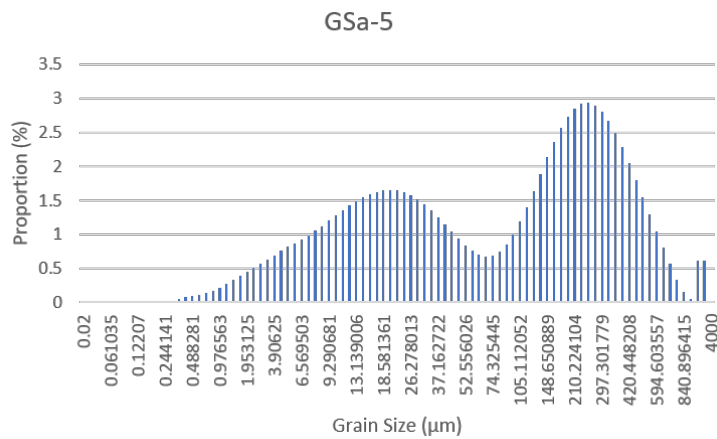
Depth (m AHD)



0.90



0.76

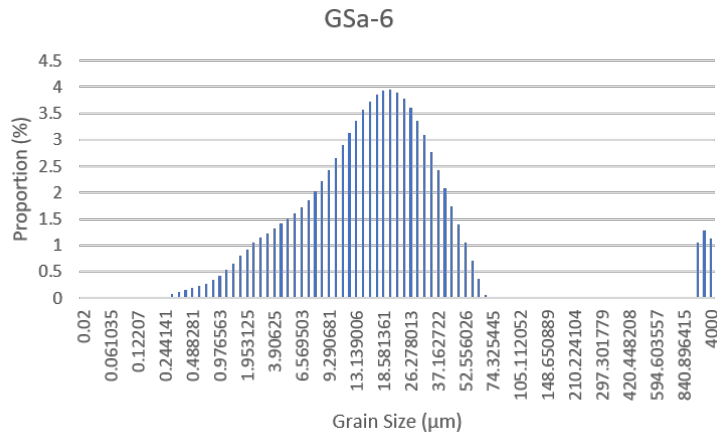


0.74

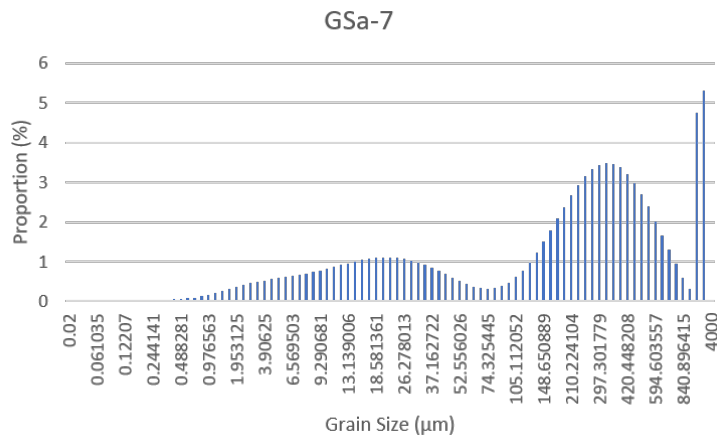
Continue to Next Page ...

Grain Size Histogram

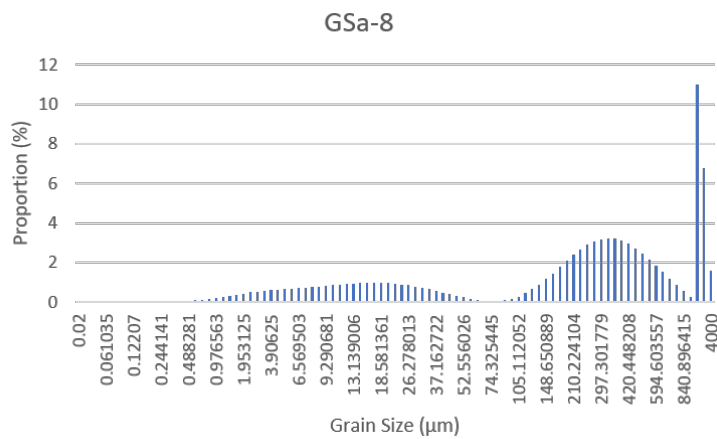
Depth (m AHD)



0.59



0.54

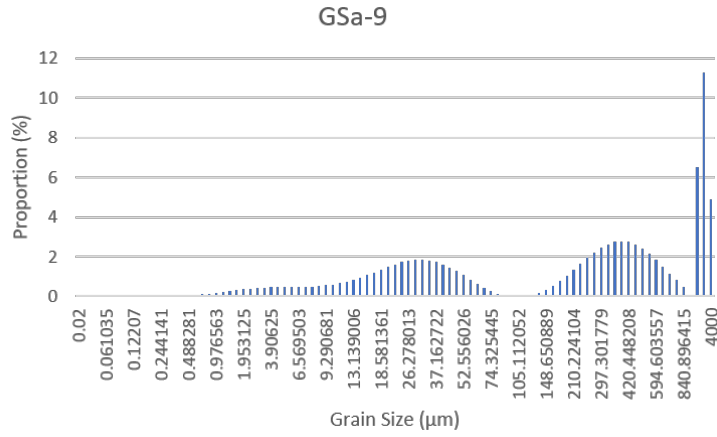


0.35

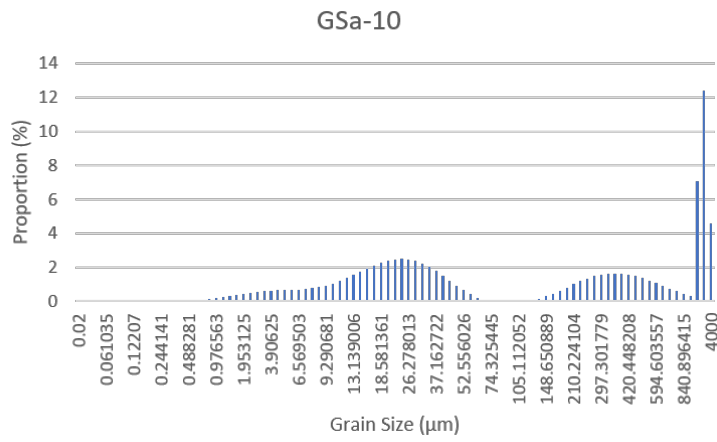
Continue to Next Page ...

Grain Size Histogram

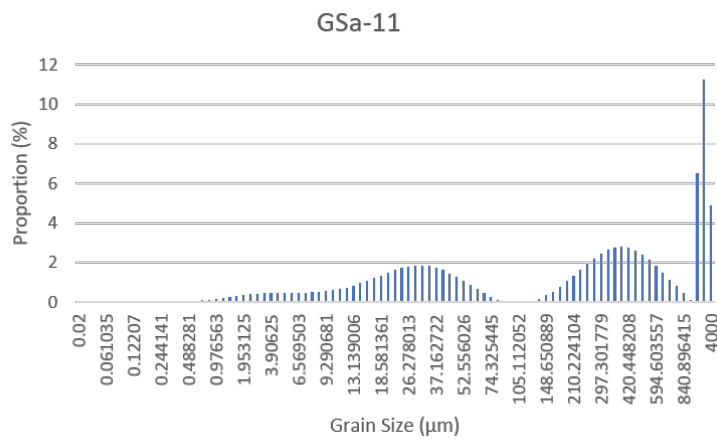
Depth (m AHD)



0.15



0.10

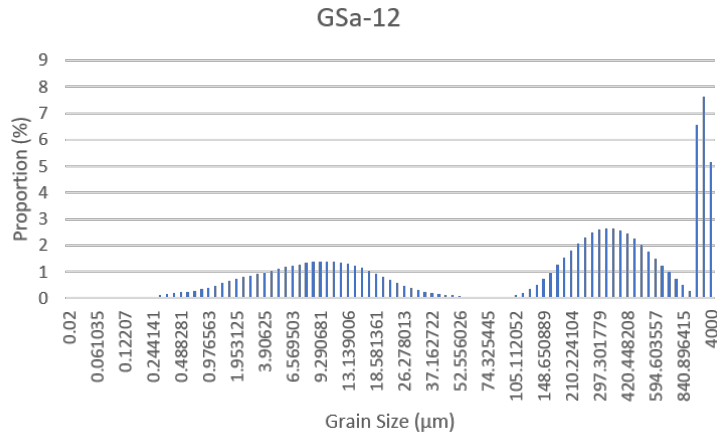


-0.15

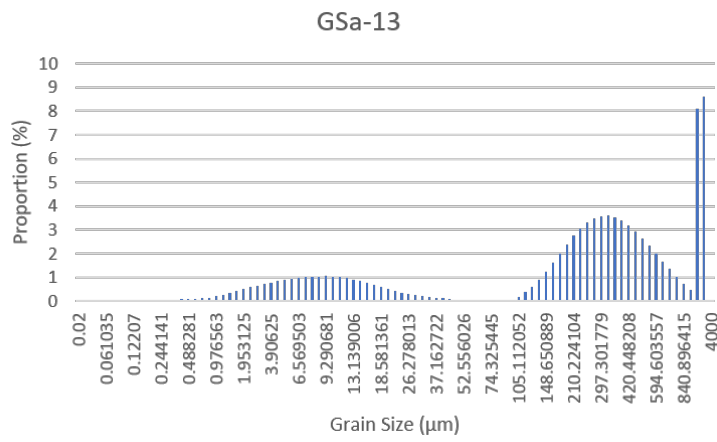
Continue to Next Page ...

Grain Size Histogram

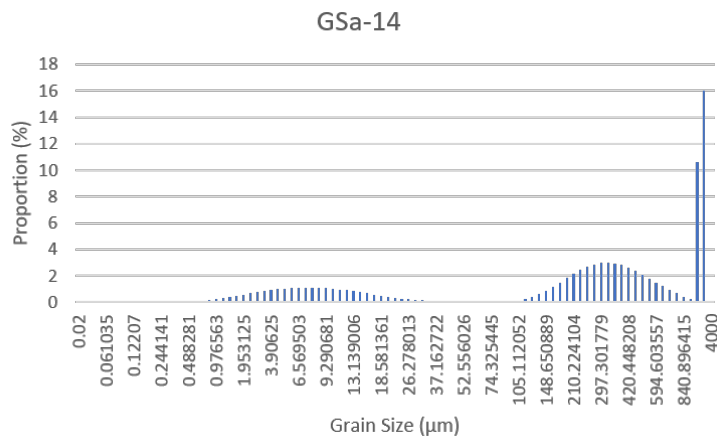
Depth (m AHD)



-0.38



-0.46



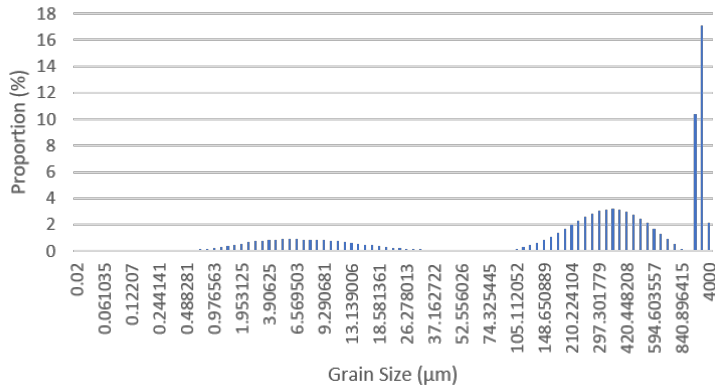
-0.54

Continue to Next Page ...

Grain Size Histogram

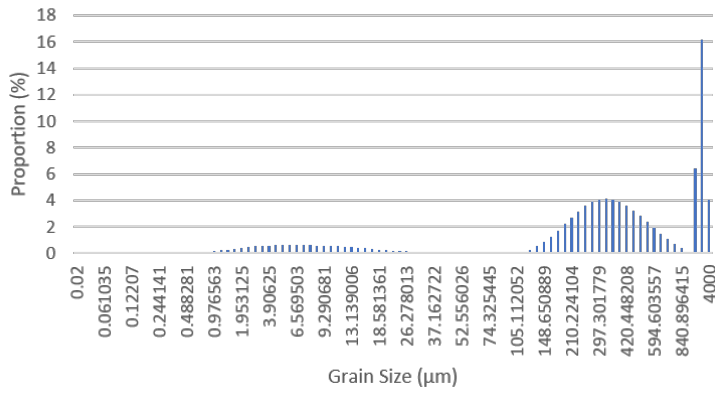
Depth (m AHD)

GSa-15



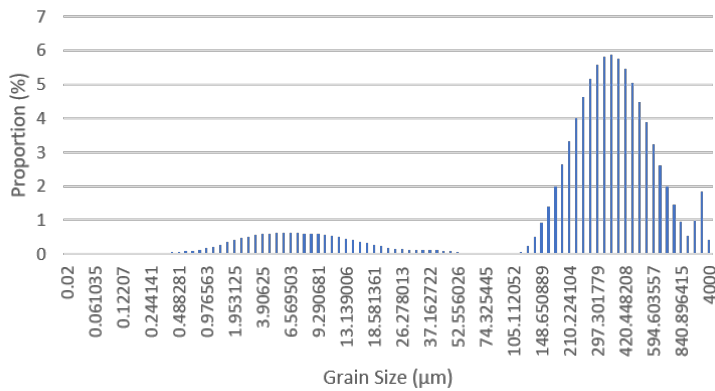
-0.63

GSa-16



-0.67

GSa-17

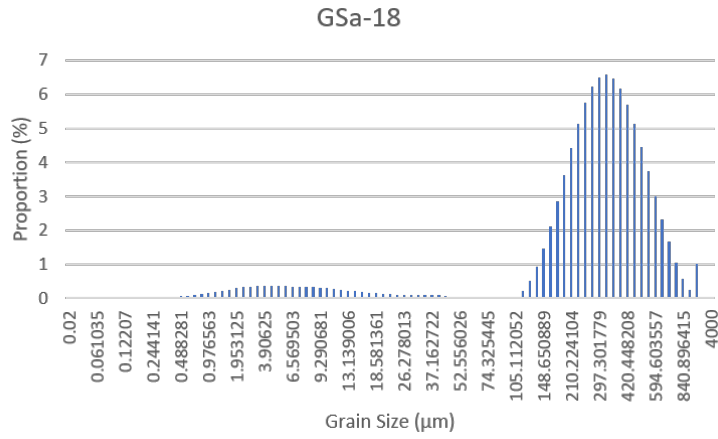


-0.95

Continue to Next Page ...

Grain Size Histogram

Depth (m AHD)



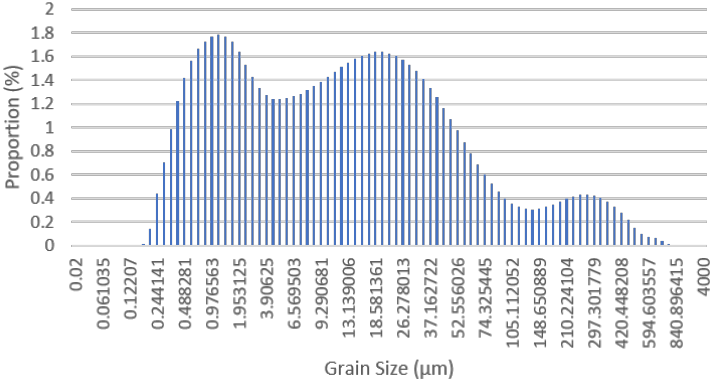
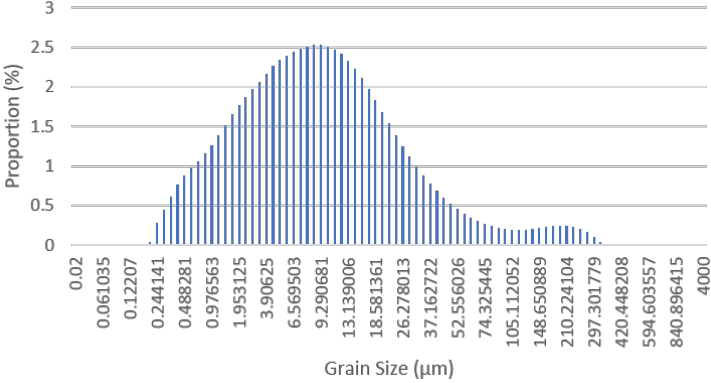
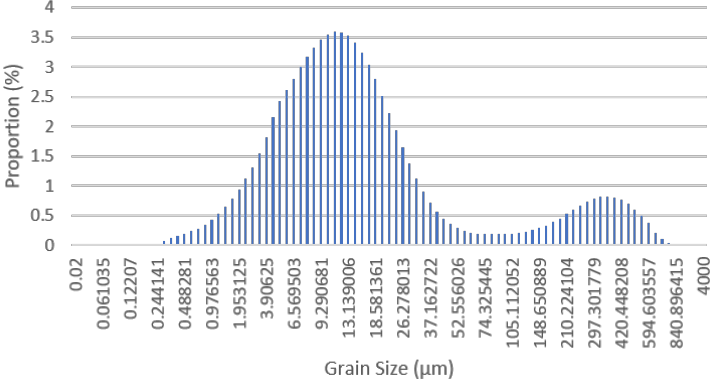
-1.21

End of Table

Table E.3: Results of the grain size analysis of mangrove core (MAN). Sample are presented with a grain size histogram and depth range (0 m AHD is approximately equivalent to mean sea level).

| Grain Size Histogram | Depth (m AHD) |
|---|---------------|
| <p>GSb-1</p> <p style="text-align: center;">Grain Size (µm)</p> | 0.73 |
| <p>GSb-2</p> <p style="text-align: center;">Grain Size (µm)</p> | 0.68 |
| <p>GSb-3</p> <p style="text-align: center;">Grain Size (µm)</p> | 0.63 |

Table E.4: Results of the grain size analysis of saltmarsh core (SM). Sample are presented with a grain size histogram and depth range (0 m AHD is approximately equivalent to mean sea level).

| Grain Size Histogram | Depth (m AHD) |
|--|---------------|
| <p>GSc-1</p>  <p style="text-align: center;">Grain Size (µm)</p> | 1.09 |
| <p>GSc-2</p>  <p style="text-align: center;">Grain Size (µm)</p> | 1.04 |
| <p>GSc-3</p>  <p style="text-align: center;">Grain Size (µm)</p> | 0.99 |

F Supplementary Maps

The following figures present the historic aerial photography used to perform the time series analysis and area change analysis.

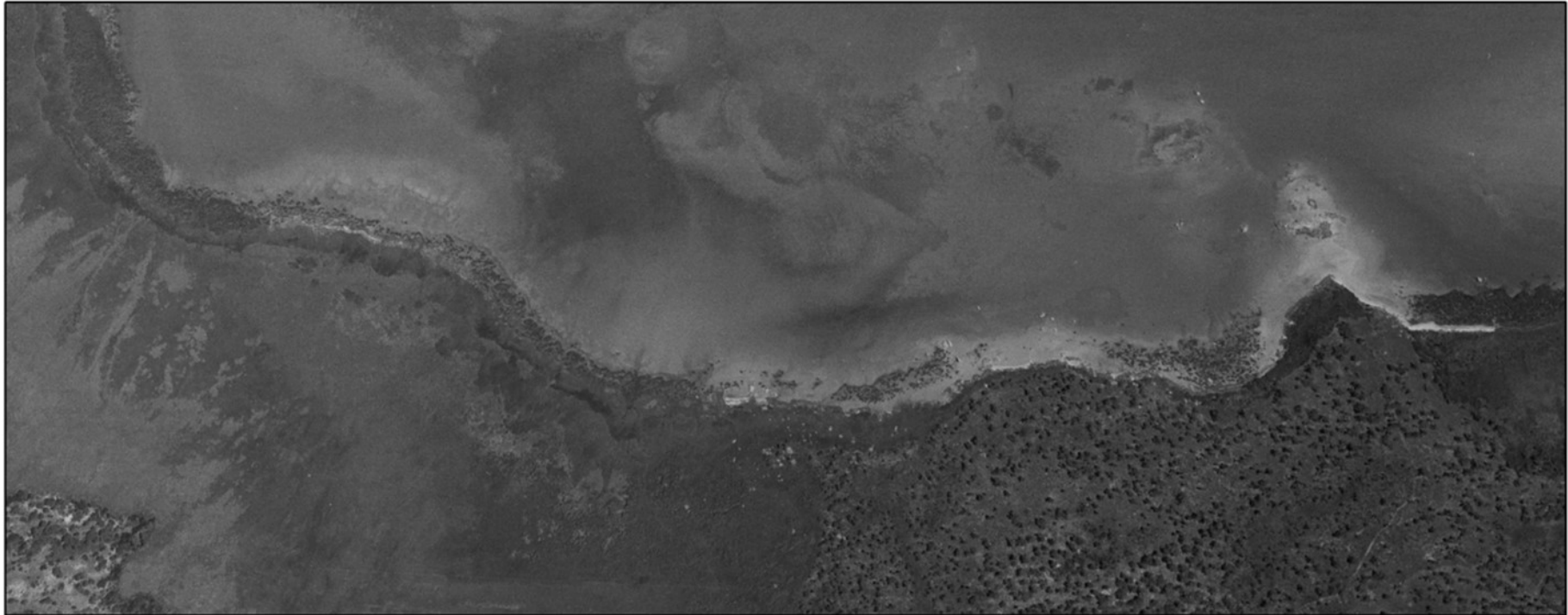


Figure F.1: Aerial photograph of Corner Inlet in 1957



Figure F.2: Aerial photograph of Corner Inlet in 1969



Figure F.3: Aerial photograph of Corner Inlet in 1978



Figure F.4: Aerial photograph of Corner Inlet in 1983



Figure F.5: Aerial photograph of Corner Inlet in 1987



Figure F.6: Aerial photograph of Corner Inlet in 2010.



Figure F.7: Aerial photograph of Corner Inlet in 2020.